SESSION 5

Plasma Physics and Magnetohydrodynamics In Space Exploration

Chairman, ADOLF BUSEMANN

DR. ADOLF BUSEMANN, *born in Lübeck, Germany, has been a member of the research staff of the Langley Research Center of the National Aeronautics and Space Administration since April 1947. He completed his undergraduate and graduate work at the Technical College at Braunschweig, Germany, graduating as an engineer in 1924 and receiving his doctorate in engineering in 1925. He started his career as an engineer at the Kaiser Wilhelm Institute (now the Max Planck Institute) in Göttingen, Germany, and later became chief engineer of the Institute. While conducting research for 6 years, Dr. Busemann also studied under Dr. L. Prandtl, renowned scientist and wind-tunnel designer, who at that time was director of the Kaiser Wilhelm Institute.*

In April 1931, Dr. Busemann began a 4-year period as a lecturer on the subjects of heat transfer, hydrodynamics, and aerodynamics in the Engine Laboratory of the Technical College at Dresden, Germany. Returning to Braunschweig in 1935 Dr. Busemann served as chief of the Gas Dynamics Division of the Aeronautical Research Laboratory until the Allied occupation 10 years later.

Following a period as a research consultant in England during 1946 and 1947, Dr. Busemann accepted an invitation in 1947 from the United States Government to come to this country and continue his career as a research scientist. At Langley Research Center, Dr. Busemann conducts original research in magnetofluid-dynamics and aerodynamics, and he acts as a consultant with the NASA on gas dynamical problems and related subjects. Dr. Busemann has authored more than 100 technical papers that have been published. He was one of two German scientists invited to deliver technical papers at the Volta Congress on high-speed aerodynamics held in Rome, Italy, in 1935. His paper was the first to propose the use of swept wings in the design of high-speed aircraft. He was elected a foreign member of both the Max Planck Association for the Advancement of Science, Germany, and the Academy of Science in Turin, Italy. He received the Carl Bosch Award for Advancement in Aeronautical Science in 1944, and is a member of the International Academy of Astronautics in Paris, France.

A resident of 18 East Southampton Avenue, Hampton, Va., Dr. Busemann became a naturalized citizen of the United States in ceremonies conducted in Norfolk, Va., on November 11, 1954. Members of his family, all of whom are now American citizens, include his wife, Mrs. Magda Krage Busemann, and three married daughters.

58. Relations Between Aerodynamics and Magnetohydrodynamics

By Adolf Busemann

SUMMARY

Although aerodynamics is approaching a state of perfection, at least in connection with turbulence, some important parts have not been completed. For example, magnetohydrodynamics, or the combination of aerodynamics and electromagnetic forces in electrically conductive fluids or ionized gases (called plasma), is a rather young science. Interesting results for technical or for astronomical application are known, but many controversies are still going on. One of the more obvious reasons that some of the results touch on a new version of very old problems is seen in the fact that under equal conditions, hydrodynamic forces and magnetic forces have opposite sign and thus reverse the situation when the magnetic field strength becomes predominant.

INTRODUCTION

The main objective of the presentations on plasma physics and magnetohydrodynamics is to demonstrate its importance for its proper placement within the university curriculum. To a certain extent this new subject is an outgrowth of aerodynamics, which has been developing to maturity not only since before man began to fly but also as the range of flying speeds has been extended throughout the subsonic and transonic range to supersonic or even hypersonic velocities. When I started my career with supersonic speeds, this speed regime could still be regarded as a quiet corner of purely academic interest where motivation and satisfaction rely on scientific curiosity and accomplishment. It may be forgotten under the glamour added by progress in aeronautics that there was enough incentive and that there were enough natural difficulties in this part of the continuum of mechanics to create a frontier spirit among those early workers on this subject. While we are entering space in the eternal demand to increase the speed of human transportation, the prospect of leaving the air and traveling through vacuum could be taken as the turning of the tide against aeronautics in retaliation for her murder of other means of transportation during the time that air travel was on the rise.

Space, however, is still not empty. The upper atmosphere under the sun's direct radiation is ionized and forms layers that change from day to night and are detected by the reflection of radio waves. Farther out, the universe is not empty either. It is filled with ionized particles that sometimes become passively entangled in magnetic fields, sometimes actively create them, and sometimes pull them along. This concept of the space environment not only is part of modern astronomy, but its development indicates one of the early nuclei around which a large portion of today's magnetohydrodynamics grew. The particle densities and the magnetic-field intensities are, of course, small compared with those on the earth's surface. Still, having no stronger competitors, their drag deserves first importance for extended space travel. With regard to the future of magnetohydrodynamics from this angle alone, the applicability to engineering which aerodynamics possessed in such a high degree as part of man's early dream of flying seems to fade out in the thin air. Combining its efforts with electromagnetism, however, aerodynamics is also engaged in making a greater dream of mankind a reality, the dream of tapping the very sources of energy which drive our universe. A great deal of research is directed toward developing the "fusion" engine, a kind of atomic diesel engine, in which a mixture is compressed beyond its threshold of stability and fuses into new products while a large energy differential derived from the combination process is being released. Ordinary materials cannot be used

to confine and compress these mixtures because they are unable to withstand the high temperatures involved. Therefore, only magnetic fields seem to be able to serve as the actual walls for confining, compressing, and ducting the mixtures although the problem remains of cooling the electric conductors, the backbones of magnetic fields. Magnetic fields have to be trained to accomplish the task of initiating the fusion, and they are the first ones present during the extraction of the energy during the expansion and have to transmit the energies to the proper destination.

In a problem of such dimensions, there is no doubt that frontier spirit in combination with glamour will remain for quite a while. All nostalgic feelings of aerodynamicists who see their field of research growing up to maturity or completion are premature; there will be in magnetohydrodynamics a second generation of researchers working in a similar way on similar problems and extending again the opportunities for a balanced theoretical and experimental approach that they learned to appreciate and that, in turn, formed their thinking.

In the belief that progress goes hand in hand with thorough understanding, regardless of how little may be accomplished at the beginning, and that experimental verification is needed to provide assurance of a proper approach, half of this session will be devoted to the theoretical, academical, or pedagogical aspect of the subject and the other half to the practical problems in a short survey. Since magnetohydrodynamic theory is such a complicated and extensive subject, not even the fundamentals can be covered in a paper of this length. The purpose here is to display the many facets of this new subject and to give cross-connections to more familiar results in order to show some of the life hidden underneath its surface.

SYMBOLS

B_0 magnetic field strength
F force
F_h hydrodynamic force
F_m magnetic force
I electric current
V flow velocity
v wave speed
μ permeability
ρ density
Γ circulation

HISTORY OF AERODYNAMICS AND ELECTRODYNAMICS

No one can predict the future of a new branch of science nor the time it will take to grow to maturity. There is no better example for learning this lesson than to compare the history of aerodynamics and electrodynamics. Wind and water are easily noticed with our own senses. Their capacity to work for mankind by driving mills and sailboats is ancient knowledge. Still, aerodynamics was not completely developed as a reasonable science prior to early flight. It more or less accompanied, with mutual support, the development of flight within the last 50 years.

Electric and magnetic fields are, as such, invisible and they did not reveal the electrodynamic forces much earlier than 1820 when Oersted discovered them. About 50 years later, in 1873, Maxwell was able to complete the electromagnetic-field theory in a form ready to give useful results. Not only is the short time remarkable, but also the fact that scientists of that time borrowed hydrodynamic pictures to interpret their invisible fields until electrodynamics learned to stand on its own feet and abandoned the attempt to call itself hydrodynamics of the ether.

Many aspects of electricity, for instance electronics and semiconductors, came much later and had a fantastic growth by themselves. Ionization, although one of the older branches dating from electrostatic times in Geissler tubes, needed further study and required a higher vacuum to simplify confusing findings. Occupied with such investigations of ionized gases in the General Electric Research Laboratory in Schenectady, Irving Langmuir in 1928 found it necessary to distinguish rather sharply between two fundamentally different states. He gave names to these extreme states by saying: "Except near the electrodes, where there are *sheaths* containing very few electrons, the ionized gas contains ions and electrons in about equal numbers so that the resultant space charge is very small. We shall use the name *plasma* to describe this region containing balanced charges of ions and electrons." (See ref. 1, p. 112.)

Plasma and sheaths are, since that time, seen as separable parts rather than extreme states on either end of a natural transient. In about the same manner, Ludwig Prandtl in 1904 mastered the basic problem of hydrodynamics of low friction by distinguishing between what he called the friction layer at the body walls—it became famous under the name boundary layer—and the potential flow farther out. Langmuir's name plasma for the ionized-gas state of balanced charges has been adopted for the whole science and it is not always contrasted with the sheaths on the electrodes. Contrary to that first distinction, it is now permissible to say that a Mercury spacecraft surrounds itself with a plasma sheath during its reentry into the earth's atmosphere. Its effect on radio communication need not be mentioned since the prolonged reentry of Astronaut Scott Carpenter in the MA–7 spacecraft is well remembered because this missing communication created, at least for the public, many minutes of uncertainty about his landing. Plasma is now used to designate a further state of matter, beyond solid, liquid, or gaseous, when temperatures are high enough to ionize the molecules or when density is low enough to prevent ions and electrons from recombining in triple collisions. It has been speculated that more than 90 percent of all matter in the universe is in this new plasma state.

Magnetohydrodynamics as a name does not indicate its relation to plasmas but rather its applications for stirring molten metals or for pumping mercury or other electrically conductive liquids. However, incompressibility is not considered necessary for use of the term. Plasma physics is almost synonymous with magnetohydrodynamics. Different names are also created, and sometimes preferred, when it is felt that magnetohydrodynamics emphasizes either incompressibility or the presence of magnetic fields too much. Examples of such names are magnetoaerodynamics, magnetofluid-dynamics, and electrofluid-dynamics.

REACTIONS ON SINGULARITIES

In the historical introduction contrasting slow and rapid development of hydrodynamics with electrodynamics, some of the striking differences between the two fields were not specified. Neither are these differences pointed out in many books concerned with only one of these two subjects.

In an idealized fluid, one must deal with point singularities in sinks and sources as well as with line singularities of the vortex type. Magnetic fields also have point singularities, such as north and south poles, as well as line singularities of the vortex type if the line is a conductor of electric currents. Both types of singularities are in complete analogy with respect to the field structure and with respect to being indicative of forces exerted by the fields. With all this analogy and the additional information that the energy in flow fields and magnetic fields is positive and proportional to the square of the field intensity, it comes as a shock when one learns that the forces are, in both cases, equal except for a systematic reversal of the sign. An attraction force changes to a repulsion force and vice versa. If the forces were made to build up field energy when a north pole is removed from a south pole, the force has to be an attraction force. If a vortex is removed from one of opposite circulation while building up the velocity field, the sign has to be an attraction again. But it seems that there are responsible forces which really cooperate in the formation of field energy. Then there are irresponsible forces doing just the opposite from what is needed and thus, exactly speaking, introducing a doubled difference for someone to resolve. The amusing part of the problem is that neither the hydrodynamic nor the electrodynamic forces are responsible altogether, but that each field has one kind of singularity that is responsible and another one that is irresponsible in dealing with the field energy. As figure 58–1 shows for point

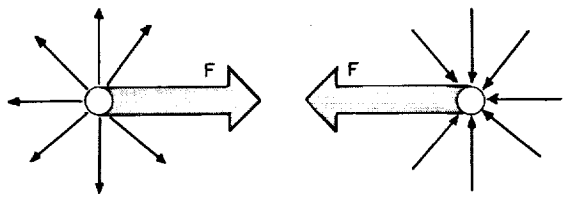

F FORCES BALANCING FIELD ENERGY
+F REACTION IN MAGNETISM
−F REACTION IN HYDRODYNAMICS
(SPONSOR: PUMPS TO MAINTAIN SOURCE STRENGTH)

FIGURE 58–1.—Forces between point singularities (poles of opposite sign).

singularities, it is the magnetic pole which has the proper sign; the hydrodynamic sinks and sources rely on pumps to maintain the source strength against nonsteady pressure differences accompanying the movements of sinks and sources. Figure 58–2 shows that in the case of line singularities, the fluid vortices have responsible forces—the basic elements of airfoil theory—whereas the magnetic vortices have irresponsible forces and rely on induced electromotive forces against the electric currents flowing in the vortex core to sponsor the doubled amount of missing field energy.

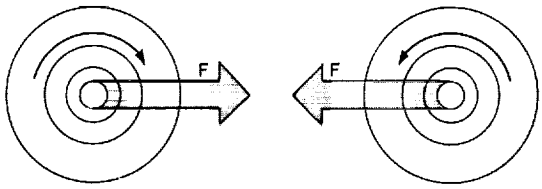

F FORCES BALANCING FIELD ENERGY
+F REACTION IN HYDRODYNAMICS
−F REACTION IN MAGNETISM
(SPONSOR: BATTERIES TO MAINTAIN CURRENT STRENGTH)

FIGURE 58–2.—Forces between line singularities (vortices of opposite sign).

It may seem for the student rather a nuisance that his memory rules for forces on singularities get hoplessly mixed up when he enters the second field after acquaintance with the first one. The physics of the combined hydrodynamic and magnetic vortices around the same core, however, takes advantage of the reversed signs for the creation of free vortices. These combinations have identical velocity and magnetic fields and lose the expected resulting force by compensating the hydrodynamic force with the magnetic field force.

LIMIT OF INFINITE CONDUCTIVITY

In order to set the stage for an easy application of this field combination, the two components must first be brought to a more comparable state of idealization. The fluid for simple vortex laws has to be of vanishing viscosity. The magnetic field in which currents are representing the magnetic vortices would show equally reduced dissipations if one goes to the limit of infinite conductivity or vanishing resistivity in the plasma. For ordinary fluids, this requirement applies to the opposite end of the conductivity scale since these fluids really are of very moderate conductivity. As concerns applications for plasmas so hot that ordinary materials cannot be used as confinement walls, it is indeed reasonable to say that the electrical conductivity may be near infinity. Plasma in the universe will also have high values of electrical conductivity in many astronomical applications and the limit of infinite conductivity can well serve as first approximation.

Any fluid moving through a magnetic field creates electric induction wherever it crosses magnetic lines. Infinite conductivity raises currents so large with any small amount of induction that the new magnetic field superimposed on the original one by the presence of the new currents is of the same order as the original field. It is, therefore, easier to deal with the total field than with its parts. The total field is now not allowed to create any induction by fluid elements crossing magnetic lines. The result is that the original magnetic lines appear to follow the fluid. Similarly, the free forces on the electric currents in the magnetic fields correspond to the magnetic field deformation and are, therefore, visible without regard to the electric currents inside the plasma. The limit of infinite conductivity is such a great simplification that everybody takes the magnetic field itself as being swallowed by the fluid and thus it has to be distorted with the fluid while exerting its reactions on account of the deformations directly to the fluid. Such a story is easy to learn and is for the main part correct.

There are a couple of exceptions connected with the fact that electric currents have to be closed. An induction field which drives electric currents in a one-way sense with no possibility of returning is not benefited by the infinite conductivity of the fluid. Such a frustrated induction field permits a certain slip of the magnetic lines through the plasma. It occurs when all magnetic lines are being replaced by similar lines while the magnetic flux is conserved. The more specific rule for the plasma clinging to the magnetic lines is, therefore, stated as follows: All elements once connected with a cer-

tain magnetic line remain always on a common line and any magnetic tube formed by magnetic lines inside the fluid has to carry the same flux for all times. The fluid of infinite conductivity which swallowed a magnetic field at birth stays with this field for life, but the identity of the lines is not guaranteed.

The confinement of a limited volume of plasma by the sole presence of a magnetic field is now not as sure as when the elements were obliged to cling to the identical magnetic line. There are, however, more refined methods whereby this lack of identity of magnetic lines may be overcome. A simple method is to use the fact that the magnetic flux is conserved. A plasma originating outside any magnetic field will, therefore, be trapped between strong fields as shown in figure 58–3 under confinement (a). A more sophisticated way of trapping the plasma is to identify the magnetic lines by their shape. In a ring of plasma, the regular magnetic lines would be circular and concentric to the axis of the ring. If a special spool around the ring causes the magnetic lines to wiggle in a steady shape so that they miss their connection after one full turn, it is possible to increase the distance of miss from the center to the outside. Such magnetic lines make many turns inside the ring before they ever close. The important part in this pattern is that there are different knots in different magnetic lines and a family born on one of them cannot jump to any other one as a substitute. These magnetic lines are topologically different and that means that they can be identified by shape.

The problem of confinement is a very good example of scientific education connected with plasma physics. There is a great deal of geometrical orientation in our three-dimensional space that can be learned in this application. The stability of configurations is another good exercise in mechanics of three-dimensional field

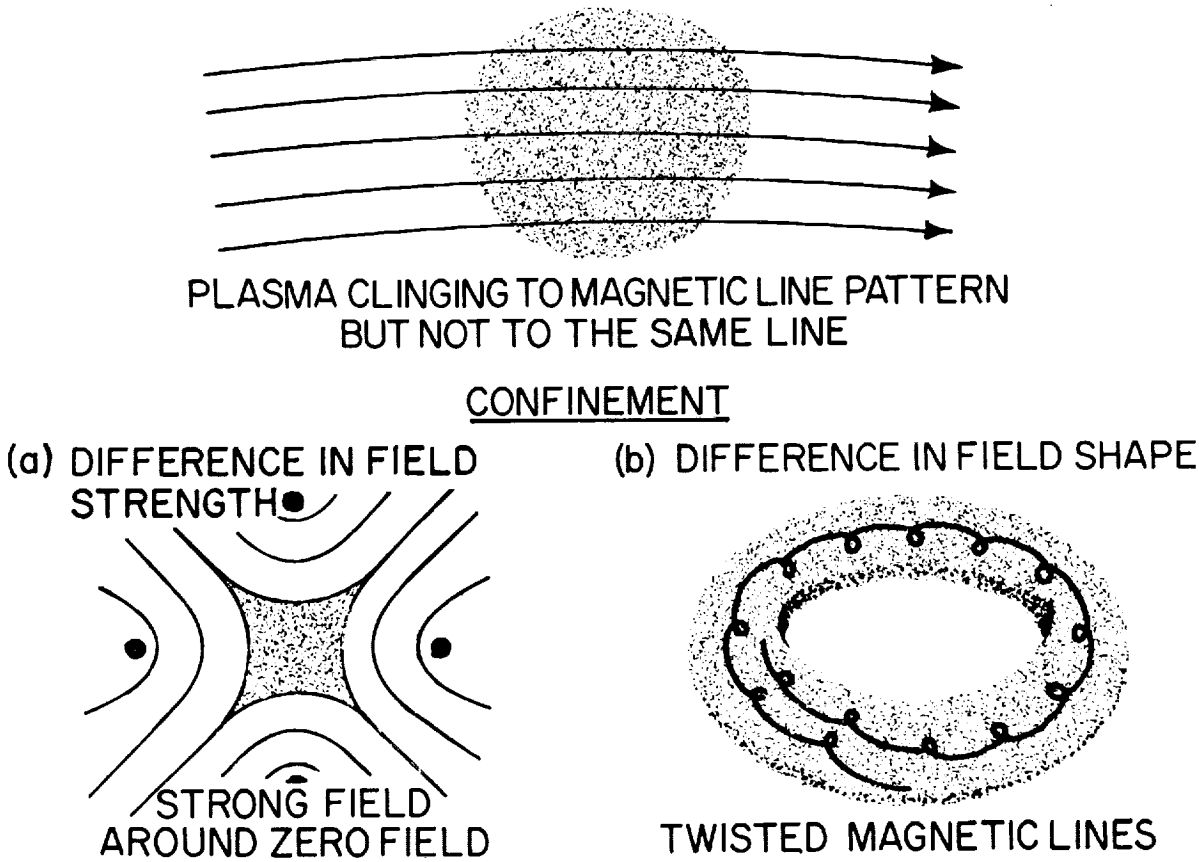

FIGURE 58–3.—Limit of infinite conductivity.

patterns. Although the education in these disciplines will remain as time goes on, the fact that the confinement problem is not solved yet has, at the present time, the added attraction of finding new tricks in acts of jailbreaking of the plasma. The fight of human ingenuity against the eternal laws of nature is still going on. Reassurance can be gained not only from the fact that mankind has always won this fight, but also from the natural examples of good confinement in astronomy and in the Van Allen belts around the earth.

FREE MAGNETOHYDRODYNAMIC VORTICES

With reference to the two-dimensional incompressible problem of free magnetohydrodynamic vortices, a parallel magnetic field of the intensity B_0 may be assumed to extend far beyond the region of interest where it is not affected by the local distortions. The plasma that is far out plays the role as the identification service for all the magnetic lines concerned. Under these conditions, the simple trapping of plasma by identical magnetic lines can be applied. Before our interest starts, a moving body may have created a single vortex in its wake in the same manner as it created a vortex in pure aerodynamics. This idea gets full plausibility when one first considers a very weak magnetic field and a fast start of a body with a sharp trailing edge as indicated in figure 58–4. No matter how weak we may assume the magnetic field to be for this purpose, the vortex left alone in the fluid of infinite electrical conductivity cannot wind up the magnetic lines of the given magnetic field B_0 forever. The final state should be an arrangement of magnetic lines coinciding with steady streamlines around the vortex. Circular magnetic lines are easily achieved if an electric current I is assumed perpendicular to the plane of figure 58–5, com-

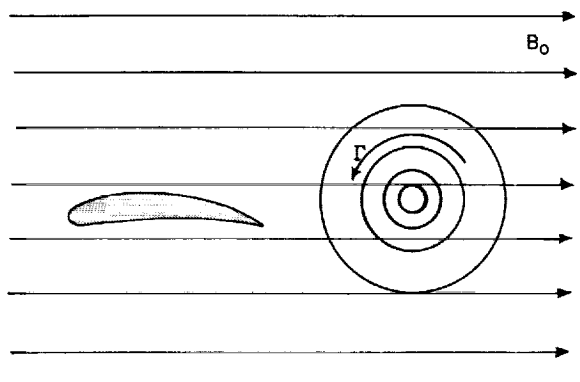

FIGURE 58–4.—Free hydrodynamic vortex with superimposed magnetic field.

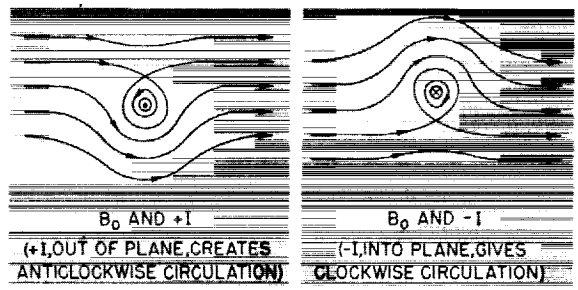

FIGURE 58–5.—Magnetic field patterns (parallel and circluatory).

ing out or going into the plane of this figure. Any finite current cannot overpower the parallel magnetic field B_0 completely and, therefore, has a stagnation point some distance from the location of the current, where circular lines change to passing lines. Two such configurations are drawn in figure 58–5, one for current out of the plane and the other for current into the plane. A resting fluid vortex is not able to show similar lines in the pattern of its streamlines. If the vortex is permitted to move, then two equal steady streamline patterns are possible as in figure 58–6.

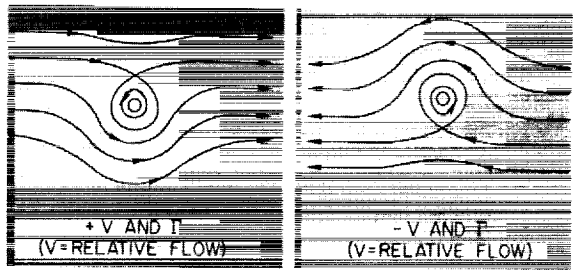

FIGURE 58–6.—Steady streamlines (parallel and circulatory).

There were, however, very valid reasons for Helmholtz to postulate that free vortices do not move with respect to their surrounding fluid neighborhood. The vortex singularity superimposed to a parallel motion would create lifting forces which a free vortex could not

absorb for any length of time. The concept of a free vortex staying within its original neighborhood of fluid particles is actually the concept of a force-free singularity, and the feature to rest within the fluid was the only way to satisfy this demand. In combinations of opposing magnetic and hydrodynamic forces, there is a much larger variety of force-free superpositions as long as an outside magnetic field is given. There is even a force-free combination with identical magnetic lines and steady streamlines if the vortex is allowed to move with a certain speed parallel to the imposed magnetic field B_0. (Compare fig. 58–5 with fig. 58–6.) Since due to the fixing of a conventional sign to the direction of the magnetic field there is still the choice of matching a clockwise or an anticlockwise magnetic field with the anticlockwise circulating vortex, the same velocity of the vortex may be taken either up or down the direction of the magnetic field. A corotating magnetohydrodynamic vortex is free of a resulting force traveling against the magnetic field vector. (See fig. 58–7.) A contrarotating free vortex has to move with the magnetic field vector B_0. Actually the condition that the electric currents have to be closed will split any fluid vortex into two magnetohydrodynamic free vortices of one-half the circulation strength but superimposed with either a magnetic circulation of the same or the opposite sign to travel in opposite directions with respect to the resting fluid and guided by the direction of the imposed magnetic field B_0.

ALF VÉN WAVES

The splitting of a former free vortex into two halves, a corotating and a contrarotating free magnetohydrodynamic vortex, opens the curtain for a play with a foursome of free magnetohydrodynamic vortices for the same magnetic field strength, having either clockwise or anticlockwise fluid circulation combined with either clockwise or anticlockwise magnetic circulation. How do they behave with each other? The completely reversed ones are either corotating or contrarotating free vortices. They are known to move together either against or with the magnetic field. The fact that, say, the corotating vortices walk together does not indicate that they have the slightest effect on each other. On the contrary, whatever the added fluid velocity would try to do, when one vortex is close to the other one, the added magnetic field strength is intended to undo. And so they walk together in complete disregard of each other as long as any distribution of corotating free magnetohydrodynamic vortices is separated from the contrarotating ones. The same holds true as long as contrarotating vortices are among themselves, the true meaning of "co" or "contra" being only a magnetic sign convention in the first place. The constant velocity and the dull neutral stability of any group of corotating or contrarotating free vortices in separation are best known in an arrangement of infinitesimal strength along lines perpendicular to the magnetic field. (See fig. 58–8.)

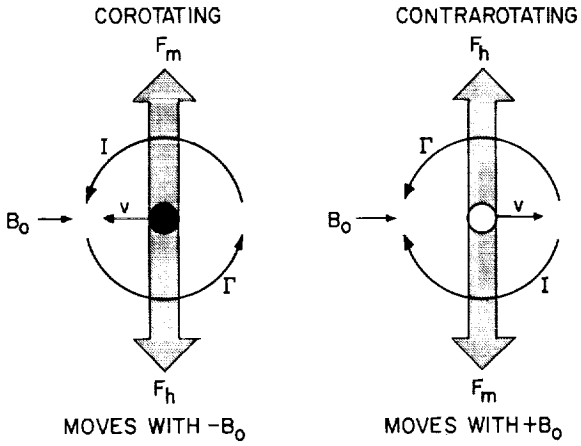

FIGURE 58–7.—Force-free combinations.

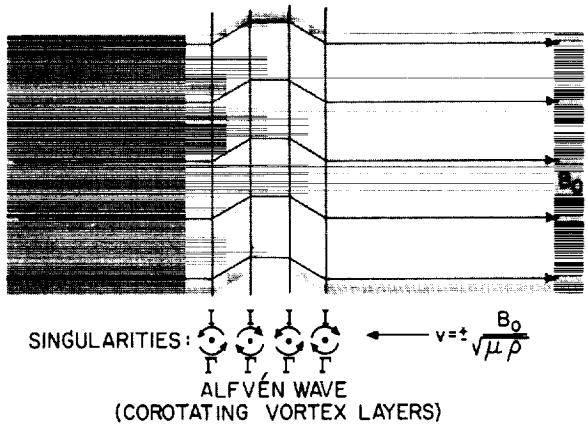

FIGURE 58–8.—Alfvén waves.

Such an arrangement represents the shear wave perpendicular to the magnetic lines and travels according to its discoverer Alfvén with the so-called Alfvén speed up or down the direction of the given magnetic field.

COMPRESSIBLE PLASMAS

This free movement of the fluid in the shear wave demonstrates two changes, one for each of the cooperating sciences. The clinging of plasma to the magnetic lines makes their usual propagation speed, the speed of light, very much slower. The structure added to the fluid by being connected to magnetic lines gives restoring forces to deformations which had none before. It also adds to the volume changes a new pressure, the magnetic pressure difference, in case the compressibility is considered and is not applied to compressions in the direction of the magnetic lines. The plasma enters, with the help of the magnetic field, the mechanics of a solid able to resist volume and shape changes but with a very obvious anisotropy according to the line structure of the magnetic field. Shear and compression waves of the Alfvén type, in combination with the acoustic waves, form a pattern of two waves for every direction with respect to the magnetic field direction. Depending upon the strength of the magnetic field, the given speed of a body moving through the plasma can be subsonic or supersonic as well as of either the sub-Alfvén or super-Alfvén types. At large Alfvén speed (the body speed being of the sub-Alfvén type), the vortices created by the body may get ahead of the body and form the surprising forward wake predicted by the theory. There are many new flow patterns possible for the flow past bodies in magnetohydrodynamics. The sharp trailing edge, one of the significant points in subsonic flow for control of lift without large corrections on account of the viscosity, lost its importance for supersonic speeds and is still a controversial factor concerning its ability to control lift at sub-Alfvén speeds when a part of the shed vortices march ahead of the body instead of staying behind.

MUTUAL INTERACTIONS OF FREE VORTICES

By separating the two groups of corotating and contrarotating vortices, a great simplicity was gained since they ignored each other's presence within either of these groups. A last remark about what happens when both groups are together may give reassurance that whatever has been suppressing the interaction between the members of each group has doubled the interest a member of one group takes in a member of the other group. The interaction, however, is complicated by the fact that when two members of the different groups are left in the vicinity of one another for any length of time, creation of new vorticity of both kinds, the corotating and the contrarotating, can be expected. (See ref. 2.) The other speakers will introduce you to many more items of the magnetohydrodynamics and plasma physics field.

Seeing the future with the eyes of the aerodynamicist, I should like to conclude that there is a continuation for almost any phase of pure aerodynamics, with great variety already under study at the very opening of the door to this combined field. Many problems apparently solved by a purely aerodynamic approach have to be reconsidered either directly from the beginning or, when higher Alfvén speeds indicate the predominance of the magnetic field strength, a "no" may turn into a "yes" when two partners cooperate who in spite of their great similarity have opposite ideas about the sign of forces.

REFERENCES

1. Langmuir, Irving: Oscillations in Ionized Gases. Vol. 5 of the Collected Works of Irving Langmuir, C. Guy Suits, ed., Pergamon Press (New York), c. 1961, pp. 111–120.
2. Busemann, Adolf: On the Kármán Vortex Street in Magnetofluiddynamics. Proc. Aerospace Scientific Symposium of Distinguished Lecturers in Honor of Dr. Theodore von Kármán on his 80th Anniversary. Sponsored by the Air Force Office of Scientific Research. Inst. Aero. Sci., 1962.

59. Fundamentals of Plasma Interaction With Electric and Magnetic Fields

By Robert V. Hess

ROBERT V. HESS, *Head, Plasma Physics Section, Aero-Physics Division, NASA Langley Research Center, received his Bachelor of Science and Master of Science equivalent from the Vienna (Austria) Institute of Technology in 1938. He studied Fluid Flow at the Massachusetts Institute of Technology in 1939. Since joining the Langley staff in November 1944, Hess has specialized in magnetoplasmadynamics, plasma acceleration, and gasdynamics. He was the first to give analytic expression of three-dimensional subsonic flow effects depending on wing aspect ratio; he predicted novel interaction effect of explosion wave with hot ground layer, subsequently experimentally confirmed. He invented a new type of chemical plasma used for telemetering experiments and electric power generation and invented a new type of plasma accelerator using Hall currents. He is author of many NASA publications on research he has conducted at Langley. Hess is a member of the Scientific Research Society of America (RESA).*

SUMMARY

The fundamental aspects of the interaction of plasmas with electric and magnetic fields are treated through specific examples from actual problems of research. For instance, the dielectric behaviour of a plasma in a strong magnetic field which applies to capacitive energy storage and Alfvén waves is discussed. The equations of motion of electrons and ions in a plasma including collisions and space charge effects are unified. The plasma is treated as a single fluid with velocity, current, and various transport properties, such as electrical conduction. The single-fluid approach is applied to a variety of methods of steady plasma acceleration and to the acceleration of ions in a plasma. Collision processes and electrical conduction are given for fully and partially ionized plasmas with and without a magnetic field. Their effect on voltage current characteristics of electrical discharges in the presence of magnetic fields is discussed for a variety of experiments. Examples of turbulent electrical conduction are given.

INTRODUCTION

Textbooks dealing with the fundamentals of plasmas in magnetic fields draw largely on examples from thermonuclear fusion problems, where problems of leakage or diffusion of a plasma across the confining magnetic field are of major concern. Since our major concern is that of plasma acceleration for which the use of electric fields crossing magnetic fields is important, our problems deal frequently with electrical conduction across a magnetic field rather than with diffusion. In this paper, an attempt is made to present the fundamentals of plasma physics up to the latest findings from this viewpoint. It will turn out that problems of anomalous, or "turbulent", electrical conduction across magnetic fields may be encountered, from which comparisons may be made with anomalous or "turbulent" diffusion processes across

46

magnetic fields which are of prime concern to the whole field of plasma physics.

The plan of the paper is to obtain a general picture through a discussion of many specific examples of plasmas interacting with electric and magnetic fields. In a broad sense, one can, however, distinguish between the pure kinetics and dynamics of such interactions and the plasma physics of actual electrical discharges in magnetic fields.

SYMBOLS

An arrow above a symbol indicates a vector quantity. Quantities are expressed in the rationalized mks system of units.

B	magnetic flux density
c	speed of light
$\bar{c}$	mean thermal velocity
C_1, C_2, C_3, C_4	constants
D	diffusion coefficient
$\frac{D(\ )}{dt}$	substantial derivative, $\frac{\partial(\ )}{\partial t}+$v. grad( )
d	Debye length
E	electric field strength
$E^*=E+v\times B$	
e	electronic charge
H	magnetic intensity
j	current density per unit area
k	Boltzmann's constant
l	length
m	mass
n	particle density per unit volume
P	polarization
p	pressure
Q	collision cross section
r	radius
s	displacement
T	temperature
v	velocity
α	turbulent coefficient
β	geometric factor
ϵ	permittivity
λ	mean-free path
μ	permeability
ρ	density
ν	collision frequency
σ	conductivity
τ	collision time, $1/\nu$
ω	cyclotron frequency

Subscripts:

x, y, z and r, θ, x refer to directions in Cartesian and cylindrical coordinates, respectively

c	coulomb
D	drift
e	electron
i	ion
L	Larmor
n	neutral
0	free space
p	plasma
i, e	ion-electron
i, n	ion-neutral
e, n	electron-neutral
$\perp$	perpendicular to the direction of . . .
turb	turbulent
osc	oscillations in plasma

Superscript:

f	finite electrodes

FUNDAMENTAL DIFFERENCES IN EFFECTS OF ELECTRIC AND MAGNETIC FIELDS

The plasma contains approximately an equal number of electrons and ions and is thus on the whole electrically neutral. The electric field exerts equal forces on the charged particles whose directions of motion are, however, opposed. These forces cancel and, as a result, an electric field in itself cannot exert a force on the plasma as a whole. A magnetic field, on the other hand, has the quality that when stationary, it cannot put energy into the plasma but merely exerts forces on it for which reactions can be measured on the magnetic coils. Since a magnetic field exerts a force on a plasma, a moving magnetic field can be expected to do work on the plasma or put energy into it. Because, however, it is actually the electric field which puts energy into the plasma, the magnetic field will put energy into the plasma or its motion through the intermediary of an electric field. It was established experimentally by Faraday and from a broader point of view by Maxwell and Einstein that a moving magnetic field is equivalent to a combination of stationary electric and magnetic fields.

I. KINETICS AND DYNAMICS OF PLASMAS IN ELECTRIC AND MAGNETIC FIELDS

Behavior of Electrons and Ions in Constant Electric and Magnetic Fields

The most fundamental case to be discussed deals with charged particles accelerated by a constant electric field in the presence of a constant magnetic field. The equation of motion of the charged particle, for example, of an ion, is then, according to basic texts such as references 1 to 11:

$$m_i\frac{d\vec{v}_i}{dt}=e\vec{E}+e(\vec{v}_i\times\vec{B}) \qquad (1)$$

The first term on the right-hand side in equation (1) is the well-known electrostatic force. Since the magnetic force does not impart energy, it is normal to the velocity $\vec{v}$ of the particle and to the magnetic field $\vec{B}$. In order to absorb the reaction to the force on the particles, the magnetic field $\vec{B}$ has to be deformed. Then, $\vec{B}$ designates the deformed field. First, an even simpler problem is treated. Assume that after the particle has attained a velocity, the electric field is removed. Then, $m_i \frac{d\vec{v}_i}{dt}$ is the centrifugal force which balances the magnetic force $e(\vec{v}_i \times \vec{B})$ which, since it is always normal to the particle velocity, produces a curvature in particle path without change in its absolute velocity and kinetic energy. From this force balance

$$m_i \frac{v_i^2}{r_{L,i}} = e|v_i|B \tag{2}$$

the radius of gyration $r_{L,i}$ (sometimes called Larmor radius) is obtained as is the angular frequency $\omega_i = v_i/r_{L,i}$ (sometimes called cyclotron frequency)

$$\left.\begin{aligned} r_{L,i} &= \frac{m_i v_i}{eB} \\ \omega_i &= \frac{eB}{m_i} \end{aligned}\right\} \tag{3}$$

The rotation of the negative electrons is opposed to that of the positive ions. The direction of rotation is based on fundamental experimental facts.

Suppose now that the electric field E is imposed. The following particle motion results (fig. 59–1):

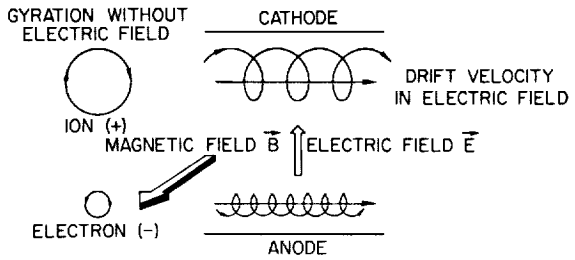

FIGURE 59–1.—Graphical representation of motions of electrons and ions.

A physical explanation for the particle drift perpendicular to the electric and magnetic field can be given as follows. The electric field accelerates ions and electrons in opposite directions and, as a result of the force balance, only energy is put into the system. The positive ions are attracted by lower or negative potential, which would be at the cathode in a discharge, and are accelerated in the direction of the electric field; whereas, the negative electrons are accelerated in the direction opposed to the electric field. The ions thus reach their maximum velocity on top and the electrons on the bottom. As a result, their Larmor radii are a maximum in this region and a minimum on the opposite side. This behaviour results in a drift normal to the electric and magnetic fields. The force exerted by the magnetic field has thus accelerated both ions and electrons in one direction normal to the electric field. The magnetic field has thus converted the energy input of the electric field, which acts in opposite directions on the electrons and ions of the plasma, into an unbalanced force in one direction.

While this description gives a good qualitative physical picture, it does not bring out the great simplicity of the motion and does not determine the value of the drift velocity. When drift velocity is attained, the acceleration of the particles normal to $\vec{E}$ and $\vec{B}$ is zero; thus

$$\vec{v}_D = \frac{\vec{E} \times \vec{B}}{B^2} \tag{4}$$

where for $\vec{E}$ perpendicular to $\vec{B}$, $v_D = \frac{E}{B}$. An observer moving with the drift velocity will detect no electric field and he will see only particles circling in the magnetic field.

Meaning of Simple Case for Practical Acceleration of a Collisionless Plasma

It was shown that the acceleration to drift velocity of particles gyrating in a strong magnetic field is due to different effects of the imposed electric field on each side of the circular motion. The minimum time for plasma acceleration would thus be, on the average, the reciprocal of the cyclotron frequency of the

heavier ions, whose mass predominates in the plasma. Correspondingly, the minimum distance of acceleration is, on the average, of the order of a Larmor radius. The neglect of collisions is justified for a plasma like the present one, which consists of only charged particles, that is, a fully ionized plasma, not only when the density is low but also when the temperature is high, as is discussed subsequently. The collisionless cases discussed herein are not merely playthings of the theoretician but are of great importance for plasma interactions with magnetic fields in space and in thermonuclear devices. The above collisionless acceleration has been approached in thermonuclear devices like the Ixion (refs. 12 and 13, sections 1 and 2), where the plasma is put into rotation in very short bursts. The use of such a system for continuous, steady plasma acceleration does not seem promising unless the losses of the highly ionized plasma to the walls are kept small like in the Ixion, where the electric and magnetic field configuration permits both confinement and acceleration of the plasma.

Collisionless Plasma Acceleration Described in Terms of Energy Input

When the drift velocity normal to the electric and magnetic field is attained, no current will flow in the direction of the electric field. As a result, a steady electric field cannot put energy into the plasma, since

$$\text{Input Rate of Energy Density}=\vec{j}\cdot\vec{E} \qquad (5)$$

with

$$\vec{j}=ne(\vec{v}_i-\vec{v}_e)$$

Equation (5) indicates that for zero $\vec{j}$ the input ratio of energy density is zero. Of course, energy can be put into a plasma with collisions because, as is well known, collisions permit the particles to break through the magnetic field. It is also well known that energy can be put into plasma with or without collisions by an electric field alone without the presence of a magnetic field. But in the presence of a steady magnetic field the electric field $\vec{E}$ must vary to permit an energy input. As indicated at the beginning of this paper, a variation of magnetic fields could also produce collisionless plasma acceleration. The study of the acceleration, however, of a collisionless plasma in a steady magnetic field, aside from applying to the present case, introduces many truly basic aspects of plasmas in magnetic fields.

Dielectric Properties of Plasma in a Magnetic Field

The current due to variation of $\vec{E}$ in a steady magnetic field can be obtained from a balance of the $\vec{j}\times\vec{B}$ force per unit volume with the accelerating force $\rho\dfrac{D\vec{v}}{dt}$; thus (from basic texts)

$$\rho\frac{D\vec{v}}{dt}=\vec{j}\times\vec{B} \qquad (6)$$

The field strength $\vec{E}$ is assumed to change slowly so that $\vec{v}$ is at no time far removed from the drift velocity $\dfrac{\vec{E}\times\vec{B}}{B^2}=\dfrac{E_\perp}{B}$; the subscript $\perp$ indicates perpendicular to the direction of drift motion. Solving for $\vec{j}$ gives

$$\vec{j}_\perp=\frac{\rho}{B^2}\vec{B}\times\frac{D\vec{v}}{dt}=\frac{\rho}{B^2}\frac{DE_\perp}{dt} \qquad (7)$$

The quantity ρ/B^2 is the product of the permittivity of free space times the dimensionless susceptibility characterizing the dielectric. Using $B^2/2\mu_0$ as magnetic pressure and $1/\mu_0\epsilon_0$ as the speed of light squared,

$$\frac{\rho}{B^2}=\frac{\rho\epsilon_0}{\dfrac{B^2}{2\mu_0}2\mu_0\epsilon_0}=\frac{\rho c^2}{\dfrac{B^2}{\mu_0}}\epsilon_0$$

A better physical picture is obtained by noting

$$\frac{\rho}{B^2}\vec{E}=n\vec{P}=ne\vec{l} \qquad (8)$$

where

$$\rho=n_em_e+n_im_i$$

and in a plasma $n_e\approx n_i$. Thus, the problem is concerned with a polarization which equals a charge times the average separation of a plasma with n particles per unit volume. This polariza-

tion is to be distinguished from the more familiar microscopic polarization of bound charges. The average charge separation in this case is limited to the sum of the Larmor radii, using the drift velocity; thus, as noted especially in reference 6,

$$r_{L,i}+r_{L,e}=\frac{m_i v_i}{eB}+\frac{m_e v_e}{eB}=\frac{m_i+m_e}{e}\frac{E}{B^2} \qquad (9)$$

Since the mass of the ions is much larger than that of the electrons, the displacement of the ions predominates. Subsequently, space-charge displacement effects will be shown in the plasma without a magnetic field, with effects of electrons predominant.

The existence of such dielectric effects of a plasma in the presence of an electric and magnetic field has very important practical consequences. It becomes possible to store electrical energy in motion, most conveniently in rotation; this energy is

$$\frac{\rho}{B^2}\frac{E^2}{2}=\frac{1}{2}\rho v_D^2 \qquad (10)$$

Such a device has been actually used as a "Hydromagnetic Capacitor" (ref. 14).

Perhaps even more significantly from a basic viewpoint the existence of a dielectric effect for a plasma in the presence of a magnetic field introduces the possibility of waves in the plasma. The electric field, of course, need not be externally imposed but is related to velocity perturbations. The well-known Alfvén waves, as is pointed out by Dr. A. Busemann in paper number 58 of this volume, can use the magnetic field either for propagation of transverse waves by using the magnetic field lines as if they were strings or for propagation of longitudinal waves by using the magnetic pressure instead of the gas pressure. Existence of such waves has great practical influence in the behavior of plasmas in a magnetic field, both in the laboratory and in space. The possibility of amplification of such waves has played a great role in the stability consideration of magnetically confined plasmas and for the study of collisionless shocks related to thermonuclear situations or to the mechanisms for the onset of the effect of solar storms on the earth's environment.

Simplified Analysis of Plasma Behavior Including Collisions and Space-Charge Effects

It has been shown so far that the electrons and ions have their displacement restricted in the presence of a magnetic field and electric field. But even without the magnetic field, restrictions on their motions exist. The most important ones are those due to collisions with each other and with neutral particles and the restriction of motion due to attractive electrostatic forces between positive and negative particles. As a result of these restrictions to their motions, the complicated particle motions in a plasma can be lumped for many practical purposes as those of a single fluid.

Since ordinary nonionized particles also have collisions but not electrostatic attraction effects, the latter will be treated in some detail. Their importance for the understanding of plasma behavior cannot be overemphasized. The electric fields built up by charge separation are given by Gauss's law or Poisson's equation as given in reference 15:

$$\text{div}\,\vec{D}=\epsilon_0\,\text{div}\,\vec{E}=e(n_i-n_e) \qquad (11)$$

Putting numbers into equation (11) indicates that differences of n_i-n_e of 10^9 particles/cm^3 in a plasma of 10^{14} particles/cm^3 will build up very large electric fields which couple the particle motion. In the first very good approximation, it may thus be assumed that $n_i \approx n_e$ and use of Poisson's equation may be avoided, whereas the electric fields produced in the plasma by charge separation are considered.

With the foregoing physical picture in mind, the equations of motion for the individual particles are considered. The more fundamental equations of kinetic theory like the Boltzmann, Focker-Planck, and Vlasov equations are avoided; also, the collision terms are expressed simply through a friction force which varies linearly with the collision frequency ν and with the difference between the particle velocities.

The balance of forces for electrons and ions are written as:

Electron force:

$$n_e m_e \frac{D\vec{v}_e}{dt}+\text{grad}\,p_e+n_e m_e \nu(\vec{v}_e-\vec{v}_i) = -n_e e(\vec{E}+\vec{v}_e\times\vec{B}) \qquad (12)$$

Ion force:

$$n_i m_i \frac{D\vec{v}_i}{dt} + \text{grad } p_i - n_i m_e \nu(\vec{v}_e - \vec{v}_i) = n_i e(\vec{E} + \vec{v}_i \times \vec{B}) \quad (13)$$

The friction force between ions and electrons and electrons and ions is obviously the same. This relationship is more evident, perhaps, when written in the full form $\left(\frac{\text{Friction force}}{\text{Volume}}\right)$

$$\nu n \frac{m_i m_e}{m_i + m_e}(\vec{v}_e - \vec{v}_i) \quad (14)$$

The reason for the appearance of m_e is that $m_e << m_i$ and thus in the center-of-mass system of the colliding particles, the heavier ions will be near to stationary with mainly the electrons being influenced by the friction.

The motion of the plasma may be expressed as a single fluid by defining the density ρ from the mass balance

$$\rho = n_e m_e + n_i m_i = \rho_e + \rho_i \quad (15)$$

and the velocity of the center of mass $\vec{v}$ from the momentum balance

$$(n_e m_e + n_i m_i)\vec{v} = n_e m_e \vec{v}_e + n_i m_i \vec{v}_i \quad (16)$$

Also, the current density $\vec{j}$ may be expressed as

$$\vec{j} = e(n_i \vec{v}_i - n_e \vec{v}_e) \quad (17)$$

with

$$\text{grad } p = \text{grad } (p_e + p_i) \quad (18)$$

Adding equations (12) and (13) and substitution from equations (15), (16), (17), and (18) gives the equation of motion

$$\rho \frac{D\vec{v}}{dt} = \vec{j} \times \vec{B} - \text{grad } p \quad (19)$$

Subtracting equations (12) and (13) with use of equations (15) to (18) and neglecting for the moment the differences in the time derivatives of the velocities results in, since $n_i = n_e$,

$$\frac{m_e \nu}{e}\vec{j} = ne(\vec{E} + \vec{v} \times \vec{B}) - \vec{j} \times \vec{B} + \text{grad } p_e \quad (20)$$

This force balance can be written in the form

$$\vec{j} = \sigma(\vec{E} + \vec{v} \times \vec{B}) + \frac{e}{m_e \nu}(\text{grad } p_e - \vec{j} \times \vec{B}) \quad (21)$$

where $\sigma = \frac{ne^2}{m\nu}$ is the electrical conductivity; equation (21) is often called the "generalized Ohm's law."

It must be emphasized that the electric field $\vec{E}$ is either externally applied or is built up inside the plasma due to space-charge separation. The measurement of the electric field inside a plasma can be a very important diagnostic tool in determining regions of magnetic interaction. In reference 15 the equations of motion of the neutral particles are included and the importance of space charge in plasma acceleration is emphasized. Before equation (21) is applied to practical cases, a few remarks about the neglected time derivatives of the velocity are appropriate. For simplicity, only the difference between the partial time derivatives is considered because this difference has more general significance. In order to bring out the main effect, collisions and other terms except the $\vec{E}$ term in the force balance of equations (12) and (13) are neglected; then,

$$ne\vec{E} = \frac{m_e}{e}\frac{\partial \vec{j}}{\partial t} \quad (22)$$

$$\frac{\partial \vec{j}}{\partial t} = \frac{ne^2}{m_e}\vec{E} \quad (23)$$

It is useful to remember that $\vec{j}$ is proportional to a velocity which, of course, is the time derivative of a displacement $\vec{s}$. Thus, the equation takes the general form (ref. 3)

$$m_e \frac{\partial^2 \vec{s}}{\partial t^2} = e\vec{E} \quad (24)$$

which is the equation for a free vibration with a restoring force $e\vec{E}$. The electric fields due to charge separation are in turn given by Poisson's equation. The polarization per unit volume due to charge separation can be obtained for an oscillating electric field in the form

$$n\vec{P} = ne\vec{s} = \frac{-ne^2}{m_e \omega_{osc}^2}\vec{E} \quad (25)$$

This leads to the natural frequency of oscillation (the so-called plasma frequency)

$$\omega_p=\left(\frac{ne^2}{m_e\epsilon_0}\right)^{1/2} \tag{26}$$

Note that in contrast to the Alfvén waves, where the oscillations of ions are predominant, in the electrostatic waves the oscillations of the lighter electrons are more important. For the propagation of electromagnetic waves through the plasma sheath discussed subsequently in paper number 61 of this volume, these electrostatic effects are essential in changing the dielectric effect of free space but are neglected here and with them the use of Poisson's equation. These waves are, of course, also very important for thermonuclear and solar phenomena and stability considerations of plasma confinement. They also play a part in possible plasma wave amplifiers.

Now, it would be very convenient to express what has been neglected in terms of length. Such a length is easily formed by dividing the mean thermal velocity by ω_p

$$\frac{\bar{c}}{\omega_p}\approx\left(\frac{kT}{m_e}\right)^{1/2}\left(\frac{m_e\epsilon_0}{ne^2}\right)^{1/2}\approx\left(\frac{kT\epsilon_0}{ne^2}\right)^{1/2}\approx d \tag{27}$$

The Debye length d has many interpretations, such as the distance where the thermal energy equals the electrostatic energy stored due to charge separation. Of course, it is also interpreted as a sheath or a region near a plasma boundary where large deviations from charge equality occur. It must be emphasized that this distance, while very useful, is not a magic length, but it has stood the test of time.

Since, in the plasma, charge equality is approximately preserved, equations (15) to (21) describing the behavior of a plasma apply to dimensions of ionized gases in excess of the Debye length. In addition, the definition of plasma requires that the dimensions characteristic of processes in the plasma (like the mean-free path and the gyration radii of electrons and ions) are larger than the Debye length

$$\lambda>d$$

and

$$r_{L,e}\text{ and }r_{L,i}>d$$

For a collisionless plasma in the presence of a magnetic field, in addition, the mean-free path must be larger than both ion and electron gyration radii

$$\lambda>r_{L,i}>r_{L,e} \tag{28}$$

It is frequently convenient to express this inequality in terms of cyclotron frequencies and the reciprocal of the collision frequency ν, that is, in terms of the collision time τ. The collision time τ is given usually by the ratio of the mean-free path and the mean thermal velocity $\bar{c}$. Thus, the product $\omega\tau$ becomes, by using equation (3) for ω and the Larmor radius,

$$\omega\tau\approx\frac{eB}{m}\frac{\lambda}{\bar{c}}=\frac{\lambda}{r} \tag{29}$$

As a result, the previously given inequality approximately corresponds to

$$(\omega\tau)_e>(\omega\tau)_i>1$$

Acceleration of a Fully Ionized, Collisionless Plasma Produced by a Magnetic Piston

The rest of the paper is chiefly concerned with examples using plasmas in steady electric and magnetic fields. But first an example is given that is important for unsteady acceleration. The simplest case appears to be that of a moving magnetic field pushing a highly ionized collisionless plasma like a magnetic piston. Under such conditions the $\vec{j}\times\vec{B}$ force per unit volume will be balanced by a pressure gradient, grad p, which establishes itself at the boundary of the plasma. This concept is a highly simplified version of a traveling-wave accelerator. The unsteady problem has thus been changed into a steady equilibrium case in the reference system of the moving magnetic field (fig. 59–2).

The equilibrium equation as given in basic texts such as references 1 to 11

$$\vec{j}\times\vec{B}=\text{grad }p \tag{30}$$

can be solved for the azimuthal current $\vec{j}_\theta$, which consists principally of electrons

$$\vec{j}_\theta=\frac{\vec{B}\times\text{grad }p}{B^2} \tag{31}$$

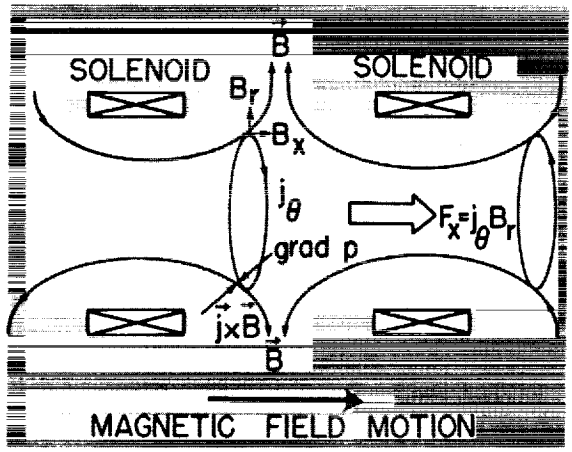

FIGURE 59–2.—Acceleration with moving magnetic piston.

For the collisionless case, using the condition that the velocity of the plasma relative to the magnetic field is zero, the force balance version of the "generalized Ohm's law" in equation (20) becomes

$$ne\vec{E}-\vec{j}\times\vec{B}+\text{grad } p_e=0$$

Using the previous equilibrium equation (30), since

$$p_i+p_e=p$$

Then

$$ne\vec{E}=-\text{grad } p_i \qquad (32)$$

Thus, the ions are kept in the magnetic field by space-charge electric fields due to electron attraction. It should be noted that in a stationary reference system, fixed to the apparatus, the electrons will pull the ions as the magnetic piston moves by. Let us contrast this case with constant magnetic field $\vec{B}$ and pressure gradient grad p with the previously discussed case of constant $\vec{B}$ and electric field $\vec{E}$. In the latter case the electric field drives electrons and ions in opposite directions and thereby establishes a current. In the presence of the magnetic field, both particles move, however, in the normal direction to both fields, so that the current in the steady state approaches zero.

In the presence of a pressure gradient the particles, however, attempt to move in the same direction. The magnetic field forces them to move normal to it and to the pressure gradient in azimuthal directions opposed to each other. Thereby a steady current can be established. Of course, the more precise counterpart to the electric-field case is the situation where a moving plasma stream is trying to cross a magnetic field, and the charged particles are forced to move in opposite azimuthal directions forming an induction current. When the effect of collision is small and magnetic-field strength is assumed constant, the rate of input of kinetic energy would equal the rate of work done by the $\vec{j}\times\vec{B}$ force in stopping the plasma. In this case where a pressure gradient balances $\vec{j}\times\vec{B}$, the forces are already balanced. A discussion of finer points in this problem are included in reference 6, section 3.

Since the term "magnetic pressure" is frequently used in connection with plasma confinement, this term is discussed next. In order to define magnetic pressure the Maxwell equation (or Ampere's law)

$$\vec{j}=\text{curl } \vec{H} \qquad (33)$$

has to be introduced. This equation expresses the magnetic field due to a given current. Inserting equation (33) into equation (30) yields, for magnetic lines of zero curvature, with $\vec{B}=\mu\vec{H}$

$$\text{grad } p+\frac{1}{2\mu}\text{grad } B^2=0$$

or

$$p+\frac{B^2}{2\mu}=\left(p+\frac{B^2}{2\mu}\right)_{ext} \qquad (34)$$

When the plasma is truly confined by the external magnetic field the external pressure must be zero, and

$$p+\frac{B^2}{2\mu}=\left(\frac{B^2}{2\mu}\right)_{ext} \qquad (35)$$

Steady Plasma Acceleration With Currents Across Electrodes

For the sample cases of plasma acceleration with currents across electrodes the electron pressure gradients may be neglected and attention is given to the currents which are predominantly due to electron motion. The generalized Ohm's law may then be written in the form (see refs. 15 and 16 and eq. (21)):

$$\vec{j}=\frac{ne^2}{m_e\nu_e}(\vec{E}+\vec{v}\times\vec{B})-\frac{e}{m_e\nu_e}(\vec{j}\times\vec{B})$$

To put the equation into a more convenient form, an expression for the collision frequency must be given. In the present approximation it equals the ratio of the mean thermal velocity $\bar{c}$ to the mean-free paths $\nu=\bar{c}/\lambda$ or the often used collision time $\tau=\lambda/\bar{c}$.

The generalized Ohm's law can be written in the form

$$\vec{j}=\sigma\left[E^*-\frac{\omega_e\tau_e}{\sigma B}(\vec{j}\times\vec{B})\right] \qquad (36)$$

where $\omega_e=\frac{eB}{m_e}$ is the cyclotron frequency of the electrons in the magnetic field, and

$$\vec{E}^*=\vec{E}+\vec{v}\times\vec{B}$$

Solving this equation explicitly for $\vec{j}$ gives

$$\vec{j}=\frac{\sigma}{1+(\omega\tau)_e^2}\left[\vec{E}^*-\frac{(\omega\tau)_e}{B}(\vec{E}^*\times\vec{B})+\frac{(\omega\tau)_e^2}{B^2}(\vec{E}^*\cdot\vec{B})\vec{B}\right]$$

For $\vec{E}^*$ perpendicular to $\vec{B}$ the last term drops out and the expression becomes

$$\vec{j}=\frac{\sigma}{1+(\omega\tau)_e^2}\left[\vec{E}^*-\frac{(\omega\tau)_e}{B}(\vec{E}^*\times\vec{B})\right] \qquad (37)$$

In Cartesian coordinates, with z in the direction of the externally imposed magnetic field the x- and y-components become

$$j_x=\frac{\sigma}{1+(\omega\tau)_e^2}[E_x^*-(\omega\tau)_eE_y^*] \qquad (38)$$

and

$$j_y=\frac{\sigma}{1+(\omega\tau)_e^2}[E_y^*+(\omega\tau)_eE_x^*] \qquad (39)$$

It is a well established fact that two major possibilities exist:

(a) The first possibility is illustrated on the left side of figure 59–3. The current is permitted to flow between theoretically infinite electrodes; then no space charge will build up inside the plasma as the charges are free to flow. As a result, $E_x^*=0$ and

$$\left.\begin{aligned} j_x&=-\frac{\sigma(\omega\tau)_eE_y^*}{1+(\omega\tau)_e^2}\\ j_y&=\frac{\sigma E_y^*}{1+(\omega\tau)_e^2}\end{aligned}\right\}\quad\left|\frac{j_x}{j_y}\right|=(\omega\tau)_e \qquad (40)$$

The x-component of the current is the so-called Hall current. Note that neither the x- nor y-components of the current actually constitute a particle trajectory.

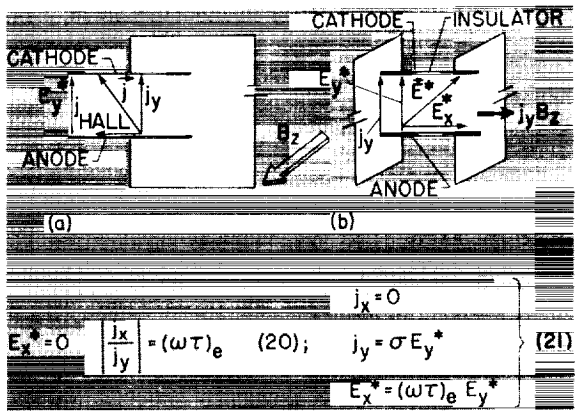

(a) Long electrodes.
(b) Short and segmented electrodes.

FIGURE 59–3.—Plasma acceleration with currents across electrodes.

(b) The second possibility is shown on the right side of figure 59–3. The current is not permitted to flow in the x-direction, that is $j_x=0$, by making short electrodes or by segmenting them and connecting with separate power supplies. The $\vec{j}\times\vec{B}$ force is now in the x-direction.

$$j_y=\sigma E_y^*$$

and

$$E_x^*=(\omega\tau)_eE_y^* \qquad (41)$$

Thus, an electric field due to space-charge separation builds up in the flow direction. Its function is to slow down the electrons which want to move ahead and speed up the ions by mutual space-charge effects so that both move at the same velocity in the axial direction. Details about this approach of plasma acceleration with researchers and companies connected with its development is discussed by M. C. Ellis in paper number 62 of this volume.

Influence of Collisions in Fully and Partially Ionized Plasmas

If figure 59–1 is compared with figure 59–3(a), it is seen that under the influence of collisions a steady current is established at the angle whose tangent is equal to $(\omega\tau)_e$. The electrons have, through collisions, established a steady motion across the magnetic field. What has happened to the ions?

The effects of the friction force on the ions have been actually neglected in the equations (12) and (13) for fully ionized plasmas. The reason is that although the ions and electrons experience the same friction force, the effect of friction on the light electrons will be much larger than the effect on the much heavier ions. In other words, since the ions are so much heavier, the center of mass moves approximately with the ion velocity and thus the effect of friction on the ion motion is negligible. The light electrons, on the other hand, can be influenced to such an extent that the friction force can balance the accelerating force in the electric field, so that a steady electron current is produced. The small magnitude of the influence of the electrons on the ion motion is also evidenced by the ratio

$$\frac{\omega_i\tau_{i,e}}{\omega_e\tau_{e,i}}=\frac{eB}{m_i}\cdot\frac{m_e}{eB}=\frac{m_e}{m_i}$$

Since the collision time between ions and electrons $\tau_{i,e}$ must equal the collision time between electrons and ions $\tau_{e,i}$, the ratio equals that of the cyclotron frequencies, which in turn is equal to the inverse ratio of the masses. In the presence of neutral atoms, the friction forces and collision times between electrons and ions are no longer balanced and different results are obtained.

As a result of this small influence of friction on the motion of the ions in a fully ionized plasma, the ions will follow their tendency toward drift motion normal to electric and magnetic fields more or less in the same fashion as in the collisionless case in figure 59–1. However, in view of the fact that the ion Larmor radius is very much larger than that of the electrons, it can be assumed that when the ion Larmor radius is also much larger than the distance between the electrodes, the ions move essentially straight across the electrodes. Under such conditions the steady electric field can put energy into the electrons, which accelerate the ions by collisions and space-charge effects. (See figs. 59–3(a) and 59–3(b).)

Now, a few brief remarks will be made on the effects of collisions on partially ionized plasma acceleration. Since neutral atoms have about the same mass as the ions, the motion of the ions can now be strongly influenced in contrast to that of the fully ionized case. The accelerating force and the friction force can balance to give a steady ion velocity. While an additional equation has to be included (refs. 8, 15, and 17) to take account of the collisions of ions and neutrals, there are no more fundamental fine points involved than those already introduced in the fully ionized case Briefly, the influence of "ion slip" with respect to the neutrals adds to the generalized Ohm's law in equation (21) a term, for $m_i=m_n$,

$$\frac{2\tau_{i,n}}{m_i n_e}\left(\vec{j}\times\vec{B}\right)\times\vec{B}$$

The loss due to this term is obtained from the scalar product with $\vec{j}$. For $\vec{j}$ perpendicular to $\vec{B}$, this term becomes (ref. 15, eq. (A–4)) and also ref. 8, eq. (6–28)):

Ion-slip loss	Joule loss	
$\frac{2\tau_{i,n}}{m_i n_e} j^2B^2$	$\frac{j^2}{\sigma}$	(42)

In contrast to the well-known Joule loss j^2/σ, the ion-slip loss is thus proportional to the square of the accelerating force per unit volume $\vec{j}\times\vec{B}$. The ratio of Joule loss to ion-slip loss is

$$2\omega_e\tau_{e,i}\omega_i\tau_{i,n} \qquad (43)$$

In view of the undesirability of these extra losses for plasma acceleration, conditions are usually tailored so as to keep them small. This can be done in a partially ionized plasma by going to relatively high densities where $\tau_{i,n}$ becomes small, or by using a fully ionized gas where $\tau_{i,n}$ goes to zero because of a scarcity of neutrals. Fully ionized plasmas are, of course, more easily produced at low densities.

The so-called *EM* (electromagnetic) region (refs. 18 and 19) is frequently mentioned in con-

nection with plasma acceleration. This region applies to fully ionized plasmas and is defined as that region where the ion Larmor radius is larger than the dimensions of the apparatus. The mean-free path is also assumed to be larger than the apparatus dimensions so that even the electrons cannot be influenced by collisions. The ions can only be accelerated by space-charge effects. The name *EM* thus refers to the case where only electric and magnetic effects act in the plasma acceleration. Evidently, it is impossible to have a steady acceleration under precisely these conditions, since as previously pointed out, no energy can be supplied to the plasma for the collisionless steady acceleration. However, from a practical viewpoint, a few collisions will alleviate this condition.

The *EM* concept can, however, be applied precisely to a time-dependent plasma acceleration and, as will be shown subsequently, to the acceleration in the direction of the electric field of ions in a plasma in steady electric and magnetic fields.

Acceleration Using Hall Currents

Two cases are shown in figure 59–4. Since in case (a) the current has a horizontal component the $\vec{j}\times\vec{B}$ force will be partly against the wall, and this effect increases with increasing that current component. The question thus arises whether one could not use the undesirable Hall current component as the driving current for the $\vec{j}\times\vec{B}$ force per unit volume. Two ways of accomplishing this result exist and are discussed in paper number 62 of this volume by Ellis. A discussion of a few fundamental questions in such arrangements is of interest. In both cases the arrangement of electric and magnetic fields will be such as to have the Hall current component in the azimuthal direction with a radial magnetic field component to give the $\vec{j}\times\vec{B}$ force per unit volume.

Briefly, in the first arrangement (fig. 59–4(a)) the Hall current j_θ is produced by interaction of a radial electric field E_r and an axial magnetic field component B_x; it subsequently interacts with the radial magnetic field component B_r to give the $\vec{j}\times\vec{B}$ force. This mechanism of Hall current acceleration was first discussed by the writer in reference 20. Most of the further experimental and theoretical developments have been made in some ingenious experiments and analyses at AVCO by R. Patrick and W. Powers (refs. 21 and 22) and by personnel of the NASA Langley Research Center (refs. 15 and 23). It should be emphasized that figure 59–4(a) represents only one possible version of this Hall accelerator. Others are discussed in paper number 62 of this volume. An analysis of the Hall accelerator in figure 59–4(a) with emphasis on the physics of the mechanism is given in reference 24.

In the acceleration method in figure 59–4(b) the azimuthal Hall currents j_θ are produced by interaction of the axial electric field E_x and the radial electric field B_r. This magnetic field B_r together with j_θ provides the driving force per unit volume. The acceleration is analyzed in some detail in the next section, as also are details about the magnetic-field distribution in figure 59–4(b).

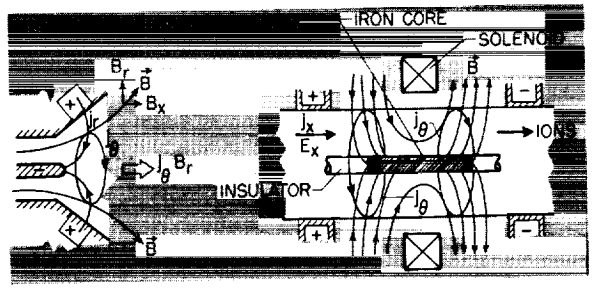

(a) Plasma Hall accelerator.
(b) Ion Hall accelerator.

FIGURE 59–4.—Acceleration of plasma and ions in plasma with Hall currents.

Several questions arise the answers to which are extremely useful in clearing up the differences in the actions of electric and magnetic fields. First, how can the Hall current which is actually a blind current component provide a $\vec{j}\times\vec{B}$ force? The answer is that the current component is called blind only because it is normal to the axial electric field through which energy is put into the electron current in the direction of the electric field. However, through the magnetic field an electron current component in the azimuthal direction is produced. This component can interact with the radial magnetic field to provide

a $\vec{j}\times\vec{B}$ force per unit volume for acceleration. The azimuthal component of the electron current will, of course, also provide added Joule losses. This effect is evident by performing a scalar vector multiplication with $\vec{j}$ for the generalized Ohm's law (eq. (21)); then, with $\vec{E}^*=\vec{E}+\vec{v}\times\vec{B}$,

$$\vec{j}\cdot\vec{E}-(\vec{j}\times\vec{B})\cdot\vec{v}=\frac{j^2}{\sigma}+\frac{(\omega\tau)_e}{\sigma B}(\vec{j}\times\vec{B})\cdot\vec{j} \quad (44)$$

where the last term is zero. However, it is the total current density which provides Joule losses. Detailed studies in reference 24 indicate, however, that the efficiency of Hall accelerators based on these simple effects should be as high as that of the basic crossed-field accelerator. If it is assumed in reference 24 for the accelerator in figure 4(a) that current density and magnetic field are the same as j_θ and B_r in the Hall current accelerator, then the Hall current which provides the driving force is higher than the current between the electrodes. The Hall current accelerators offer further possibilities of reduction in losses by plasma containment away from walls by magnetic fields as in a magnetic nozzle. This effect is rather large in the configuration of reference 22 (similar to that of fig. 4(a)), where bulging current paths maintain a plasma in a supersonic magnetic nozzle. The final design will probably be a combination of Hall acceleration and magnetic-nozzle effects. The low efficiencies calculated in reference 25 are based on the choice of a configuration of electrodes and magnetic fields where in the limit of large $(\omega\tau)_e$ the current across the electrodes cannot cross the magnetic field lines. Thus dissipation rather than acceleration is mostly obtained. With proper choice of configuration (ref. 24), this problem can be avoided with resulting higher efficiencies.

Theory for Acceleration of Ions in a Plasma With Hall Currents

In the conventional ion accelerator, the ions are accelerated in the absence of electrons and as a result, according to Childs law, the ion current is limited by space-charge effects. A discussion of such acceleration is given in paper number 48(c) "Electrostatic Thrustors" by Warren D. Rayle. One way to overcome the space-charge limitations for conventional electrostatic ion accelerators is to accelerate the ions inside of a plasma in the presence of electrons. Naturally, as in the conventional ion accelerator, the ions emerging from the accelerator must be neutralized by electrons.

The concept of ion acceleration in plasmas was first described in the work of a A. Bratenahl, S. Janes, and A. Kantrowitz from AVCO (ref. 26) as a means for boosting the acceleration in a traveling wave accelerator through superposition of an axial electric field. No direct mention was made of the action of azimuthal Hall currents. The classification of this system of ion acceleration under Hall current accelerators has emerged only gradually. A. Sutton in a review of plasma accelerators (ref. 25) discussed a Hall current accelerator with longitudinal electric field and compared its efficiency with that of a conventional crossed-field accelerator. The physical aspects of this system as an ion accelerator and of the motion of the electrons, however, were not brought out. Detailed descriptions of the acceleration as a steady Hall current ion accelerator with axial electric field and radial magnetic field were given at a meeting on magnetoplasmadynamics held at the Langley Research Center in April 1962, where discussions of Hall current ion accelerators were given by G. R. Seikel and E. Reshotko from the NASA Lewis Research Center, by G. L. Cann from Electro-Optics, Inc. and by R. V. Hess, J. R. Sevier, and R. N. Rigby from the Langley Research Center. At a later date, results of their investigations appeared as references 27 to 29. F. Salz, R. G. Meyerand, and E. C. Lary from United Aircraft have performed fundamental experiments coupled with analysis on such a system (refs. 30 and 31). So have Janes, Dotson, and Wilson from AVCO (ref. 19). J. S. Luce and J. W. Flowers from Oak Ridge National Laboratory have discussed use of an energetic arc confined in an axial magnetic field for ion acceleration in a plasma (ref. 32). Some communications from J. S. Luce, now with Aerojet General, Nucleonics, point to certain common features with ion Hall accelerators.

The following analysis of the Hall current ion accelerator is of a similar form as that given by the writer and J. Sevier at the meeting on magnetoplasmadynamics held at the Langley Research Center, with added remarks concerning the physical mechanism. Assuming the use of a fully ionized gas and steady state acceleration, that is $\vec{E}$ and $\vec{B}$ constant, the "generalized Ohm's law" explicitly expressed in terms of the current density $\vec{j}$ (eq. (37)) is

$$\vec{j}=\frac{\sigma}{1+(\omega\tau)_e^2}\left[\vec{E}^*-\frac{(\omega\tau)_e}{B}(\vec{E}^*\times\vec{B})\right] \quad (45)$$

Expressing $\vec{j}$ in coordinate form yields

$$j_\theta=\frac{\sigma}{1+(\omega\tau)_e^2}[v_xB_r-(\omega\tau)_e(E_x-v_\theta B_r)] \quad (46)$$

and

$$j_z=\frac{\sigma}{1+(\omega\tau)_e^2}[(E_x-v_\theta B_r)+(\omega\tau)_e v_x B_r] \quad (47)$$

The $\vec{j}\times\vec{B}$ force per unit volume is

$$j_\theta B_r=\frac{\sigma B_r}{1+(\omega\tau)_e^2}[v_xB_r-(\omega\tau)_e(E_x-v_\theta B_r)] \quad (48)$$

It is indicated that in addition to the axial motion v_x, the possibility of a rotational motion v_θ exists. For the present purpose this rotational motion is ignored by assuming that the Larmor radius of the ions is much larger than the length of acceleration. If this were not the case, other methods would have to be tried to prevent the ions from going into azimuthal drift motion normal to E_x and B_r, since the azimuthal Hall current would tend to be sacrificed. The direction of rotation can be reversed by making the ions travel through reversing magnetic fields as indicated, for example, in figure 59–4(b). The $j_\theta B_r$ force per unit volume is in the same direction for reversed B_r, since j_θ is also reversed. Use of one to several magnetic field reversals through arrangement of several solenoids to form a series of magnetic cusps is discussed in references 19 and 27 to 29. The nature of acceleration for large values of $(\omega\tau)_e$ is of interest. Then, assuming $v_\theta\to 0$,

$$j_\theta\to\sigma\left[\frac{v_xB_r}{(\omega\tau)_e^2}-\frac{E_x}{(\omega\tau)_e}\right] \quad (49)$$

and

$$j_x\to\sigma\left[\frac{E_x}{(\omega\tau)_e^2}+\frac{v_xB_r}{(\omega\tau)_e}\right] \quad (50)$$

Using the expression

$$\sigma=\frac{ne^2}{me}\tau_e$$

there results

$$j_\theta\to -ne\frac{E_x}{B_r} \quad (51)$$

and

$$j_x=ne(v_{i,x}-v_{e,x})=nev_x \quad (52)$$

Now v_x is the velocity of the center of mass, which for a fully ionized plasma is, as can be seen from equation (16), essentially the velocity of the ions. The current j_x is proportional to the difference in the velocities of ions and electrons; thus,

$$j_x=ne(v_{i,x}-v_{e,x})\to nev_{i,x}, \text{ thus } v_{e,x}\to 0 \quad (53)$$

Also, since the ion velocity in the azimuthal direction is assumed to be zero,

$$j_\theta=ne(v_{i,\theta}-v_{e,\theta})\to -nev_{e,\theta} \quad (54)$$

For the sake of completeness the equation of motion, which for the fully ionized plasma is about the same as that for the ions, is given:

$$nm_i\frac{Dv_{i,x}}{dt}=(\vec{j}\times\vec{B})_x=-j_\theta B_r=neE_x \quad (55)$$

Let us summarize the results. The equations of motion for the fully ionized plasma as a whole and of the individual particles yield in the collisionless limit of large $(\omega\tau)_e$ and correspondingly large $(\omega\tau)_i$ values the following results. The velocity of the electrons v_e in the axial direction approaches zero (eq. (53)) and the full drift velocity is attained in the azimuthal direction (eqs. (51) and (54)). The magnetic field exerts a force per unit volume $-j_\theta B_r$ (eq. (55)), which nearly stops the electron motion; thus in the center of mass system which moves with the ions this force points in the positive direction. The axial current is a pure ion current (eq. (53)). The acceleration of the ions is in the direction of the axial electric field (eq. (55)).

The magnetic field by nearly stopping the axial electron motion has performed the func-

tion of unbalancing the equal and opposite forces on the electrons and ions exerted by the axial electric field. The electric field, which usually puts only energy into the plasma, can now put momentum in the plasma through the ions.

The very fundamental question arises as to what is the true function of the magnetic field and the $j_\theta B_r$ force per unit volume in providing a thrust on the apparatus. Since a thrust constitutes an integrated effect of the forces acting in the system, it does not matter where the electrons are stopped in the apparatus, as long as they are being stopped so that the directed energy of the ions can be used for thrust. To bring out certain fundamentals, assume for the moment that the plasma is fully ionized and collisionless. If no magnetic field were applied, a thrust would be obtained by having the axial motion of the electrons stopped by the anode, while the ions escape through the cathode. Without a magnetic field the electrons can gain very high velocities in the electric field and would cause considerable energy loss and thus a reduction in efficiency. The possibility, of course, exists of using the anode as the ion source so that the actual waste of energy is greatly reduced, since the ions have to be produced somewhere.

The avoiding of a possible energy loss is, however, only one reason for the use of the magnetic field. Another lies in the fact that without the magnetic field it is difficult to build up a potential inside of the plasma, which is necessary to accelerate the ions. The reason is that since charge continuity must be preserved, for electrons and ions,

$$n_e e v_e = C_1$$

and

$$n_i e v_i = C_2$$

their respective charge densities will be high when their velocities are low and low when their velocities are high. As a result large differences in charge densities will exist near the electrodes. Thus the Debye distance d (eq. (27)) is small, and the plasma beyond a reasonable multiple of this distance will be shielded from the voltage drop across the electrodes. In other words, the voltage drop will be restricted to thin sheaths near the electrodes and the ion acceleration, as well as the electron acceleration, occurs inside the sheaths. As a result, the ions could lose some axial thrust at the cathode.

The function of the magnetic field is to distribute the voltage drop over the whole plasma. This is accomplished by slowing down the electrons so that, according to the laws of charge continuity, the charge density of the electrons can build up. Thus, in a manner of speaking, a sheath is distributed along the axial direction of the accelerator furnishing a distributed potential drop for accelerating the ions. This distributed potential drop is not in conflict with the definition of a plasma, where $n_e \approx n_i$. The reason is that, as pointed out in the discussion of Gauss's law (eq. (11)), only a very small percentage of charge unbalance, as compared with the total charge concentration, is necessary to produce large electric fields inside of the plasma.

Words of caution are necessary in relating the stopping of the electrons in the axial direction by the magnetic field to the establishment of a charge distribution, which in turn yields the electric fields for ion acceleration inside of the plasma. If one were to state merely that the charges are stopped without stating how they are stopped, the law of charge continuity would offer no answer to the nature of the charge distribution. A determination of the magnetic field configuration to yield the optimum charge distribution for ion acceleration would require simultaneous solution of the equations of motion of the ions, Gauss's law, and the law of charge continuity.

The question has also been asked whether the Hall ion accelerator is a $j \times \vec{B}$ accelerator or an electrostatic accelerator. For the collisionless case where $\vec{j} \times \vec{B}$ and $n_e \vec{E}$ are equal, this becomes a question of semantics. Of course, it must be kept in mind that without magnetic field, the electric field $\vec{E}$ would not be properly distributed in the plasma.

Where collision losses, especially those due to ionizing collisions, are included, the electrostatic effect will no longer be a direct measure of ion acceleration, since the electric field or the voltage drop across the electrodes must also overcome these losses. The $j_\theta B_r$ force per unit

volume will be a true indicator of the accelerating force on the system. The losses are discussed subsequently in the section "Voltage-Current Characteristics of Hall Ion Accelerator."

PLASMA PHYSICS OF ELECTRICAL DISCHARGES IN MAGNETIC FIELDS

Thus far, the kinematics and dynamics of plasmas in electric and magnetic fields have been treated. In the sections that follow emphasis will be given to the effect of a magnetic field on the electrical conductivity, ionization, and complete discharge characteristics.

General Effect of Magnetic Field on Electrical Conductivity

If the Hall current is permitted to flow (fig. 3(a)), the current between electrodes is given by equation (40)

$$j_y=\frac{\sigma E^*_y}{1+(\omega\tau)_e^2}$$

The conductivity is thus effectively reduced by the factor shown in equation (40). Take the case of large magnetic fields where $(\omega\tau)_e>>1$ and use σ in the form

$$\sigma=\frac{n_e e^2}{m\nu}$$

without a magnetic field, where $\nu=1/\tau$. With $\omega=eB/m_e$, then with a magnetic field,

$$\sigma_{B\perp}=\frac{m_e n_e \nu}{B^2} \tag{56}$$

The current density in a strong magnetic field is

$$j_y=\frac{n_e m_e}{B^2}\nu E^*_y$$

Thus the dielectric storage effect is again found in a strong magnetic field (eq. (7)), this time for the electrons and modified by collisions.

It is evident that in the presence of a strong magnetic field an increase in collision frequency ν will help the electrical conduction by reducing the dielectric storage effects, whereas without the magnetic field an increase in ν lowers the conduction. In other words without collisions the electrons would be forced to go into drift motion normal to the electric and magnetic fields and collisions help them to move in the direction of the electric field.

Electrical Conductivities in Partially and Fully Ionized Plasmas Without Magnetic Fields

The collision frequency in the electrical conductivity σ can be expressed in the form

$$\nu=\frac{\bar{c}}{\lambda}=\bar{c}(n_n Q_{e,n}+n_e Q_{e,i}) \tag{57}$$

where $\bar{c}$ is the mean thermal velocity, λ the mean free path as defined in reference 10, page 105, n_n and n_e are the concentrations of neutrons and electrons, $Q_{e,n}$ the collision cross section of electrons with neutral atoms, and $Q_{e,i}$ the collision cross section of electrons and ions. The value of $Q_{e,n}$ is very difficult to determine theoretically as it depends on the detailed electric structure of the atom. Since the positive and negative charges are balanced in an atom, the electron will have to approach very closely to feel the presence of the atom. Analysis of the interaction requires a quantum mechanics approach which may become very complicated; thus one often relies on experiments. The electrons and ions act as single poles and, as such, they can also make fairly close collisions, but the long-range effect of large-angle scattering effects due to many small-angle scattering effects can become very important in a plasma where many particles are present.

The elementary electrostatic laws inherent to the short-range as well as long-range electrostatic interactions are next briefly discussed. For the detailed picture, see, for example, reference 7 (page 249), and reference 1; for a simplified version, see reference 2. The force between two charges is inversely proportional to the square of the distance and the mutual potential is inversely proportional to the distance. At the point of closest approach of the charges their distance is of the order of the effective radius of the charge influence. The collision cross section is of course proportional to the square of this radius. As a result the collision cross section is inversely proportional to the square of the potential energy. Expressing the interaction in terms of thermal energy instead

of potential energy yields the result that the so-called "Coulomb" collision cross section

$$Q_c \propto \frac{1}{T^2} \tag{58}$$

is inversely proportional to the square of the temperature. Since the mean thermal velocity $\bar{c}$ is proportional to $T^{1/2}$ (eq. (27)), the collision frequency for a given ionized particle density n_e is

$$\nu_c \propto \frac{n_e}{T^{3/2}} \tag{59}$$

For a partially ionized plasma, when the collisions of electrons and neutrals predominate, for a given n_n and $Q_{c,n}$,

$$\nu_n \propto n_n T^{1/2} \tag{60}$$

The constancy of $Q_{c,n}$ is thereby a carry-over from the elastic-sphere approach of kinetic theory. Actually, $Q_{c,n}$ may decrease or increase with temperature, in a temperature range before coulomb collisions become important (related for example to the Ramsauer effect, ref. 33, which requires a quantum-mechanics explanation). For the present purpose $Q_{c,n}$ is assumed to be independent of temperature; this condition would also hold for the billiard ball approach of classical kinetic theory.

It must be strongly emphasized that use of the collision cross section $Q_{c,i}$ for fully ionized plasmas does not necessarily imply that the plasma has to be fully ionized. This is especially true if a plasma tends to become ionized at comparatively low temperatures and thus the collision cross section between electrons and ions begins to dominate when the percentage of ionization is very small.

The conductivity σ for Coulomb collisions is

$$\sigma_c = \frac{n_e e^2}{m\nu} \propto T^{2/3} \tag{61}$$

whereas, for collisions of electrons with neutral atoms,

$$\sigma_n \propto \frac{n_e}{n_n} T^{-1/2} \tag{62}$$

For the Coulomb conductivity the concentration of charged particles thus has cancelled out, except for a weak dependence in a logarithmic term related to the long range interaction effects, this term is not included here, but can be found in the basic texts (ref. 1 to 11).

The fact that the Coulomb conductivity depends only weakly on the particle density is not surprising if classical kinetic theory for a gas consisting only of one species of atoms is considered. There, the transport coefficients such as viscosity or thermal conductivity are independent of density but solely dependent on temperature. It can be considered that for charged particles or Coulomb interactions the particles act alike in spite of their different masses because the interaction effects are based on the like charges of the particles.

Electrical Conductivity of Fully and Partially Ionized Plasmas in Magnetic Fields

As shown in equation (56), the conductivity of a plasma across a magnetic field B is given by

$$\sigma_{B\perp} = \frac{m_e n_e \nu}{B^2}$$

For a fully ionized plasma, if ν_c is taken from equation (59)

$$(\sigma_{B\perp})_c \propto \frac{n_e^2}{T^{3/2}} \frac{1}{B^2} \tag{63}$$

whereas for a partially ionized plasma with ν_n taken from equation (60)

$$(\sigma_{B\perp})_n \propto \frac{n_e n_n}{B^2} T^{1/2} \tag{64}$$

assuming that the collision cross section $Q_{c,n}$ remains constant with varying T. Note that the coulomb conductivity across the magnetic field, $(\sigma_{B\perp})_c$, depends now also on the charged particle density. The magnetic field by acting differently on electrons and ions, has reduced the effect of equality of particles with like charges, on which was based the strong dependence of σ_c on temperature.

Effect of Finite Extensions of Electrodes on Electric Conductivity in Magnetic Fields

In AVCO's work (ref. 34) the interesting result was shown that if the magnetic field

lines are made to extend beyond the electrode region, the currents will not flow straight across the magnetic field but will bulge in the direction of the magnetic field lines. The bulging of the current is related to the fact that the electrons like to move (in a corkscrew motion) along the magnetic lines when there are comparatively few corresponding collisions, that is $(\omega\tau)_e$ is considerably larger than 1. The ratio of the azimuthal Hall current density to the radial current density is as in the case of infinite electrodes (eq. 40))

$$\frac{j_\theta}{j_r}=(\omega\tau)_e$$

For the limiting case of very short electrodes, the radial current density is credited to F. J. Fishman in the appendix of reference 34.

$$j_r=\frac{\sigma E_r}{\sqrt{1+(\omega\tau)_e^2}} \tag{65}$$

for infinite electrodes. For very strong magnetic fields this implies

$$j_r\rightarrow\frac{\sigma E_r}{\omega\tau}=\frac{ne}{B}E_r \tag{66}$$

The electrical conductivity normal to the magnetic field thus becomes independent of collisions in this limit and is the same for fully and partially ionized plasmas (using the superscript f for finite electrodes).

$$(\sigma_{B\perp})^f=\frac{ne}{B} \tag{67}$$

Then, $j_r=\frac{nm_e\omega E_r}{B^2}$, where the dielectric effect in a strong magnetic field again makes its appearance.

One should be reminded that also for diffusion in magnetic fields important effects are introduced by finite dimensions of the apparatus, related to the tendency of electrons to move along magnetic lines for high values of $(\omega\tau)_e$. This so-called Simon diffusion (for example, refs. 9 and 22) has, however, different reasons from those discussed here.

Conductivity and Voltage Current Characteristics of Electrical Discharges in Magnetic Field

The development of the expressions for electrical conductivity show that aside from its direct dependence on the magnetic field it depends also on the electron concentration n_e (or on the ratio of n_e/n_n, where n_n is the concentration of neutral atoms) and the temperature. The form of the dependence, however, depends on the magnetic field.

No mention has been made of the possible variation of these parameters under variation of electric field. Such a constancy of the parameters can be enforced, for practical cases, by introducing, into the crossed electric and magnetic fields, a plasma of a given ionization whereby the function of the discharge is just to keep the parameters constant. Furthermore, it could be assumed that the cathode is thermionically emitting so that only slightly higher electric fields are required to produce the electrons necessary for ionization.

From a practical viewpoint it is not only of interest that these parameters are constant but how much energy need be supplied by the electric field to keep them constant. Also, it is important to know how each parameter varies with an increased energy input; for example, it is of great practical importance how the electron concentration n_e may be increased without excessive increase in the temperature T.

Much useful information about the behavior of a discharge can be gained from its voltage-current characteristics. Since no attempt will be made to develop a general theory on this involved matter, examples from some recent research developments at NASA and elsewhere will be given.

Voltage Plateaus for Widely Differing Discharges in Magnetic Fields

Experiments have shown that a large number of arc discharges without magnetic fields have negative voltage-current characteristics. This result is due to the fact that when the discharge just begins to become ionized, very rapid ionization processes can occur; these processes increase n_e very rapidly so that the discharge may require only a low temperature and low electric field or voltage to furnish an increased current.

As the ionization of the plasma increases and the electrical conductivity changes from that of a partially ionized plasma (eq. (62))

$$\sigma \propto \frac{n_e}{n_n} T^{-1/2}$$

to that of a more highly ionized plasma, where the Coulomb collisions predominate (eq. (61))

$$\sigma_c \propto T^{3/2}$$

The voltage must increase, therefore, to increase the current when the increase in temperature is not large. The existence of a positive voltage-current characteristic for discharges with predominant Coulomb collisions has been observed in reference 35 at atmospheric pressure and in reference 21 at pressures from 10 to 100 mm Hg at very high curents. In view of the fact that, in changing from a partially to a more highly ionized plasma, the voltage-current characteristic can change from negative to positive, a voltage plateau can occur without a magnetic field.

Arc discharges in fairly well ionized plasmas of pressures from 1 to 100 mm Hg in magnetic fields up to 13,000 gauss with currents up to 270 amperes have been produced in experiments by W. Grossmann, Jr., at the Langley Research Center. The electric field is in the radial and the magnetic field in the axial direction. In these experiments a constant voltage with increasing current was observed. Measurements by researchers at AVCO (ref. 34) and at Langley for a similar discharge indicate the existence of Hall currents. For both experiments using tungsten cathodes uniform disk discharges were observed; more about these results are given in paper number 62 of this volume by M. C. Ellis. A report on the existence of the voltage plateau and its possible interpretation was given in a joint paper by W. Grossmann and the writer (ref. 23). In AVCO's work the existence of a "voltage plateau" was not explicitly recognized. It can, however, be obtained by replotting figure 8 in reference 34. A brief analysis, performed by Philip Brockman at the Langley Research Center, using the assumption that a large share of the power goes into rapid ionization has indicated this same result.

Since the plasma is fairly well ionized the question arises: how can the ionization affect the conductivity and the voltage-current characteristics, since the Coulomb conductivity without the magnetic field shows only a temperature dependence? As indicated from the expressions of the conductivity in a magnetic field in the Coulomb range (eq. (63))

$$(\sigma_{B\perp})_c \propto \frac{n_e^2}{T^{3/2}} \frac{1}{B^2}$$

or for the finite electrode case (eq. (67))

$$(\sigma_{B\perp})^f \propto \frac{n_e}{B}$$

in the presence of the magnetic field, an increase in ionized particles can affect the conductivity. Thus, a voltage plateau with increasing current due to rapid ionization processes can occur.

It should be emphasized that voltage plateaus have been also observed under vastly different conditions. For example, the well-known Alfvén-Fahleson voltage plateau (refs. 36 and 37) in an apparatus of similar geometry occurs for very low densities under conditions where the ion Larmor radius is smaller than the gap between electrodes. As a result the ions perform azimuthal drift motion normal to the radial electric field and the axial magnetic field. The electron currents are assumed to be small. The ions transfer their drift energy via the electrons which in turn use it to rapidly ionize the neutral atoms. The latter move slowly in view of their collisions with the apparatus wall. (See also analysis in ref. 38.)

The reason for the voltage plateau in the present case is vastily different since the ions are not set into collisionless drift motion, the densities being much higher. The energy for ionization is fed into the plasma directly by the electrons. A detailed analysis of this discharge including radiation effects and possible nonequilibrium ionization effects due to electron temperatures in excess of atom temperatures is being performed by H. Hassan at North Carolina State College under contracts to NASA. (For a discussion of such nonequilibrium effects, see ref. 39.)

The voltage plateau noted by both the Alfvén-Fahleson research and by research at

Langley are related to rapid ionization processes in plasmas. The energy is fed rapidly into ionization, while the ionization is still too low to put the plasma as a whole in rotation. Once the ionization becomes high enough and begins to be saturated, energy can be put into accelerating the plasma with a resultant voltage increase and the establishment of a positive voltage-current characteristic.

Recently a voltage plateau was also reported for a fully ionized rotating plasma in the Ixion (ref. 12, part II). The reasons for this voltage plateau are vastly different. Apparently the rotating plasma reaches a velocity limit due to friction with the walls. As a result it can no longer be accelerated and the voltage reaches a plateau.

Voltage-Current Characteristics of Hall Ion Accelerator

In the discussion of the Hall ion accelerator a fully ionized collisionless plasma was assumed corresponding to values $(\omega\tau)_e$ approaching infinity. For practical situations, of course, τ is finite. To analyze the effects of collisions one could adopt the viewpoint that the ionized plasma has been freely provided and that not much energy is required to maintain it. Since the matter of concern here is with fully ionized, almost collisionless plasmas for ion acceleration, if possible with a negligible amount of neutral atoms, the operation must be at considerably lower pressures than 1 mm Hg. While it is often easier to produce higher ionization at low pressures just because there is less gas to ionize, it is also more difficult to maintain it because of greater losses to the walls unless, of course, the plasma is kept away from the walls with magnetic fields. In the basic experiment performed by R. N. Rigby (ref. 29) of the Langley Research Center and continued by R. H. Weinstein, a radial magnetic field was imposed across an axial discharge (with the use of a flux concentrator in the center as shown in the schematic drawing in fig. 59–4(b)). The purpose was to see what happens when the $j\theta B_r$ interaction is optimized with a pure radial magnetic field B_r with expected penalties in losses. A similar configuration was used in reference 31, however, without reversed magnetic fields along the axis.

From the previous discussion better understanding of the practical implications in relaxing the collisionless fully ionized state is possible. For this case the only energy required is that for accelerating the ions. No energy is supplied by the axial electric field to the azimuthal electron current j_θ because without elastic collisions and without requirements on the electrons to perform ionizing or inelastic collisions, they do not require an energy input in the steady state. In order to provide steady energy for ionization an axial current will, however, need to exist. Through it some energy is also fed into heat, some of which is lost to the wall.

In the experiments, which will be discussed in more detail by M. C. Ellis (paper number 62 of this volume), an increase of voltage was required for a current increase. The slope of the voltage-current characteristic increases with increasing magnetic field and decreasing pressure. The slopes are too steep to suggest the effect of axial or azimuthal velocity (through $v_x B_r$ or $v_\theta B_r$) responsible for the main effect in the increase of E_x (see eqs. (46) and (47)). The increasingly positive voltage-current characteristic with increasing magnetic field can be obtained from equations (63) and (64) for the conductivity σ by assuming that the electron concentration n_e and the temperature T do not vary much as voltage and current are increased.

The important fact is that if approximately constant values of n_e and T can be shown to exist over a wide variety of slopes of the voltage-current characteristics, the slopes will be solely a function of the magnetic field. (Of course careful measurements of n_e and T over a wide variety of conditions are important.) Assuming that the discharge covers the same cathode area for increasing magnetic field, the electric field-current density characteristic can be substituted for the voltage-current characteristics. There follows, when no current bulging is possible as in the Hall ion accelerator, with $(\sigma_{B\perp})_e$ from equation (63):

$$\frac{E_x}{j_x}=\frac{1}{(\sigma_{B\perp})_e}\propto B^2$$

Experiments in the low pressure range at high $(\omega\tau)_e$ indicate a slope proportional to $\vec{B}$. This could be the result of current bulging along the magnetic field lines, since using the conductivity from equation (67) would result in

$$\frac{E_x}{j_x}=\frac{1}{(\sigma_{B\perp})'}\propto B_r$$

However, the experimental arrangement in the Hall ion accelerator does not encourage current bulging. Thus, there must be different reasons for the linear dependence on $\vec{B}$ of the slope of the voltage-current characteristic. They will be discussed in the following section.

First, a few remarks about the significance of Hall current measurements are important. As previously mentioned the voltage gradient or electric field E_x along the axis of the device is no longer responsible solely for the acceleration of the ions but must also furnish the energy to overcome losses due to ionization or heating. The electric field along the axis and the voltage drop across the electrodes will thus be higher than that required for acceleration. A measurement of the voltage variation along the axis will as a consequence not be an explicit measure of the directed energy put into the ions. The $j_\theta B_r$ force per unit volume, however, actually represents the true accelerating force. Measurement of the Hall current in the azimuthal direction thus is desirable for a knowledge of the distribution of accelerating forces along the accelerator. Measurements of both j_θ and E_x can, of course, furnish important information concerning the losses. Hall current measurements have been performed by R. N. Rigby (ref. 29) and have been continued by R. H. Weinstein, J. Burlock, and T. M. Collier of the Langley Research Center.

Effect of "Plasma Turbulence" on Electrical Conductivity and Voltage-Current Characteristics in a Magnetic Field

The problem of "turbulent" or anomalous diffusion has become one of the most critical problems of plasma physics. (It is noteworthy that the turbulence in plasmas is not the same process as in fluids). On its avoidance depends the success of thermonuclear fusion. The problem is essentially that whenever deviations from a quiescent plasma state occur, the tendency exists for a diffusion more rapid across the magnetic field than that determined by the classical result (see refs. 1 to 11)

$$D_{B\perp}=\frac{D}{1+(\omega\tau)_e^2} \tag{68}$$

where D, the diffusion coefficient, say for electrons, can be expressed by

$$D=C_3\lambda\bar{c}=C_3\lambda^2\nu \tag{69}$$

in the presence of a strong magnetic field by making the proper substitutions

$$D_{B\perp}=\frac{D}{(\omega\tau)_e^2}=\frac{1}{\frac{e^2\lambda^2}{m^2c^2}}\frac{D}{B^2}=C_3r_{L,e}^2\nu \tag{70}$$

It has now been found (refs. 1 to 11) that for anomalous or turbulent diffusion, the diffusion is inversely proportional to $\vec{B}$

$$(D_{B\perp})_{\text{turb}}=C_4\frac{D}{B} \tag{71}$$

instead of being inversely proportional to B^2. This relation is the so-called Bohm diffusion. The reason for such behavior is, roughly, that amplified oscillations occur in the plasma and produce electric fields normal to the magnetic lines; as a result a drift motion occurs across the magnetic field. Since such drift motion is inversely proportional to $\vec{B}$ (and proportional to $\vec{E}$), a diffusion coefficient inversely proportional to $\vec{B}$ instead of B^2 is established.

It has long been known that discharges across magnetic fields can maintain much higher currents than would be expected on the basis of the classical law that suggests a conductivity inversely proportional to B^2. The operation of the PIG (Phillips Ionization Gage) discharge at low pressures has shown such behavior (see also refs. 40 and 41 for more recent work). A study of a PIG discharge with radial electric and axial magnetic fields was made at the Langley Research Center (ref. 15), and the mechanism for oscillations was studied. In the axial discharges with radial magnetic fields, oscilla-

tions were observed by researchers at AVCO (ref. 19), at United Aircraft (refs. 30 and 31), and at the Langley Research Center (ref. 29).

For determination of the "turbulent" electrical conduction in a discharge crossing a magnetic field, the voltage-current characteristic again offers a very useful tool. For turbulent conduction oscillating electric fields can build up in the azimuthal direction superposed on the Hall current (refs. 15 and 42, for a possible amplification mechanism), which together with the radial magnetic field permit a drift of the electrons along the axial direction. As a result the axial current is given by

$$\left.\begin{aligned} j_z &= \alpha\beta n_e e \frac{E_z}{B_r} \\ j_z &= (\sigma_{B\perp})_{\text{turb}} E_z \end{aligned}\right\} \tag{72}$$

with

$$(\sigma_{B\perp})_{\text{turb}} = \frac{\alpha\beta n_e e}{B_r} \tag{73}$$

This expression is found in reference 43 (see also ref. 44). (In these references $\vec{B}$ is axial and $\vec{E}$ is radial.) In this expression the nature of the drift is included by the inverse proportionality of the electrical conductivity to B_r. The effect of the azimuthal electric field oscillations producing the enhanced conduction across B_r is included by a factor α; the factor β depends on the particular geometry.

Assuming that n_e, α and β do not vary much with increasing currents, the slope of the voltage characteristic is then

$$\frac{E_z}{j_z} \propto B_r \tag{74}$$

This fits the variation of the slope of the voltage-current characteristics in the Hall ion accelerator for low pressures given in reference 29. Such fit was also found by researchers at AVCO (ref. 19) and United Aircraft (ref. 31). It thus appears that we are dealing with turbulent electrical conduction.

The question arises of how to reduce this turbulence. One way as pointed out in reference 19 is to use truly well-ionized plasmas. Then the magnitude of axial electron currents to maintain the energy input through the axial electric field is reduced. The axial electric field required to feed the ionization energy into the plasma, feeds it also into the oscillations. Thus, for proper injection of a fully ionized fast moving plasma the possibility exists of keeping the oscillations and the turbulence down. Another way is to operate a Hall accelerator at higher pressures as is done for the Hall accelerators with radial electric fields. Such an approach is also used for the Hall ion accelerator by G. Cann (ref. 28) and in some of the configurations used at the Langley Research Center. Another possibility arises by using a time-dependent reversal of the radial magnetic field with resulting reversal of the azimuthal electron motion to delay the growth of instabilities. This concept is suggested by recent experiments in ref. (45), indicating that instabilities of a magnetically confined discharge could be delayed by rapid current reversals; this, however, would be detrimental to propulsion. A many-phase traveling magnetic field rotating around the annulus would cut down the occurrence of zero magnetic field, but it may also prevent the electrons from oscillating back and forth if they are tied to the rotating magnetic field. The use of externally imposed waves has also been suggested.

Finally, attention should be drawn to the coincidence that the slope of the voltage-current characteristic for turbulent electrical conductivity (eq. (73)) is inversely proportional to $\vec{B}$, but the slope for nonturbulent conductivity with current fringing along the magnetic lines (eq. (67)) is also inversely proportional to B, but for vastly different reasons. In this connection details of the experimental arrangement in reference 43, for which turbulent conduction and diffusion laws have been established, is of interest. A highly ionized plasma is produced in an axial discharge which is confined by an axial magnetic field. Perpendicular to this field a small current is drawn to an auxiliary ring electrode. Since the ring electrode is of finite dimension, a slight possibility exists of some current bulging in the direction of the magnetic field lines, although the other electrode is the long discharge plasma. In references 43 and 44, however, the turbulent noise level is also

checked and apparently the theory of turbulent conduction or diffusion is well established. It is also of interest that in reference 43 a current actually drawn from the main plasma is used to check the effects of plasma turbulence in the presence of a magnetic field. The implication is given that similar turbulent laws should apply to diffusion across the magnetic field. The idea is that although there exist differing mechanisms for the production of turbulence, the actual effect of the fully developed turbulence should give a voltage-current slope inversely proportional to $\vec{B}$. Since there are a variety of macroscopic and microscopic amplification mechanisms (see discussion on stability in ref. 7 and ref. 46) in the plasma with different individual character, the final answer is not yet quite clear although large-scale turbulence is known to decay to small-scale turbulence.

FINAL REMARKS

The purpose of this paper is mainly to point out that a profound knowledge of the deeper implications of known aspects of plasma physics or measurement techniques is necessary before experimental results can be attributed to anomalous effects. The history of plasma physics is full of such situations. On the other hand, once new effects are discovered they can be found in many situations; the field of plasma "turbulence" is a good example. On both counts the role of the university which combines teaching with research is of great importance.

REFERENCES

1. Spitzer, Lyman, Jr.: Physics of Fully Ionized Gases. Interscience Publ., Inc. (New York), 1956.
2. Glasstone, Samuel, and Lovberg, Ralph H.: Controlled Thermonuclear Reactions. D. Van Nostrand Co., Inc., c.1960.
3. Chandrasekhar, S. (S. K. Trehan, compiler): Plasma Physics. The Univ. of Chicago Press, c.1960.
4. Linhart, J. G.: Plasma Physics. Interscience Publ., Inc. (New York), 1960.
5. Rose, David J., and Clark, Melville, Jr.: Plasmas and Controlled Fusion. The M.I.T. Press and John Wiley & Sons, Inc., c.1961.
6. Anon.: Notes on Plasma Dynamics, M.I.T., Aug. 1959.
7. Wandel, C. F., ed.: International Summer Course in Plasma Physics, 1960. Risö Rep. No. 18, Danish Atomic Energy Comm., Nov. 1960, pp. 119–248.
8. Cowling, T. G.: Magnetohydrodynamics. Interscience Publ., Inc., (New York), 1957.
9. Simon, Albert: An Introduction to Thermonuclear Research. Pergamon Press (New York), 1959.
10. Kennard, Earle H.: Kinetic Theory of Gases. McGraw-Hill Book Co., Inc., 1938.
11. Ecker, G.: Electrode Components of the Arc Discharge. Reprinted from Ergebnisse der Exakten Naturwissenschaften, Bd. XXXIII, Springer-Verlag (Berlin), 1961.
12. Baker, D. A., Hammel, J. E., and Ribe, F. L.: Rotating Plasma Experiments. I. Hydromagnetic Properties. The Physics of Fluids, vol. 4, no. 12, Dec. 1961, pp. 1534–1548.

    Baker, D. A., and Hammel, J. E.: Rotating Plasma Experiments. II. Energy Measurements and the Velocity Limiting Effect. The Physics of Fluids, vol. 4, no. 12, Dec. 1961, pp. 1549–1558.
13. Ebel, M. E., Kroll, N. M., et al.: Plasma Propulsion Studies—Summer, 1959. LA–2408 (Contract W–7405–ENG. 36), Los Alamos Sci. Lab., Univ. of California, Aug. 3, 1960.
14. Anderson, Oscar, Barker, William R., et al.: Hydromagnetic Capacitor. Jour. Appl. Phys., vol. 30, no. 2, Feb. 1959, pp. 188–196.
15. Hess, R. V., Burlock, J., Sevier, J. R., and Brockman, P.: Theory and Experiments for the Role of Space-Charge in Plasma Acceleration. Electromagnetics and Fluid Dynamics of Gaseous Plasma. Vol. XI of Microwave Res. Inst. Symposia Ser., Polytechnic Press of Polytechnic Inst. of Brooklyn, c.1962, pp. 269–305.
16. Kemp, Nelson H., and Petschek, Harry E.: Two-Dimensional Incompressible Magnetohydrodynamic Flow Across an Elliptical Solenoid. Res. Rep. 26, AVCO Res. Lab., Apr. 1958.

17. WOOD, GEORGE P., CARTER, ARLEN F., LINTZ, HUBERT K., and PENNINGTON, J. BYRON: A Theoretical Treatment of the Steady-Flow, Linear, Crossed-Field, Direct-Current Plasma Accelerator for Inviscid, Adiabatic, Isothermal, Constant-Area Flow. NASA TR R-114, 1961.
18. KANTROWITZ, ARTHUR R., and PETSCHEK, HARRY, E.: An Introductory Discussion of Magnetohydrodynamics. Res. Rep. 16, AVCO Res. Lab., May 11, 1957.
19. JANES, G. S., DOTSON, J., and WILSON, T.: Electrostatic Acceleration of Neutral Plasmas—Momentum Transfer Through Magnetic Fields. Presented at Third Symposium on Advanced Propulsion Concepts (Cincinnati, Ohio), Oct. 2–4, 1962. (Sponsored by U.S. Air Force and Gen. Elec. Co.)
20. HESS, ROBERT V.: Experiments and Theory for Continuous Steady Acceleration of Low Density Plasmas. Vol. I of Proc. XIth Int. Astronautical Cong., Carl W. P. Reuterswärd, ed., Springer-Verlag (Vienna), 1961, pp. 404–411.
21. POWERS, W. E., and PATRICK, R. M.: A Magnetic Annular Arc. Engineering Aspects of Magnetohydrodynamics, Clifford Mannal and Norman W. Mather, eds., Columbia Univ. Press, 1962, pp. 5–18.
22. PATRICK, R. M., and POWERS, W. E.: Plasma Flow in a Magnetic Annular Arc Nozzle. Presented at Third Symposium on Advanced Propulsion Concepts (Cincinnati, Ohio), Oct. 2–4, 1962. (Sponsored by U.S. Air Force and Gen. Elec. Co.)
23. GROSSMANN, WILLIAM, Jr., and HESS, ROBERT V.: Existence of a Voltage Plateau for a Discharge Crossed With a Magnetic Field at Elevated Pressures. Presented at the Summer Meeting, American Phys. Soc. (Seattle, Wash.), Aug. 27, 1962.
24. SEVIER, JOHN R., HESS, ROBERT V., and BROCKMAN, PHILIP: Coaxial Hall Current Accelerator Operation at Forces and Efficiencies Comparable to Conventional Crossed-Field Accelerators. ARS Jour. (Tech. Notes), vol. 32, no. 1, Jan. 1962, pp. 78–80.
25. SUTTON, GEORGE W., and GLOERSEN, PER: Magnetohydrodynamic Power and Propulsion. Magnetohydrodynamics, Ali Bulent Cambel, Thomas P. Anderson, and Milton M. Slawsky, eds., Northwestern Univ. Press (Evanston, Ill.), c. 1962, pp. 243–268.
26. BRATENAHL, A., JANES, G. S., and KANTROWITZ, A. R.: Plasma Acceleration in the Electromagnetic Region II. Bull. American Phys. Soc., ser. II, vol. 6, no. 4, June 22, 1961, p. 379.
27. SEIKEL, G. R., and RESHOTKO, E.: Hall Current Ion Accelerator. Bull. American Phys. Soc., ser. II, vol. 7, no. 6, June 19, 1962, p. 414.
28. CANN, G. L., TEEM, J. M., BUHLER, R. D., and BRANSON, L. K.: Magnetogasdynamics Accelerator Techniques. AEDC-TDR-62-145 (Contract No. AF 40(600)-939), Arnold Eng. Dev. Center, July 1962.
29. RIGBY, ROBERT NORRIS: Some Phsyical Properties of an Axial Electric Arc in a Radial Magnetic Field. M. S. Thesis, The College of William and Mary in Virginia, 1962.
30. LARY, E. C., MEYERAND, R. G., Jr., and SALZ, F.: Ion Acceleration in a Gyro-Dominated Neutral Plasma—Theory. Bull. American Phys. Soc., ser. II, vol. 7, no. 7, Aug. 27, 1962, p. 441.
31. SALZ, F., MEYERAND, R. G., Jr., and LARY, E. C.: Ion Acceleration in a Gyro-Dominated Neutral Plasma—Experiment. Bull. American Phys. Soc., ser. II, vol. 7, no. 7, Aug. 27, 1962, p. 441.
32. LUCE, J. S., and FLOWERS, J. W.: The High Specific Impulse, Arc-Ion System. ORNL-3031 (Contract No. W-7405-eng-26), U.S. Atomic Energy Comm., Apr. 21, 1961.
33. MASSEY, H. S. W., and BURHOP, E. H. S.: Electronic and Ionic Impact Phenomena. The Clarendon Press (Oxford), 1952.
34. POWERS, WILLIAM E., and PATRICK, RICHARD M.: Magnetic Annular Arc. The Physics of Fluids, vol. 5, no. 10, Oct. 1962, pp. 1196–1206.
35. BUSZ, G., and FINKELNBURG, W.: Thermische Lichtbögen hoher Temperatur und niedriger Brennspannung. Z. Phys., Bd. 138, Heft 2, 1954, pp. 212–225.
36. ALFVÉN, H.: Collision Between a Nonionized Gas and a Magnetized Plasma. Magneto-Fluid Dynamics, F. N. Frenkiel and W. R. Sears, eds., Pub. 829, Nat. Res. Council, Nat. Acad. Sci., 1960, pp. 710–713.
37. FAHLESON, ULF V.: Experiments With Plasma Moving Through Neutral Gas. The Physics of Fluids, vol. 4, no. 1, Jan. 1961, pp. 123–127.
38. LIN, SHAO-CHI: Limiting Velocity for a Rotating Plasma. The Physics of Fluids, vol. 4, no. 10, Oct. 1961, pp. 1277–1288.
39. HURWITZ, H., JR., SUTTON, G. W., and TAMOR, S.: Electron Heating in Magnetohydrodynamic Power Generators. ARS Jour., vol. 32, no. 8, Aug. 1962, pp. 1237–1243.

40. KAUFMAN, HAROLD R.: The Electron-Bombardment Ion Rocket. Presented at Third Symposium on Advanced Propulsion Concepts (Cincinnati, Ohio), Oct. 2–4, 1962. (Sponsored by U.S. Air Force and Gen. Elec. Co.)
41. BINGHAM, R. L., CHEN, F. F., and HARRIES, W. L.: Preliminary Studies of a Reflex Arc. MATT–63 (Contract AT(30–1)–1238), Plasma Phys. Lab., Princeton Univ., Feb. 1, 1962.
42. BUNEMAN, O.: Instability of Electrons Drifting Through Ions Across a Magnetic Field. Tech. Rep. No. 251–1 (Contract AF49(638)–660), Stanford Electronics Labs., Stanford Univ., July 20, 1961.
43. YOSHIKAWA, S., and ROSE, D. J.: Anomalous Diffusion of a Plasma Across a Magnetic Field. The Physics of Fluids, vol. 5, no. 3, Mar. 1962, pp. 334–340.
44. YOSHIKAWA, SHOICHI: Electrical Conductivity of a Turbulent Plasma. The Physics of Fluids, vol. 5, no. 10, Oct. 1962, pp. 1272–1277.
45. RUGGE, HENRY F., and PYLE, ROBERT V.: Instability of the Positive Column of an AC Discharge in a Magnetic Field. Bull. American Phys. Soc. Abstract D12. Ser. II, vol. 7, no. 7, Aug. 27–29, 1962, p. 442.
46. KADOMTSEV, B. B.: Turbulent Loss of Particles From a Discharge in a Strong Magnetic Field. Soviet Physics—Tech. Phys., vol. 6, no. 10, Apr. 1962, pp. 882–888.

AUTHOR'S NOTE: *After this paper was presented at the conference, the 4th Annual Meeting of the Division of Plasma Physics of the American Physical Society was held in Atlantic City, N.J., from November 28 to December 1, 1962, where further instability mechanisms in crossed electric and magnetic fields were suggested by Albert Simon from General Atomic and by G. Briffod, M. Gregoire, and C. Manus, Centre d'Etudes Nucleair de Saclay, France. In the latter paper, also, interesting experiments for the onset of the instabilities were shown. At this meeting, also, recent Hall current measurements were discussed in a paper by R. V. Hess, R. N. Rigby, and R. H. Weinstein of the NASA Langley Research Center, with emphasis on the use of the Hall currents for the measure of the onset and existence of turbulent conduction.*

60. The Electric Drag Forces on a Satellite in the Earth's Upper Atmosphere

By George P. Wood

GEORGE P. WOOD, *Head, Magnetohydrodynamics Section, Aero-Physics Division, NASA Langley Research Center, received his Bachelor's and Master's degrees in Physics from the University of Mississippi and also did graduate work at the Johns Hopkins University. Wood joined the Langley staff as a junior physicist in July 1940. He is recognized as an international authority on optical interferometric observation of flows and in magnetohydrodynamics. He has specialized in heat transfer, optical interferometric study of transonic and supersonic flows, and magnetohydrodynamics. He published the first paper in the United States dealing with aerodynamic heating at supersonic speeds and was the first to achieve steady-state crossed-field acceleration of high-density plasma. He is author of 25 NASA technical publications on research he has conducted at Langley.*

SUMMARY

A theoretical study has been made of the electric drag forces acting, as a result of the electric charge on the sphere, on a spherical satellite in free-molecule flow in the upper atmosphere. The analysis has been applied to a 4-meter-diameter earth satellite at an altitude of 1,500 kilometers. The calculations have yielded charge-density distribution and potential distribution in the sheath, the ion trajectories, the increased ion-impact drag, the ion-scattering drag, and the induction drag due to the earth's magnetic field. These three electric drags total about 3½ percent of the drag of the uncharged sphere for average conditions between maximum and minimum of sunspot activity. The percentage would be approximately doubled at the maximum and approximately halved at the minimum.

INTRODUCTION

This paper describes one of the applications of plasma physics and magnetohydrodynamics in space research.

One of the uses of artificial earth satellites is the determination of the density of the upper reaches of the earth's atmosphere. Explorer IX (1961 Delta 1) is a satellite that was placed into orbit by the NASA in February of 1961 for the purpose of measuring the density of the atmosphere. It is a 12-foot-diameter hollow lightweight sphere that was constructed of two layers of thin plastic and two layers of aluminum foil and was inflated after being placed in orbit. This satellite is rather large, yet of small mass, and its orbit is considerably affected by the aerodynamic drag exerted by the atmosphere. From the observed effect of this drag on the orbit, the density of the atmosphere at least at the altitude of perigee, which is about 700 kilometers, can be inferred.

The upper atmosphere of the earth, however, is a plasma, and electrostatic and electromagnetic interactions can take place between the plasma and the satellite, the outer layer of which is a metal and carries a charge. These interactions cause drags on the satellite that are additional to the conventional aerodynamic drag that occurs in an un-ionized environment. Although these additional drags may turn out

10

to be small, as they do in the present case, it seems advisable to calculate them in order to be able to take them into account in the determination of atmospheric density.

A number of papers are available on the subject of the electric drag of satellites (refs. 1 to 8). Some of the analyses apply, however, only to charged bodies that are small compared to a Debye length, and for an altitude of 1,500 kilometers (the altitude used herein as an example) the Debye length is only 3 centimeters. In some of the analyses the satellite is assumed to be charged to many tens of volts, whereas in the case to be considered herein the potential of the satellite is only a fraction of a volt. Some of the published works treat only one of the three electric drags. In others, the concepts themselves are erroneous. (A comprehensive and useful review of the subject is given in ref. 9.) It therefore seemed advisable to perform the analysis and computation in such a way that the results are applicable to the average altitude of Explorer IX. The present analysis applies to satellites that are large compared to a Debye length (a satellite diameter of 4 meters is used) and that are at altitudes high enough that free-molecule flow obtains (an altitude of 1,500 kilometers is used). A more extensive treatment has been given in reference 10.

SYMBOLS

B magnetic induction, webers/m^2
e charge on singly ionized positive ion, coulombs
i current, amperes
j current density, amperes/m^2
k Boltzmann's constant, joules/°K
l length, m
m mass, kg
n number density, m^{-3}
Q charge, coulombs
r, θ, ψ spherical coordinates
T temperature, °K
U nondimensionalized potential, $e\phi/kT$
v velocity, m/sec
x, y, z Cartesian coordinates
ϵ permittivity, farads/m
ζ nondimensionalized length, r/λ_D
η transformed coordinate, $\log_e \frac{\zeta}{\zeta_s}$
λ_D Debye length, $\left(\frac{\epsilon kT}{n_{e,\infty} e^2}\right)^{1/2}$
σ conductivity, mhos/m
ϕ potential, volts

Subscripts:
e electron
i ion
∞ ambient
s satellite

DESCRIPTION OF ELECTRIC DRAGS

A satellite experiences electrostatic drags because it acquires a charge. At an altitude of 1,500 kilometers, the principal constituent of the atmosphere is helium. For average conditions over a solar cycle, one-fourth of the helium atoms are ionized by radiation from the sun in the far ultraviolet. The number density of electrons and of ions is equal and both are at the same temperature. (See table 60–I, which shows conditions at an altitude of 1,500 kilometers.) The satellite velocity is greater than the ion velocity; therefore, the satellite sweeps up the ions. The electrons, on the other hand, being of small mass and being tied to the lines of force of the earth's magnetic field, spiral in very small circles around these lines and, having much greater velocity than the satellite, impinge on the satellite at a higher rate than

TABLE 60–I.—*Conditions at an Altitude of 1,500 Kilometers*

		Ions	Electrons
Mass density, kg/m³	2×10^{-16}		
Number density, m⁻³	3×10^{10}	7×10^{9}	7×10^{9}
Temperature, °K	1,300	1,300	1,300
Magnetic flux density, weber/m²	2.3×10^{-5}		
Debye length, m	3×10^{-2}		
Satellite velocity, m/sec	7×10^{3}		
Thermal velocity, m/sec		3×10^{3}	2×10^{5}
Mean free path, m		4×10^{2}	3×10^{4}
Radius of gyration, m		3	5×10^{-2}
Revolutions/collision		10	8×10^{4}

the ions. The satellite therefore quickly builds up a negative charge and a negative potential of such magnitude that the rates of impingement of ions and electrons become equal. At an altitude of 1,500 kilometers, charged particle densities and velocities are such that this negative potential is 0.4 volt.

The ultraviolet portion of the sun's radiation can also cause photoelectrons to be emitted from the surface of the satellite, but because the aluminum surface is not really clean and is oxidized, the photocurrent at this altitude can only reduce the equilibrium charge on the satellite toward zero. In order to obtain a maximum value for the electric drag, the effects of photoemission were neglected. This condition would correspond either to a dirty surface or to the satellite's being in the earth's shadow. The calculations were therefore made for a negative potential of 0.4 volt on the satellite.

Three electric drag forces can act on a satellite. Two of these forces are electrostatic in nature and are identified herein as Coulomb drags. The third is electromagnetic and is termed the induction drag. One of the Coulomb drags is due to the increase in the rate at which ions impinge on the satellite (and thus mechanically transfer momentum to it) because of the Coulomb forces between the charge on the satellite and the charges on the ions. This phenomenon is illustrated in figure 60–1 for the case of no magnetic field. Because of the negative charge on the satellite, the cross section for ion impingement is increased. When, however, the satellite is crossing the lines of force

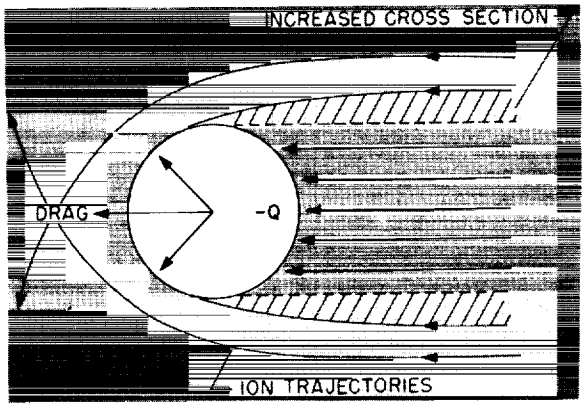

FIGURE 60–1.—Coulomb drags (without magnetic field).

of the earth's magnetic field, a voltage gradient is induced in the satellite, which thus becomes polarized. Thus, the increase in the cross section for ion impingement is not symmetrical about the satellite. This condition is shown in figure 60–2.

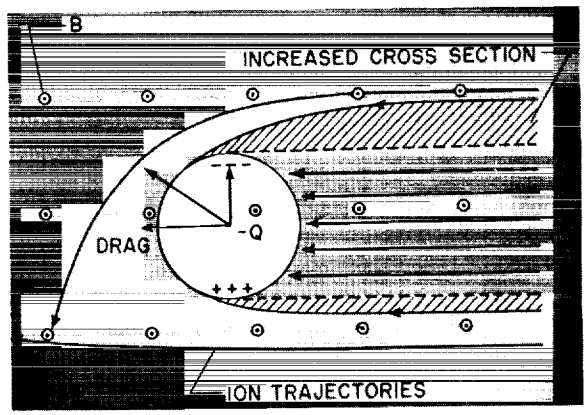

FIGURE 60–2.—Coulomb drags (with magnetic field).

The second Coulomb drag is due to the fact that ions whose trajectories are affected by the electrostatic force but which do not actually impinge on the satellite are deflected or scattered and thus exert a force on the satellite. This type of drag is illustrated in figure 60–1 for the case of no magnetic field. The force between the ion and the satellite varies in both direction and magnitude but can be illustrated qualitatively by a single force as shown. The resultant of the forces exerted by all the scattered ions is a force in the drag direction. When the earth's magnetic field is taken into account, the scattering is no longer symmetrical, as is shown in figure 60–2. The resultant force vector due to scattering of ions can in this case be resolved into two components, one along the drag direction and one in the lateral direction.

Induction drag occurs only when a magnetic field is involved and can be qualitatively described as follows. (See fig. 60–3.) Ions impinge preferentially on the portion of the front of the satellite that is more negative, and electrons traveling along the magnetic lines of force impinge most copiously on the portion of the two sides that is more positive. The positive ions and the negative electrons have to combine, so there is a flow of electrons in the satellite

which is equivalent to a positive current as shown. The well-known electromagnetic force on a current in a magnetic field is the vector product of the current density and the magnetic flux density $j \times B$ per unit volume. This force has a component in the lateral direction and a component in the drag direction.

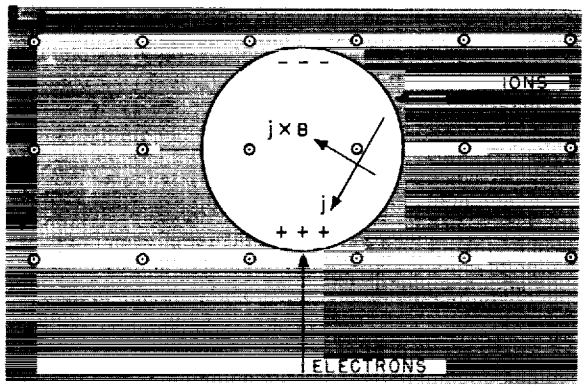

FIGURE 60–3.—Induction drag.

CALCULATION OF SHEATH

The foregoing discussion indicates that, before these three electric drags can be calculated, a knowledge of the trajectories of the ions is required. The ion trajectories are found by solving the equations of motion of the ions. Solving the equations of motion requires in turn a knowledge of the electric potential distribution around the satellite. The electric field of the satellite does not extend to infinity but is limited to a few tens of centimeters by a sheath that forms around the satellite. It is the potential distribution in this sheath that is required. To find it, ion and electron density distributions in the sheath are needed.

Because the ions are very massive as compared with the electrons, the ion density in the sheath can, as a good first approximation, be considered to be constant and equal to that outside the sheath. Most of the redistribution of charge density in the sheath is made by the electrons.

The electrons in the undisturbed atmosphere can be taken to be in thermodynamic equilibrium, as was verified by measurements taken with Explorer VIII (1960 Xi 1). Then if the satellite surface were a perfect reflector of electrons, the electrons in the sheath would be distributed according to the Boltzmann law; thus,

$$n_e = n_{e,\infty} \exp\left(\frac{e\phi}{kT}\right)$$

But since the satellite surface is an almost perfect absorber of electrons, those electrons that initially have sufficient kinetic energy to reach the surface are not reflected, and of course no electrons come through the satellite from the other side to replace them. The Boltzmann distribution must therefore be modified near the satellite surface to account for this deficit in the distribution of receding electrons. The modification is effected in the following manner. At any point in the sheath at which the potential is ϕ, the electrons that have velocities toward the surface of the satellite have a Maxwellian distribution with velocities ranging from zero to infinity, but their number density is reduced by the Boltzmann factor $\exp\left(\frac{e\phi}{kT}\right)$. The electrons that have velocities away from the surface, which are those that have been reversed in direction by the potential field, are reduced in number density by the Boltzmann factor and have only that part of a Maxwellian distribution that extends from $-\sqrt{\frac{2e(\phi-\phi_s)}{m_e}}$ to zero. Those missing from the Maxwellian distribution were intercepted by the surface. The electron density at the point where the potential is ϕ is then

$$n_e = n_{e,\infty} \exp\left(\frac{e\phi}{kT}\right) \sqrt{\frac{m_e}{2\pi kT}} \int_{-\sqrt{\frac{2e(\phi-\phi_s)}{m_e}}}^{\infty} \exp\left(\frac{m_e v^2}{2kT}\right) dv$$

$$= \left[\frac{1}{2} + \frac{1}{2} \operatorname{erf} \sqrt{\frac{e(\phi-\phi_s)}{kT}}\right] n_{e,\infty} \exp\left(\frac{e\phi}{kT}\right)$$

The right-hand side of this equation is the Boltzmann distribution modified by the expression in the brackets.

The potential distribution and the charge-density distribution in the sheath were found by solving Poisson's equation

$$\nabla^2\phi=\frac{e}{\epsilon}(n_e-n_i)$$

Dimensional quantities were made nondimensional as follows: Distance from the center of the satellite r was expressed in terms of Debye lengths, potential in terms of temperature (in volts), and number density in terms of ambient number density. Poisson's equation in spherical coordinates then becomes

$$\frac{1}{\zeta^2}\frac{\partial}{\partial\zeta}\left(\zeta^2\frac{\partial U}{\partial\zeta}\right)+\frac{1}{\zeta^2\sin\theta}\frac{\partial}{\partial\theta}\left(\sin\theta\frac{\partial U}{\partial\theta}\right)=e^U\left[\frac{1}{2}+\frac{1}{2}\operatorname{erf}\sqrt{U-U_{\theta=\pi/2}-\frac{(v_s\times B)r_s}{kT}\cos\theta_s}\right]-1$$

The ohmic voltage gradient j/σ is not taken into account in this equation because it is negligible as compared with the polarizing voltage gradient $v_s\times B$. The orientation of the coordinate systems used for the calculation of the sheath is shown in figure 60–4. These coordinate systems are fixed in the satellite. The boundary conditions for the sheath are:

$U=0$ at $\zeta=\infty$ (actually used was $\zeta=20$)

$$U=U_{\theta=\pi/2}+\frac{(v_s\times B)r_s}{kT}\cos\theta_s \text{ at } \zeta=\zeta_s$$

$$\frac{\partial U}{\partial\theta}=0 \text{ at } \theta=0,\pi$$

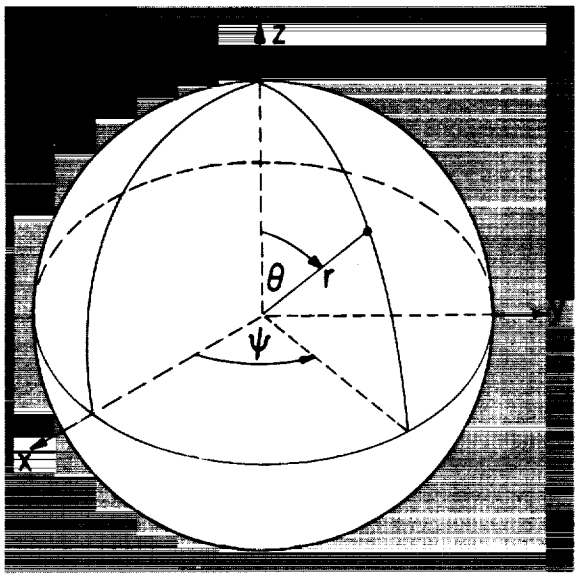

FIGURE 60–4.—Spherical and Cartesian coordinate systems.

This last boundary condition is based on the assumption that the wake has a negligible effect on the sheath on the front half of the satellite and that the sheath can therefore be calculated as though it were symmetrical about the z-axis. The region of the sheath, an area bounded by circular arcs, was transformed into a rectangular area by the substitution

$$\eta=\log_e\frac{\zeta}{\zeta_s}$$

With this substitution, Poisson's equation becomes

$$\frac{\partial^2U}{\partial\eta^2}+\frac{\partial U}{\partial\eta}+\frac{\partial^2U}{\partial\theta^2}+\cot\theta\frac{\partial U}{\partial\theta}=r_s^2e^{2\eta}\left\{e^U\left[\frac{1}{2}+\frac{1}{2}\operatorname{erf}\sqrt{U-U_{\theta=\pi/2}-\frac{(v_s\times B)r_s}{kT}\cos\theta_s}\right]-1\right\}$$

(The angle θ_s is the angle defining the point on the satellite surface which projects along the direction of the earth's magnetic field lines to the point where the potential is U.) This equation was written as a system of difference equations which were solved simultaneously for a network of 51 by 51 mesh points by an iteration procedure on an IBM 7090 electronic data processing system. One hundred twenty iterations were found to be sufficient.

The results for the potential U in the sheath are shown in figure 60–5, where contours of constant U are drawn. It should be emphasized that, since the radius of the satellite is so much greater than the thickness of the sheath ($r_s=66.67\lambda_D$), it was necessary, in order to be able to show the structure of the sheath, to use vastly different distance scales for the two regions, inside and outside of the satellite. The ratio of the scales is 1 to 33.33. The results for the charge density $\frac{(n_i-n_e)}{n_{i,\infty}}$ in the sheath are given in figure 60–6, which shows contours of constant charge density. (Here again different scales were used for the satellite and the sheath.) It can be seen that the retarding action of the negative charge on the satellite, together with the absorption of electrons that contact the surface, results in very much reduced electron number densities very close to the surface. The thickness of the sheath is shown by figure 60–5 to depend on the local value of

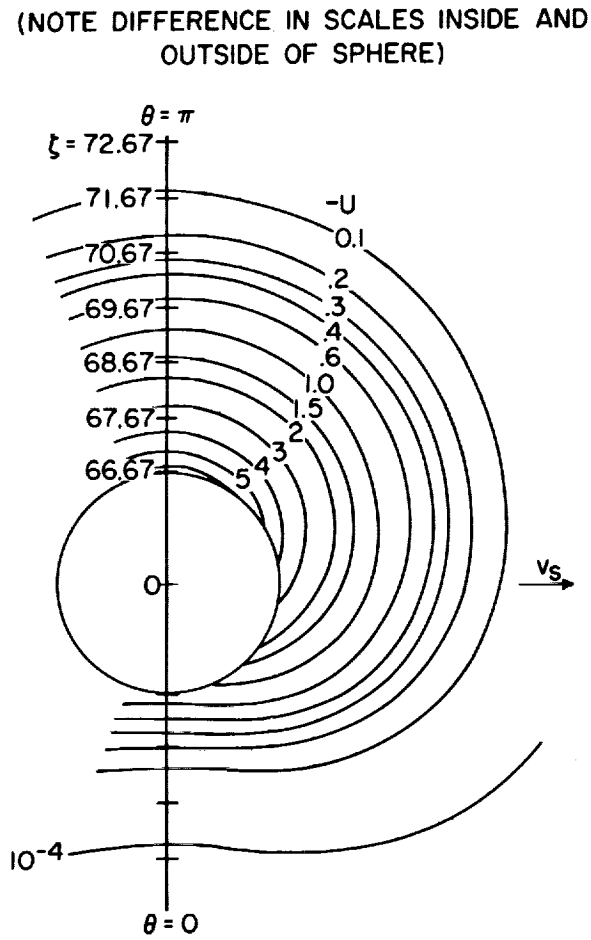

FIGURE 60–5.—Contours of potential U in the sheath.

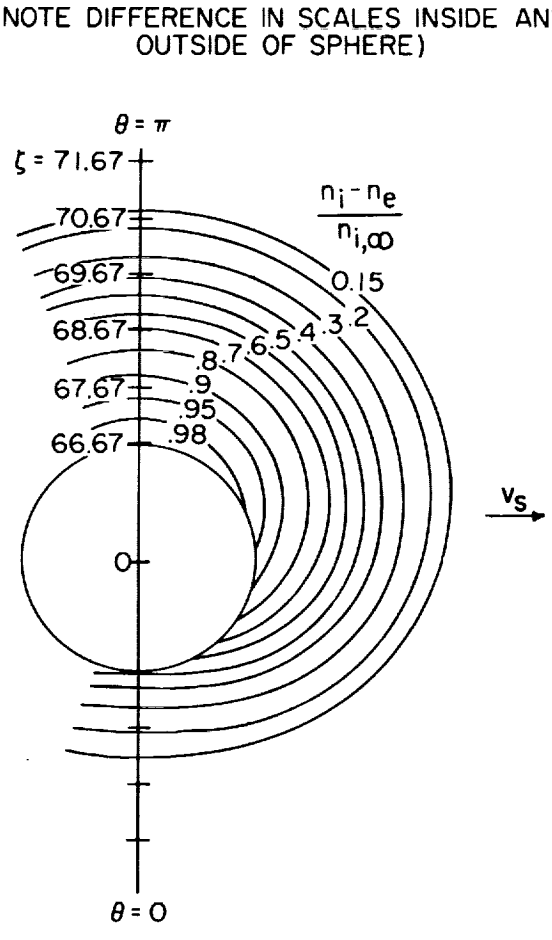

FIGURE 60–6.—Contours of constant charge density in the sheath.

the potential on the satellite surface and to vary from about 0.8 to 1.5 Debye lengths, if the edge of the sheath is taken to be the location of $1/e$ of the surface potential. Since the sheath on the front half of the satellite has symmetry about the z-axis (the vertical axis in the plane of the paper in figs. 60–5 and 60–6), three-dimensional surfaces of constant potential and constant charge density can be generated by rotating these figures about that axis.

CALCULATIONS AND RESULTS FOR ION TRAJECTORIES

The trajectories of the ions were found from a solution of the Lagrangian form of the equations of motion,

$$\ddot{\zeta}-\zeta\dot{\theta}^2-\zeta\sin^2\theta\,\dot{\psi}^2+\frac{e^2 n_{i,\infty}}{\epsilon m_i}\frac{\partial U}{\partial\zeta}=0$$

$$\zeta^2\ddot{\theta}+2\zeta\dot{\zeta}\dot{\theta}-\zeta^2\cos\theta\sin\theta\,\dot{\psi}^2+\frac{e^2 n_{i,\infty}}{\epsilon m_i}\frac{\partial U}{\partial\theta}=0$$

$$\zeta^2\sin^2\theta\,\dot{\psi}=\text{Constant}$$

where the dots over symbols denote differentiation with respect to time. The two derivatives of potential ($\partial U/\partial\zeta$ and $\partial U/\partial\theta$) that appear in these equations had been calculated and stored in the process of calculating the potential and the charge density in the sheath. They were used in solving these equations numerically on the IBM 7090 electronic data processing system. A fifth-order integration routine that employed a fourth-order Runge-Kutta method was used. Each interval was computed by two complete half-interval steps and comparison was made with the whole interval step for accuracy agreement.

Typical results are shown in figure 60–7 for the most negative (−0.72 volt) and the least negative (−0.076 volt) regions on the sphere. The trajectories shown are in the plane $\psi = \pi/2$. It is only for this condition that the ion trajectories are planar and are not unreasonably difficult to calculate. The trajectories appear to agree qualitatively with those calculated by Jastrow and Pearse (ref. 1). For the low satellite potential used herein, comparatively few ions are deflected from the sheath into the wake. Again, this result is in general agreement with the results in reference 1.

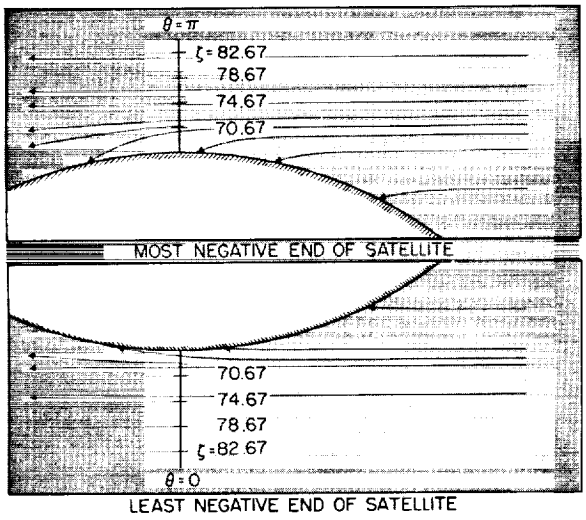

Figure 60–7.—Ion trajectories.

CALCULATION OF COULOMB DRAG

On the basis of the results obtained in the preceding section, the portion of the Coulomb drag of a 4-meter sphere at 1,500 kilometers due to ion scattering has been estimated and shown to be not more than 0.05 of 1 percent of the drag of the uncharged sphere. The portion of the Coulomb drag due to increased ion impringement is calculated from the effective cross-sectional area of the satellite for ion impingement. This effective area, obtained from the calculated trajectories, is shown in figure 60–8. It is 10 percent larger than the projected area of the sphere. The degree of ionization obtained from table 60–I is 23 percent. Therefore the Coulomb drag due to

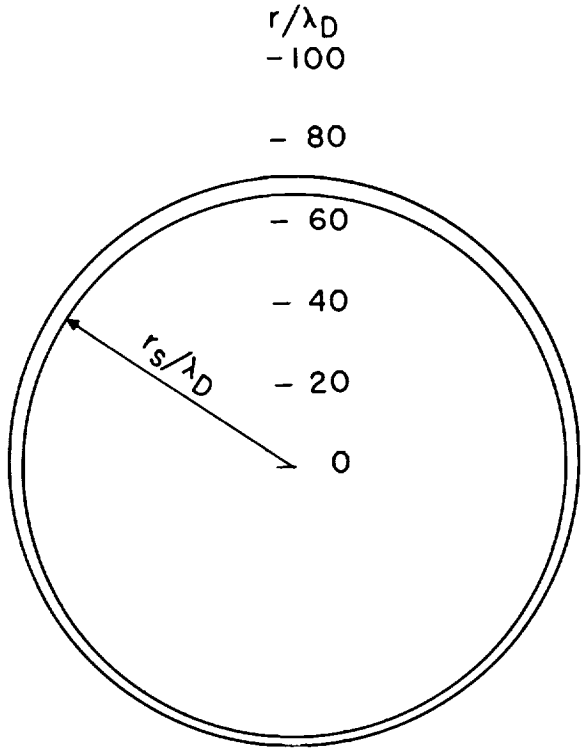

FIGURE 60–8.—Cross section for ion impact.

increased ion impacts is 2.3 percent of the drag of the uncharged sphere.

The conditions in the atmosphere at an altitude of 1,500 kilometers that were used herein are presumably close to average conditions over a cycle of sunspot activity. At sunspot maximum, when the degree of ionization is about twice as large as average, the ratio of the Coulomb drag to the drag of the uncharged sphere would be approximately twice as great as at average conditions. At sunspot minimum, where the degree of ionization is about half that used herein, the ratio of Coulomb to uncharged-sphere drag would be approximately half that shown here.

CALCULATION OF INDUCTION DRAG

The method used herein for calculating induction drag is the following. First, the current in the satellite normal to B must be obtained; to obtain this current, the satellite is considered to be divided into circular elements or rings centered on an axis perpendicular to the directions of both satellite velocity and magnetic flux as shown in figure 60–9. From

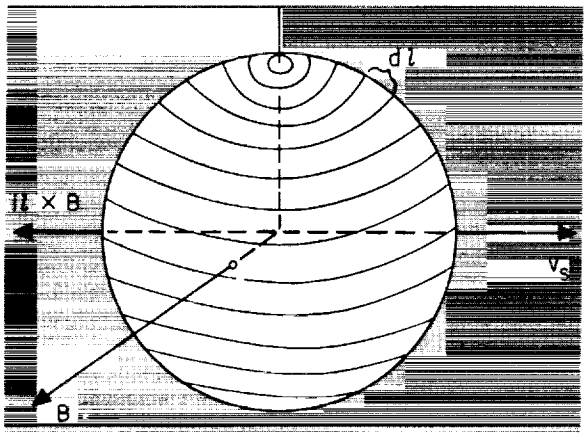

FIGURE 60-9.—Geometry for calculation of induction drag.

the trajectories of the ions, the ion current to the first element is obtained. The electron current to that element is given by the well-known kinetic-theory differential expression for the flux of particles crossing a surface in one direction (with velocities normal to the surface between v and $v+dv$) integrated between the kinetic-energy limits of $-e\phi_s$ and ∞; that is, the electron current density to the spherical surface is

$$j_e = en_{e,\infty}\left(\frac{kT}{2\pi m_e}\right)^{1/2} \sin\theta\cos\psi \exp\left(\frac{e\phi_s}{kT}\right)$$

The net current to the first element is then the difference between the ion current and the electron current to that element. This net current has to flow into the second element, from which this net current plus the net inflow of ion and electron current from the plasma into the second element has to flow into the third element, and so on. Any current flow in the plane of a circular element can be ignored because, for it, $i\times B$ is not in the drag direction. The total induction drag is obtained by summing for all elements the product $i(dl\times B)$.

The magnitude of the induction drag was found to change very little if, instead of using the actual ion trajectories to determine the ion current to the different elements, the satellite is assumed to run into a stationary ion gas. The ion current density to the spherical surface is thus

$$j_i = n_{i,\infty} e v_s \sin\theta\sin\psi \qquad 0\leqq\psi\leqq\pi$$

The net current flowing downward at each one of the circular elements where the polar angle is θ is

$$i=\int_0^\theta\int_0^{2\pi}(j_i-j_e)r_s^2\sin\theta\,d\psi d\theta$$

$$=2n_{i,\infty}ev_sr_s^2\left(\frac{\theta}{2}-\frac{\sin 2\theta}{4}\right)$$

$$-4n_{e,\infty}er_s^2\left(\frac{kT}{2\pi m}\right)^{1/2}\exp\left(\frac{e\phi_{\theta=\pi/2}}{kT}\right)$$

$$\int_0^\theta \sin^2\theta\exp(\alpha\cos\theta)d\theta$$

where

$$\alpha=\frac{eBr_sv_s}{kT}\approx 2.85$$

From this the induction drag is found to be

$$\int i(dl\times B)=\int iBr_s\sin\theta d\theta$$

$$=Br_s^3\left\{n_{i,\infty}ev_s\left(\pi+\frac{2}{3}\right)\right.$$

$$-4n_{e,\infty}e\left(\frac{kT}{2\pi m}\right)^{1/2}\exp\left(\frac{e\phi_{\theta=\pi/2}}{kT}\right)$$

$$\int_0^\pi\left[\int_0^\theta\sin^2\theta\right.$$

$$\left.\left.\exp(\alpha\cos\theta)d\theta\right]\sin\theta\,d\theta\right\}$$

From this expression the induction drag is found to be 1.8×10^{-9} newton, or 1.2 percent of the drag of the uncharged sphere. This is the induction drag calculated for the velocity vector v_s and the magnetic vector B normal to each other. In general, the angle between these two vectors will be less than $\pi/2$ and the induction drag will accordingly be less.

CONCLUDING REMARKS

The potential and the charge distribution in the sheath on a 4-meter-diameter sphere and the drag of the sphere resulting from its electric charge have been calculated for an altitude of 1,500 kilometers. The results are perhaps more accurate than any previously obtained.

The Coulomb drag due to scattering has been shown to be essentially zero. The Coulomb

drag due to increased ion impingement is shown to be 2.3 percent of the drag of the uncharged sphere at average conditions during a solar cycle. The percentage would be approximately doubled for the degree of ionization prevailing at the maximum of the solar cycle of sunspot activity and would be approximately halved at the minimum. These values for Coulomb drag are obtained without taking account of photoemission. If photoemission has the expected effect for an aluminum surface, these values would be decreased. They can therefore be taken to be upper limits which occur when the satellite is in the earth's shadow.

The induction drag due to the electric generator action of the satellite has been shown to be 1.2 percent of the drag of the uncharged sphere for the orientation for which the induction drag is a maximum.

REFERENCES

1. JASTROW, R., and PEARSE, C. A.: Atmospheric Drag on the Satellite. Jour. Geophys. Res., vol. 62, no. 3, Sept. 1957, pp. 413–423.
2. CHOPRA, K. P., and SINGER, S. F.: Drag of a Sphere Moving in a Conducting Fluid in the Presence of a Magnetic Field. Reprint from 1958 Heat Transfer and Fluid Mechanics Institute. Stanford Univ. Press, pp. 166–175.
3. KRAUS, LESTER, and WATSON, KENNETH M.: Plasma Motions Induced by Satellites in the Ionosphere. The Physics of Fluids, vol. 1, no. 6, Nov.–Dec. 1958, pp. 480–488.
4. CHANG, H. H. C., and SMITH, M. C.: On the Drag of a Spherical Satellite Moving in a Partially Ionized Atmosphere. Jour. British Interplanetary Soc., vol. 17, no. 7, Jan.–Feb. 1960, pp. 199–205.
5. JEFIMENKO, OLEG: Effect of the Earth's Magnetic Field on the Motion of an Artificial Satellite. American Jour. Phys., vol. 27, no. 5, May 1959, pp. 344–351.
6. BEARD, DAVID B., and JOHNSON, FRANCIS S.: Charge and Magnetic Field Interaction with Satellites. Jour. Geophys. Res., vol. 65, no. 1, Jan. 1960, pp. 1–7.
7. WYATT, P. J.: Induction Drag on a Large Negatively Charged Satellite Moving in a Magnetic-Field-Free Ionosphere. Jour. Geophys. Res., vol. 65, no. 6, June 1960, pp. 1673–1678.
8. DAVIS, A. H., and HARRIS, I.: Interaction of a Charged Satellite with the Ionosphere. NASA TN D-704, 1961.
9. CHOPRA, K. P.: Interactions of Rapidly Moving Bodies in Terrestrial Atmosphere. Rev. Modern Phys., vol. 33, no. 2, Apr. 1961, pp. 153–189.
10. HOHL, FRANK, and WOOD, GEORGE P.: The Electrostatic and Electromagnetic Drag Forces on a Spherical Satellite in a Rarefied Partially Ionized Atmosphere. For presentation at Third International Symposium on Rarefied Gas Dynamics (Paris, France), June 26–30, 1962. (NASA)

N63-11387

61. Plasma Frequency and Radio Attenuation

By Paul W. Huber and Clifford H. Nelson

PAUL W. HUBER, *Head, Plasma Applications Section of the Aero-Physics Division, NASA Langley Research Center, received his Bachelor of Science degree in Electrical Engineering from Ohio Northern University in May 1942. Joining Langley after graduation, Huber has specialized in the general field of research dealing with real-gas-flow properties. Some of the contributions in this field have included early measurements of vibrational heat-capacity lag in various gases, early measurements of pressure versus time and boundary-layer development in shock tubes, the first direct measurement of Mach stem development and surface effects for spherical blast waves, and the first direct measurement of radio-frequency wave attenuation in a specifiable plasma. Huber is a member of the American Rocket Society. He is author of numerous NASA publications and has presented symposium papers and published journal papers.*

CLIFFORD H. NELSON, *Head, Measurement Research Branch, Instrument Research Division, NASA Langley Research Center, received his Bachelor of Science degree in Electrical Engineering from the University of Washington in June 1938. Nelson is active in the development of flight instrumentation for airborne and space vehicles and techniques for transmitting data by telemetry. He has specialized in the development of techniques for determining the properties of the plasma sheath surrounding space vehicles during atmospheric entry. He is presently investigating the problems of radio telemetry blackout associated with this plasma sheath. Earlier, Nelson was responsible for the development and application of a line of self-contained recording instruments used in flight research with piloted aircraft up to and including the X–15. This array of flight instrumentation has been unequaled on the basis of accuracy and reliability of operation and has received international recognition through the AGARD publications. Nelson is a member of the Instrument Society of America and the Engineers' Club of the Virginia Peninsula.*

SUMMARY

The problem of radio-frequency attenuation due to the interaction of an electromagnetic wave and a plasma layer is reviewed with particular attention to that aspect dealing with communications during the reentry phase of space-flight missions. The need for concerted effort on the problem is first brought out by the projection of radio blackout data from current missions to that of second-generation missions. The electromagnetic plasma parameters are discussed in relation to their influence on the wave propagation properties. It is shown that theoretical models of wave-plasma interaction (absorption and reflection) can be synthesized to approximate the reentry plasma-layer problem, which is interaction with relatively dense plasmas having gradients of finite extent with respect to a signal wavelength. Comparison of flight results with those obtained with a simplified conceptual model is presented. Finally, various means by which the attenuation problem may be alleviated or circumvented are reviewed and the capabilities for laboratory and flight model tests are outlined.

666582 O—62——23

35

INTRODUCTION

Almost everyone is familiar with one radio attenuation problem associated with reentry from space flight, this of course being the Mercury-Atlas radio blackout period experienced by the Astronauts. It was observed in these missions that there was a period of a few minutes in which communications both from and to the capsule were totally obstructed by the ionization layer formed about the body during the reentry phase of the mission (ref. 1). Although this was by no means the first time such a phenomenon has been observed, it did nevertheless serve to dramatically reemphasize the importance of the problem and, indeed, to substantiate the current factual as well as conceptual thinking to a surprising degree.

It had been previously established, from many tests of unmanned vehicles and from evaluation of gross theoretical models of the electromagnetic-wave—plasma interaction problems, that radio interference effects can and do exist in both the boost and reentry phases and can compromise the operational, not to mention the psychological, aspects of space flight. The really disturbing part about the situation is that for the second-generation space-flight missions, such as Apollo and other planned space and planetary probes, these effects appear to be greatly magnified in the light of present technology, so that data systems as well as monitoring and command systems may be seriously impaired. In some instances, however, tracking by means of radar may be improved (ref. 2). It is well, then, to review and examine the present status of knowledge and technology in regard to radio attenuation with a view toward delineation of the problem areas and avenues which might be pursued in the hope for solutions.

The general flight blackout problem can be briefly reviewed by first examining the data from Mercury space-flight missions. Figure 61–1 illustrates the relationship of the plasma layer or ionization layer with respect to the vehicle, its aerodynamic flow field, and the communications system. The plasma layer is located between the surface of the vehicle and the main shock wave, and not only does it completely surround the body but it may extend to a distance of many body dimensions behind the vehicle. The important point to be noted is that the radio-frequency (RF) signals both from the capsule and from the ground are reflected and/or absorbed by the plasma layer which is thus acting as a shield to obstruct communications from both directions.

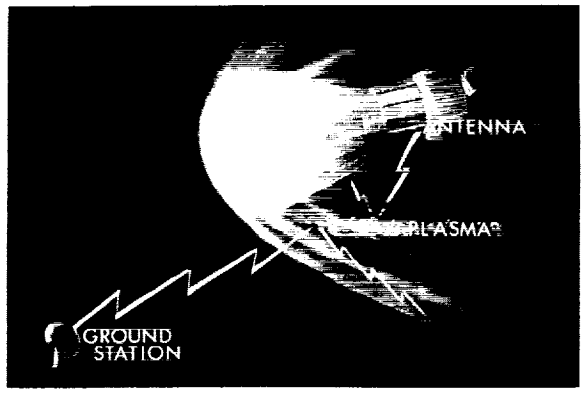

FIGURE 61–1.—Signal blackout due to plasma layer.

Figure 61–2 shows the velocity-altitude spectrum in which this signal impairment is manifested for the Mercury spacecraft VHF voice telemetry as well as the C-band radar-beacon signal. The upper shaded region is an experience curve gained from a variety of other flight experiments. A possible Apollo path is shown by the dashed curve for comparison. The Mercury beacon signal was not completely blacked out but was greatly attenuated for the short period shown. The VHF signal was blacked out completely for a few minutes, in which time the capsule traversed a distance measured in hundreds of miles. For the Apollo curve shown in this figure, the beacon signal would be cer-

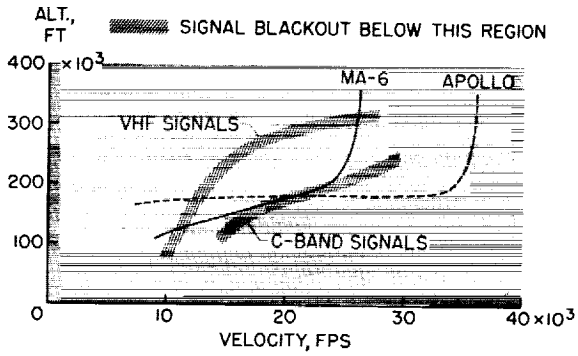

FIGURE 61–2.—Radio frequency blackout regions for Mercury-Atlas communications.

tainly blacked out completely and the VHF blackout period would be expressed in terms of thousands of miles traversed by the capsule. Lack of communications during such a lengthy period could very well mean a greatly increased requirement for the onboard navigation and flight evaluation system, which in turn is measured in increased payload or decreased mission capability, not to mention reliability.

SYMBOLS

B	magnetic induction
c_o	speed of light
E	electric field intensity, $r+js$
e	charge on electron
f	signal frequency
k	propagation parameter, $\alpha+j\beta$
k_1	value of propagation parameter in uniform plasma
m	mass of electron
N	concentration
n	index of refraction
Q	average effective momentum transfer cross section for electron-particle collision
R	amplitude of reflected wave
T	amplitude of transmitted wave
r	real part of E
s	imaginary part of E
t	time
V	real part of $(k/k_0)^2$
W	imaginary part of $(k/k_o)^2$
w_e	mean thermal velocity of electrons
x, y, z	space coordinates
α	phase parameter
β	attenuation parameter
Δ	thickness of shock layer
λ	wavelength
ν	electron collision frequency
ϕ	angle of incidence
ω	angular signal frequency, $2\pi f$
ω_b	cyclotron frequency, $\frac{eB}{mc_0}$
ω_p	plasma frequency, $\left[\frac{4\pi e^2 N_e}{m}\right]^{1/2}$

Subscripts:

b	dependent on B
e	electron
i	particle other than electron
o	in vacuum
p	plasma
$\parallel$	E vector parallel to plane of incidence
$\perp$	E vector perpendicular to plane of incidence
∞	semi-infinite homogeneous plasma with N_e discontinuous at boundary
1, 2	designate particular values of y

CHARACTER OF PLASMA LAYER

In order to study some of the fundamental aspects of the interaction of electromagnetic (E.M.) waves and plasmas, in particular, plasmas of the type associated with blunt-body reentry into an earth or planetary atmosphere, the reentry plasmas must first be defined or characterized. It is necessary to know both the magnitude and spatial extent of plasma properties during reentry. The determination of the shock-layer flow field, and hence plasma properties, about blunted bodies in hypersonic flow is indeed a complex mixture of disciplines. These disciplines include hypersonic aerodynamics, high-temperature thermodynamics, multicomponent chemical kinetics, and viscous ablating flow, even for the simpler continuum-flow concept of primary interest. Although it is not within the scope of this presentation to review these theoretical methods, suffice it to say that only a very limited number of such computations have been made for highly blunted bodies and these are either restricted to the nose region or are for thermochemical equilibrium and/or inviscid flow (refs. 3 to 6). Such results do, however, provide a good indication of the influence of the various flight parameters on the plasma characteristics and serve as inputs for first-order radio attenuation estimates. There are few, if any, direct experimental plasma measurements available for application to this problem. The general character of the plasma in the shock layer, as based on present knowledge (ref. 3), is illustrated in figure 61–3. The plots show the spatial variation of the electromagnetic plasma parameters—free electron concentration and electron collision frequency—along a path normal to the body surface for an aft location on a blunted body at a possible reentry flight condition. Note particularly the nonlinear, nonmonotonic variation of N_e, the peak value of N_e, and the relatively constant value of ν. It might also be noted that the only part of the layer which is of particular consequence with regard to RF attenuation is that part with a value of N_e higher than approximately 10^6 cm^{-3}. The number 10^6 is of significance in that this is about the maximum electron concentration in the ionosphere (refs. 7 to 9) through which, of course,

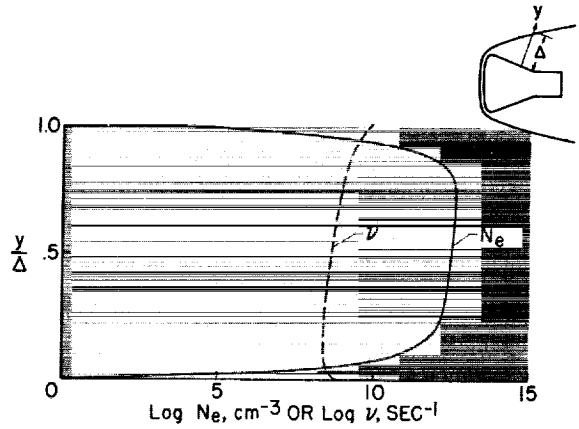

FIGURE 61–3.—Typical variation of electromagnetic parameters in shock layer.

any space communications system must be capable of transmitting a priori.

Since the reentry plasma layer has been defined, at least in qualitative fashion, the problem of electromagnetic wave interaction with this plasma can now be considered. Probably the best way to do this is to look first at the simplest type of an interaction, bringing out the important plasma parameters and their influence on the wave propagation nature. It should then be possible to consider the influence on the propagation of the various nonidealities which comprise the actual plasma-wave model and, thereby, attempt to synthesize a more comprehensive picture of the problem.

PLASMA PROPERTIES FOR ELECTROMAGNETIC WAVE INTERACTIONS

From a solution of Maxwell's equations for the simplest interaction, that of a plane wave in a uniform plasma, expressions can be derived to show the perturbations on the electromagnetic wave due to the presence of the plasma—that is, propagation characteristics in the plasma as compared, for example, with propagation characteristics in a free-space medium. By using also the equation of motion of an electron in an infinite uniform plasma undergoing harmonic oscillation (the ions may be considered stationary for RF frequencies), it can be further shown that there is a parameter known as plasma frequency which defines a range in the wave frequency spectrum in which these perturbations are not small (refs. 8 and 10 to 13). It is this range—where signal frequency is of the order of or less than the property called plasma frequency—that is of particular interest. Within this range, a significant part of the wave electric energy can become transformed into electron kinetic energy and thus alter the wave characteristics. The result is manifested by displacement currents and conduction currents in the plasma, depending furthermore upon the rate at which electrons can collide with other particles in the plasma and the strength of any imposed magnetic field. (Radiation damping due to electron oscillation is negligible for RF frequencies.) Therefore, the plasma properties for wave propagation—that is, the index of refraction and attenuation coefficient—are expressible in terms of the parameters: plasma frequency, collision frequency, and magnetic-field strength.

Since the plasma-frequency parameter is the most important of the plasma properties, it is discussed first. This parameter is also called characteristic frequency and sometimes critical frequency and is a convenient lumped parameter having the dimensions of frequency. However, it is an inherent property of the plasma. For example, consider in an infinite plasma that some of the electrons are displaced from their equilibrium position in the plasma due to the application of some force on the electron. A restoring space charge field is then created which, if the displacing force is suddenly removed, causes the electrons to oscillate about their equilibrium at a frequency proportional to the plasma frequency. The value of the restoring field (and the plasma frequency) is dependent exclusively on the free electron concentration in the plasma—that is, the number of free electrons in a unit of volume. It is intuitively obvious that, when the exciting frequency (signal frequency) becomes equal to this characteristic frequency of oscillation, the electromagnetic properties of a plasma may exhibit marked changes, as indeed they do.

The other important plasma property is called electron collision frequency and is representative of the rate at which electrons interact with other particles in the plasma. (See refs. 11 and 14 to 17.) This property indicates the

lossy or dissipation properties of the plasma resulting from the transport of electron energy. These electron interactions may be binary with neutral species or ions, or with several particles concurrently, and may be elastic or inelastic, all depending on the thermal and state properties of the plasma and the strength of the electromagnetic wave.

It is well to point out that the reentry plasmas which are of importance to RF attenuation generally fall into the category of weakly ionized, dense gases—that is, most of the particles are neutral atoms and molecules and a relatively small fraction are free electrons and ions, but the density of electrons and rate of electron collisions are relatively high.

SIMPLE INTERACTION MODEL

The simplest type of wave-plasma interaction is illustrated in figure 61–4 where a plane wave propagating in free space is normally incident upon a semi-infinite uniform plasma. The boundary in this model is a discontinuous jump from the free-space values to the plasma values of the propagation parameters. After impingement of the incident wave upon the plasma, two waves are generated: one propagated into the plasma (the transmitted wave) and the other reflected away from the plasma. The following properties of these waves may be determined from the solutions appropriate to this model (ref. 13):

$$n=\frac{\alpha c_o}{\omega}=\left[\frac{V+\sqrt{V^2+W^2}}{2}\right]^{1/2}$$

$$\frac{\beta c_o}{\omega}=\left[\frac{-V+\sqrt{V^2+W^2}}{2}\right]^{1/2}$$

where

$$V=1-\left[\left(\frac{\nu}{\omega_p}\right)^2+\left(\frac{\omega}{\omega_p}\right)^2\right]^{-1/2}$$

$$W=\frac{\nu}{\omega}\left[\left(\frac{\nu}{\omega_p}\right)^2+\left(\frac{\omega}{\omega_p}\right)^2\right]^{-1/2}$$

$$R_\infty{}^2=\frac{(\alpha_o-\alpha)^2+(\beta_o-\beta)^2}{(\alpha_o+\alpha)^2+(\beta_o+\beta)^2}$$

$$\omega_p=2\pi(8970)\sqrt{N_e}$$

$$\nu=\overline{w}_e\sum_i N_i Q_i$$

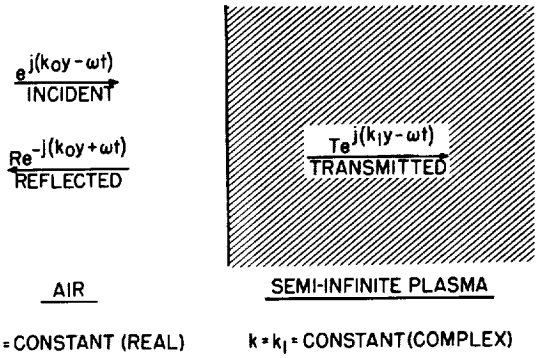

FIGURE 61–4.—Simple wave-plasma model (semi-infinite uniform plasma).

In these equations the propagation parameters, index of refraction (or phase constant) and the extinction (or attenuation) coefficient, are seen as functions of the plasma frequency and collision frequency at a given signal frequency. The reflection coefficient for this semi-infinite type of reflection is seen also as a function of the plasma properties. For this wave-plasma model only one reflection occurs, and the strength of the reflected wave is constant in time and space. The transmitted wave, however, is weakened due to absorption in the plasma for each unit of plasma thickness traversed. In each element of plasma, a portion of the wave electric energy is lost to electron kinetic energy which, when equilibrated, appears as an increase in the thermal energy of the plasma, although this increase is of a thermally negligible amount. The fractional loss of wave energy, however, is by no means negligible over a large portion of the wave frequency spectrum as can be illustrated by a plot such as that shown in figure 61–5 which is similar to a sketch in reference 18. It is seen that, for wave frequencies much less than the plasma frequency, the plasma is highly reflective and almost all the energy is reflected away. In such a case the plasma acts like a conductor; penetration of the wave into the plasma is small, and equivalent displacement currents in the plasma act to change only the index of refraction. At the other end of the spectrum ($\omega>\omega_p$) where the signal frequency is very high, the plasma is completely transparent to the wave (acts as a good dielectric) and no consequential effects are noted. In the intermediate frequency region,

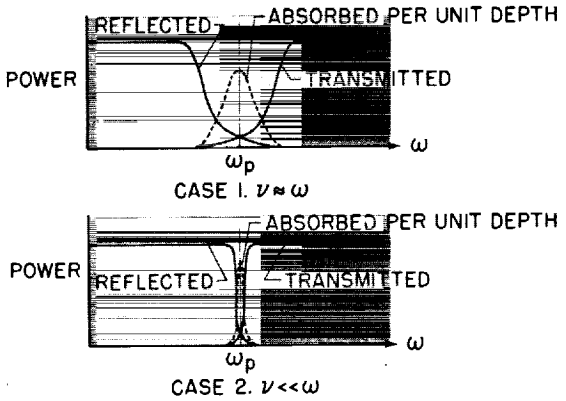

FIGURE 61–5.—Influence of parameters on wave propagation.

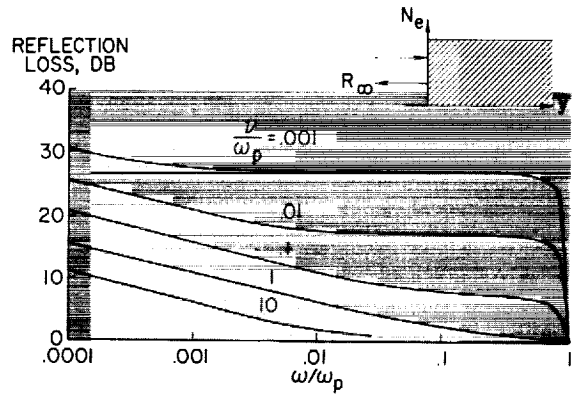

FIGURE 61–7.—Signal loss due to reflection at semi-infinite plasma interface.

however, the situation is quite mixed, depending, in addition to the plasma frequency, upon the value of the electron collision frequency. In this frequency regime, the plasma is like a lossy dielectric and some of the wave energy is reflected back and the remaining energy is lost by plasma absorption. The region where $\omega \approx \omega_p$ is frequently referred to as the cutoff region. It is seen, therefore, from these results that the most important plasma parameter for determination of wave propagation characteristics is the plasma frequency or, in the most explicit terms, the free-electron concentration.

Figures 61–6 and 61–7 show in normalized form the explicit dependence of absorption per unit plasma thickness and of the reflection on the electromagnetic plasma parameters for the simple wave-plasma model. To be noted in figure 61–6 (from ref. 19) is the interesting result that for very low frequencies the absorption loss falls off. If, therefore, the reflection losses are not too great, the use of very low frequency (as well as very high frequency) is suggested.

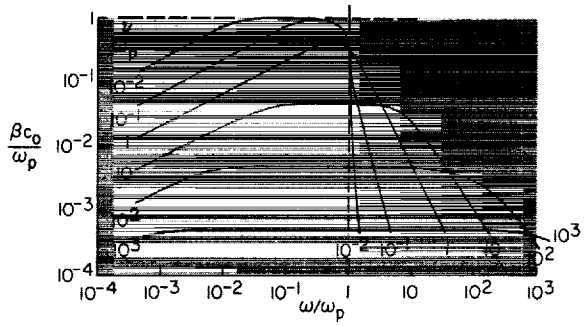

FIGURE 61–6.—Normalized plane-wave attenuation in a uniform plasma.

NONUNIFORM, FINITE-THICKNESS MODELS

It is interesting to consider the effect of replacing the abrupt change of properties at the air-plasma interface with a more gradual and continuous change. The general problem of wave propagation at normal incidence through a nonuniform plasma has been formulated by John S. Evans of the Langley Research Center (see ref. 20) and involves numerical integration, through the plasma layer, of the following equations:

$$\frac{d^2r}{dy^2}+k_o^2(rV-sW)=0$$

$$\frac{d^2s}{dy^2}+k_o^2(sV+rW)=0$$

where r and s are the real and imaginary parts, respectively, of the electric vector. The numerical integration of the propagation equations is done by using the Runge-Kutta method on an IBM 7090 electronic data processing system. Such a program can be used to find the transmitted and reflected wave strengths for any pathwise variation of plasma properties whether discontinuous or gradual, but, of course, the number of integration steps is dependent upon the magnitude of the gradients. An analytical method (ref. 21) has also been developed which is applicable to special types of plasma property variations (linear ramps and combinations of ramps and uniform plas-

mas) for transmission at normal incidence. Solutions are obtained in the form of complex Airy functions and numerical evaluation performed by a machine. Since the results of these two programs are compatible, they are not separately discussed but are used hereinafter to illustrate effects of plasma nonuniformity. Figure 61–8 shows such an effect on the reflected wave strength for a linear variation of properties from free-space to plasma values. It is seen from this figure that the reflected power drops markedly from the discontinuous-jump value when the ramp length (linear region) increases to a fraction of the signal wavelength, the effect being only weakly dependent on the plasma absorptivity for the shorter ramp lengths. It can be also shown that gradients other than the linear ramp gradient produce effects generally similar to those shown in this figure, but such details as these are not discussed herein. With regard to the absorption properties, it can be shown that for gradients in the plasma the absorption is generally closely evaluated by summation or integration of the local absorption coefficients along the propagation path, the gradients not being of first-order influence (ref. 22).

The next aspect to be considered is the effect of finite extent of the plasma (as contrasted to the semi-infinite plasma) on the reflection properties of the plasma. Since it was just shown that gradients having dimensions greater than 1/10 wavelength or so reduced the reflection significantly, there would naturally be the

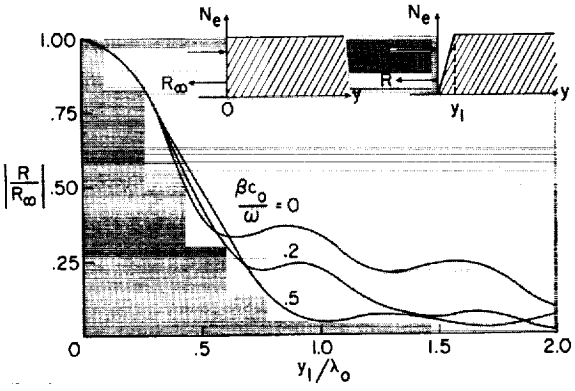

FIGURE 61–8.—Effect of plasma gradient on the semi-infinite plasma reflection. $n=0.5$.

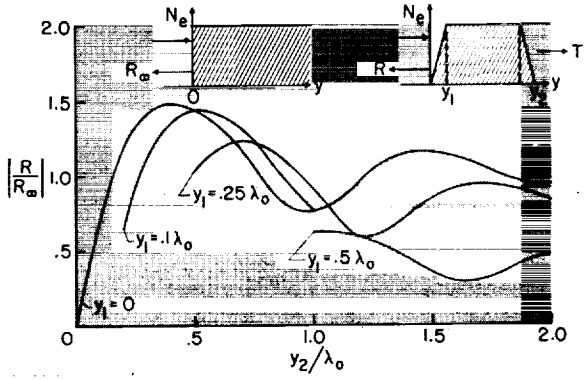

FIGURE 61–9.—Effect of finite extent of plasma on the reflection. $n=0.5$; $\frac{\beta c_o}{\omega}=0.1$.

question of what happens when the plasma thickness is comparable to the wavelength of the signal. Figure 61–9 shows the effect of plasma extent (i.e., layer or slab thickness) on reflection for two types of plasma boundaries—a discontinuous jump and a linear ramp gradient, each type occurring at both the forward and rearward plasma boundaries. Although the interferometer effect—that is, interference and reinforcement at fractional wavelength multiples—might be expected, the fact that the plasma absorptivity can be high also when the refractivity is high would generally tend it toward the highly damped case. However, to illustrate most simply the effect of plasma extent on reflection, a weakly absorbing plasma is shown here. It is seen for this plasma that the reflectivity of the layer indeed varies periodically with the plasma extent measured in multiples of the signal wavelength. (The wavelength in the plasma is not equal to the free-space wavelength.) For high absorptivity, such as the more usual reentry plasma case, the wave cannot penetrate very far (i.e., fraction of a wavelength) into the plasma before much of its strength is dissipated, and the interferometer effect is then masked.

SIMPLIFIED ATTENUATION CONCEPT APPLIED TO FLIGHT RESULTS

Since the plasma model at least grossly resembles the actual plasma problem (compare figs. 61–3 and 61–9) the situation for plane-

wave RF transmission at normal incidence can now be briefly summarized. When the plasma is thick and $\omega<\omega_p$, the effects of gradients on reflection are unimportant, since the signal will be nearly all lost by absorption anyway. When the plasma is thin and $\omega<\omega_p$, the reflection problem may be the determining one, and the signal losses will not be as high as those predicted by the semi-infinite, discontinuous model. When $\omega>\omega_p$, there is no problem for any thickness; when $\omega\approx\omega_p$, the magnitude of the problem for both reflection and absorption depends furthermore on the value of ν—that is, depends on altitude as well as thickness. Of course, ω_p, which is always the prime parameter, depends on both velocity and altitude. To illustrate the possible range of variation of the plasma parameters N_e and ν during reentry, plots of the normal shock and equilibrium far-wake values calculated at the Langley Research Center are shown in figure 61–10 for a blunt-body trajectory such as Mercury. Note the strong increase in plasma parameters in the early reentry period. The cases shown should be representative of the most extreme and least extreme values likely to occur in the shock layer. Since rather large bodies will generally be used for the manned space missions—that is, plasmas of the thick variety—the problem can be reduced to the simple question of when is the maximum value of plasma frequency in the shock layer higher than the signal frequency. In order to assess the value of such an attentuation yardstick, a study of figure 61–11 is of interest. In this figure are shown, on a velocity-altitude map, the contours of plasma frequency which might be characteristic of maximum shock-layer values occurring at an aft location on a large blunt body. These values were computed at the Langley Research Center according to the following simplified aerothermodynamic flow model for a frozen flow, far wake. It was assumed that the stagnation (or normal shock) flow streamline reached a condition of thermochemical equilibrium in the nose region (all the reaction and relaxation rates infinite) and then was expanded very suddenly (as around the corner and into the afterbody region) to ambient pressure. In the expansion, no chemical recombination was assumed to occur, which means the composition was frozen at the nose value (internal energy was allowed to follow the expansion) and is analogous to a flow model of very slow reaction rates. Such a flow model is a gross oversimplification of the actual finite rate, three-dimensional flow case but is certainly more appropriate than other simplified conceptual models—for example, the normal-shock flow or equilibrium-wake flow values shown in figure 61–10. (Note the ticks at 260 mc and 5.5 kmc.) It is seen that, fortuitously or not, the points in the MA–6 flight between which blackout occurred (>53-db attenuation) correspond very closely to the points at which the signal frequency equaled the computed plasma frequency. For the C-band beacon signal, actual blackout did not occur but the signal dropped to nearly the noise level of the receivers and was, in fact, highly attenuated (approximately 37 db). It would, of course, be dangerous, at this point, to consider

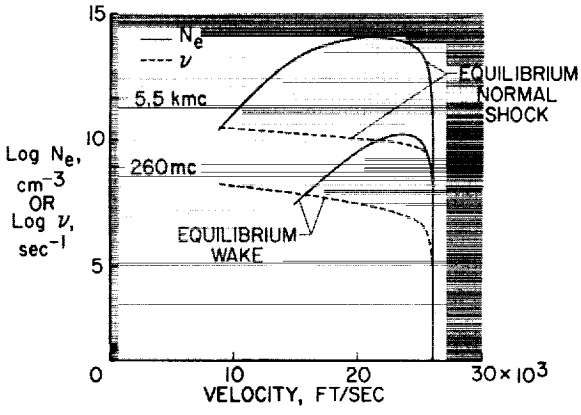

FIGURE 67–10.—Variation of N_e and ν during reentry.

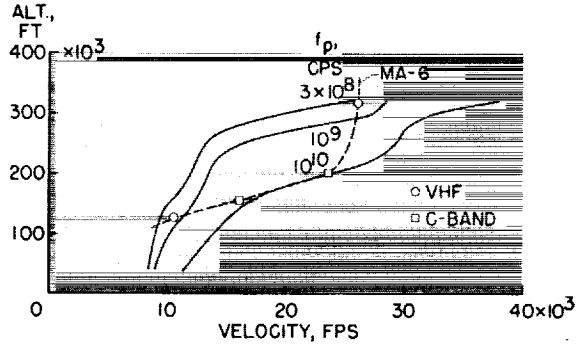

FIGURE 61–11.—Comparison of flight blackout data with simplified concept.

such agreement as being indicative of general applicability of such a concept to other bodies or to other flight trajectories.

OTHER INTERACTION MODELS

Propagation at oblique incidence to the plasma layer should be considered in the RF attenuation problem since the look angle of the wave path will not always be normal or near normal, as for the models discussed so far. Oblique propagation has not yet, however, been worked out for the case of a dissipative nonuniform plasma of small extent—that is, where gradients occur in small parts of a wavelength, as appropriate to the reentry plasma. The magneto-ionic (propagation through the ionosphere) theories treat the oblique propagation from the standpoint of geometric optics, in which the nonuniformities are assumed to occur very gradually with respect to signal wavelengths. (See ref. 23.) To illustrate the qualitative nature of the actual problem, some results obtained for a thin, lossy, uniform plasma applied to propagation at oblique incidence are presented in figure 61–12. These results are from a program developed for the IBM 7090 electronic data processing system by Calvin Swift of the Langley Research Center. For the oblique case, the wave propagation must be shown in two modes, $T\parallel^2$ and $T\perp^2$, since the two modes will behave differently due to polarization effects. The $T\parallel$ mode is that part

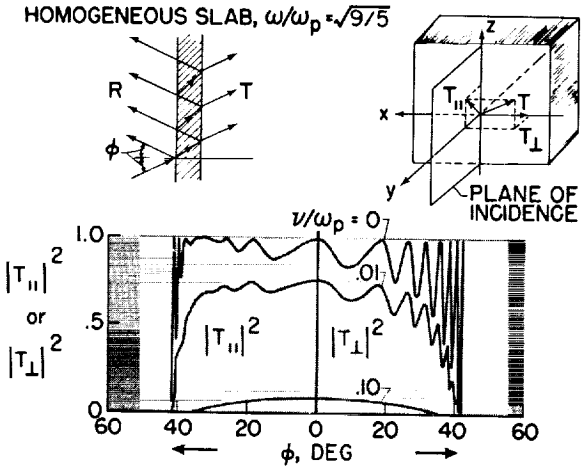

FIGURE 61–12.—Effect on transmission of signal incidence angle.

of the transmitted E vector which is parallel to the plane of incidence and the $T\perp$ mode is that part which is perpendicular to the incidence plane, as shown in the figure. The periodic nature of the transmitted power ratio $|T|^2$ as a function of incidence angle is also seen in the figure and is due to multiple reflections occurring at the two interfaces (indicated in the sketch on the left). For the dissipative case, this effect is washed out by wave absorption. The important result is that, as in the case of optical refraction at oblique incidence, there is a critical angle of incidence beyond which no transmission through the medium is possible because of complete reflection of the wave.

The other interaction model which has not as yet been discussed is propagation in the presence of an imposed magnetic field. This is a very important problem, since it offers the possibility of providing "transmission windows" in parts of the wave frequency spectrum which would otherwise be opaque to RF transmission (ref. 24). The effect may be briefly explained as follows. In the presence of a static magnetic field, a free electron describes a circular motion about the field lines at a frequency (the gyrofrequency) which is proportional to the strength of the magnetic field and with a radius of gyration which decreases as the field increases. Since the electron motion in the plane transverse to the magnetic field is thereby altered, new propagation modes may be introduced, depending upon the orientation of the electromagnetic wave. For example, if a wave is propagated parallel to the field lines and the field is infinitely strong, then no electron motion can occur in the plane transverse to the propagation direction and, hence, there can be no interaction even when $\omega < \omega_p$. This problem has been studied for the model of a lossy, uniform, semi-infinite plasma for normal incidence of circularly polarized waves propagating parallel to the field lines and for propagation of electromagnetic waves transverse to the field lines. The first case is of particular interest since the location of the window is not dependent upon the value of the plasma frequency but only upon the strength of the magnetic field for a collisionless plasma. For a

plasma with collisions the reduction of attenuation becomes less significant as the collision frequency increases. Figure 61–13 shows the effects of varying magnetic-field strength and collision frequency on the absorption properties, and figure 61–14 shows the effects on the reflection properties (in normalized form) of a semi-infinite, uniform plasma for normal incidence of right-hand circularly polarized waves when the field lines are parallel to the propagation direction. No results are yet available for nonuniform, finite-thickness plasmas.

There are a number of other interaction problems which may be of importance in certain situations, and they are only mentioned since there is considerable complexity and uncertainty involved in their formulation and assessment. (1) The near-field propagation problem involves alteration of the field of the antenna due to proximity of the plasma and, near the antenna, the wave is not like a plane wave, as was assumed for all the models considered. (2) Mismatch of impedance and detuning of the antenna, due to proximity of the plasma, have the effect of reducing the efficiency of the radiating system, and hence a signal degradation. (3) Voltage breakdown of the antenna elements may occur for high-power levels or low-density plasmas (resulting from field ionization near the antenna) and may greatly reduce the signal. (4) A nonplane plasma layer (radius of curvature less than wavelength) may introduce deviations from the plane-wave-slab model.

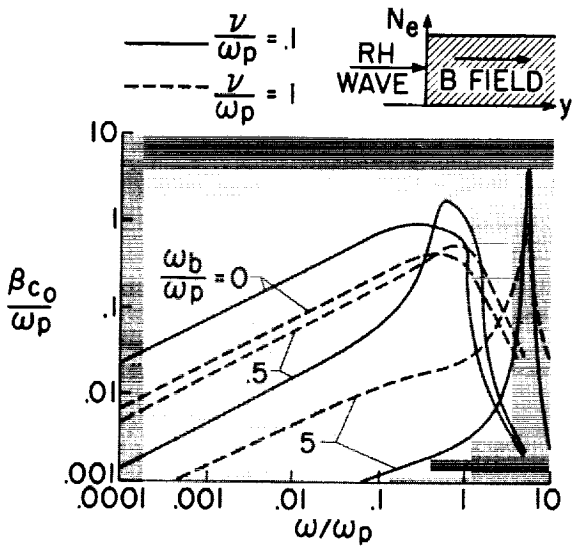

FIGURE 61–13.—Effect of magnetic field on wave-plasma absorption.

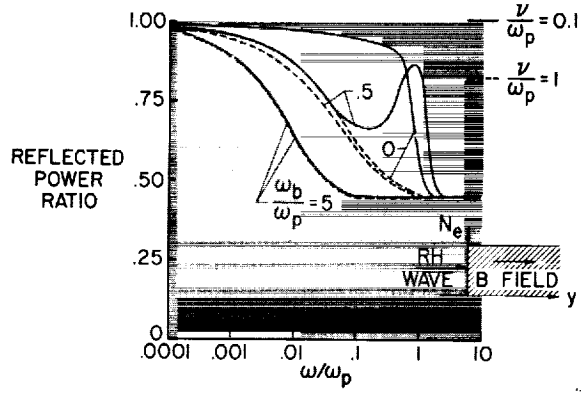

FIGURE 61–14.—Effect of magnetic field on reflected power ratio.

MEANS FOR ACCOMPLISHING RADIO-FREQUENCY FLIGHT COMMUNICATION

From the discussion of the wave interaction problem for a plasma of the type to be expected in flight, some feeling for the parametric dependence of the problem has now been obtained. It would be well then to enumerate and assess the possible schemes which might be considered for maintaining transmission through the plasma during the critical part of the flight.

(1) Selection of signal frequency:

It has been shown that, for signal frequencies higher than the plasma frequency, transmission is possible. (See also ref. 25.) It can also be shown that in some cases (depends also on ν) very low frequencies will permit transmission. Because of the large investment in worldwide communications systems, as well as other problems, selection of frequency is not practicable outside of rather narrow limits. However, if such was possible, the Mercury spacecraft would require the X-band and the Appollo spacecraft would require at least the K_a-band for continuous transmission (see figs. 61–2 and 61–11), if the concept in figure 61–11 applies. This, in turn, introduces acquisition problems and atmospheric absorption problems, but neither of these is insurmountable. Selection of very low frequencies entails problems with atmospheric noise and antennas and is of inconclusive value, based on present knowledge.

(2) Use of applied magnetic fields:

This scheme was, of course, not evaluated for the actual reentry-type plasma model, but by basing an estimate on the numbers from the uniform semi-infinite case and using peak shock-layer plasma properties, required magnetic-field strengths can be estimated. It would appear from such an assessment that the scheme requires magnetic-field producing systems of impracticably large size for the large manned vehicles, even considering the cryogenic superconductors. For small vehicles, however, the scheme offers very promising possibilities, since the field strengths can still be high at the smaller absolute distance out from the body surface where peak ω_p occurs.

(3) Aerodynamic shaping:

This scheme involves the use of small bodies which might be mounted on the larger body to protrude outside of the main plasma layer. If the small body is the RF radiator, then the layer obstructing transmission will be relatively thin. It is certain that the absorption losses will be reduced in such a scheme, but the change in reflection loss is inconclusive lacking numerical evaluation of the actual case (scaling problem). The scheme is certainly an attractive one, provided that the cooling problems associated with the small probe and its mount are not too restrictive.

(4) Material injection:

This scheme might be referred to as the brute force scheme, since the material injection is for the purpose of cooling and/or neutralizing the plasma, as a means for reduction of the ionization. The injection of material may act as a heat sink (to lower the thermal state and, hence, ionization) and/or be electrophilic (to reduce the free-electron concentration by attachment). (See ref. 26.) The result is, hopefully, to open up a hole in the plasma layer for signal transmission or, in the case of small-body nose injection, to eliminate the ionization layer entirely. Also, selection of proper ablation products may act to reduce attenuation if the mixing and diffusion processes are great enough. On the other hand, ablation may work against the scheme, if the ablation products are easily ionizable.

(5) Miscellaneous schemes:

Other schemes which might be mentioned but are not discussed due to the uncertainty involved in the formulation and evaluation of the ideas are as follows: (a) Use of the plasma layer as an electromagnetic radiator by some means of coupling the transmitter to the sheath; (b) use of modulated electron beams to introduce new propagation modes into the plasma; (c) modulation of the plasma properties from within to accomplish a modulation on a reflected continuous-wave signal from the ground (similar to, or a variation of, the Luxemburg effect); (d) use of modulated laser; and (e) finally, if there is no other resort or if real-time telemetry is not absolutely required, the storage and playback, or storage and recovery, type of systems may be used for the various flight data. This is not a very happy solution for manned flight.

OTHER FLIGHT RADIO-FREQUENCY PROPAGATION PROBLEMS

A problem of much interest with regards to tracking, detection, and discrimination of hypersonic vehicles during reentry is that of radar scattering from the vehicle and its plasma layer, including primarily the wake or trail plasma. (See refs. 2 and 27.) It has been observed that the signal may be at times absorbed by the gas cap (strong plasma layer around the nose) of the vehicle or that the reflected signal may actually be enhanced due to an apparent increase in the vehicle size, which is actually an increase in the radar cross section due to the growth of the plasma into the wake. This wake plasma may be very extensive at times and depends on many uncertain factors, such as ionization of ablation products in the wake, frozen recombination of the body flow-field plasma when expanded into the wake, and action of diffusion and mixing processes in the wake and ambient atmosphere (refs. 28 to 31). This is analogous to the meteor trail phenomena to a large extent but occurs at velocities lower than the usual meteor atmospheric entry.

Another interesting problem which is of great concern to communications and tracking from the launch site is that of rocket plume attenuation. In such a phenomenon, there is ionization in the rocket exhaust products or at the plume-air interface (again, due to the action of some uncertain factors) which results in a per-

turbation of the signal propagation through the plume (ref. 32). These uncertain factors may include chemi-ionization (nonequilibrium ionization in a combustion process) in the plume or at the interface, nonequilibrium expansion of the rocket combustion products, or seeding of the plume with ablated rocket-nozzle material. A much less likely factor is that of equilibrium ionization in the plume or plume-air mixture.

Another currently perplexing problem is that of signal propagation during the entry of a space vehicle into a planetary atmosphere, such as Venus or Mars, in order to effect telemetry of information about the planetary properties before a hard landing. The primary difference between this problem and an earth reentry communications problem is in the definition of the flow-field plasma properties resulting from the different chemistry involved (different atmospheric constituency). Once the electromagnetic properties of the plasma layer can be specified, the wave propagation problem should be no less tenable than another.

Finally, the problem of plasma noise should be mentioned, since this source of incoherent RF radiation may be troublesome over a wide frequency range. This radiation originates from within the plasma and may be due to processes known as Bremstrahlung (free-free transitions) recombination, or from unstable plasma oscillations due to electron density gradients. In any case, a plasma noise level is added to the communications system noise level, and this is not desirable.

LABORATORY AND FLIGHT RADIO-FREQUENCY ATTENUATION STUDIES

Generally, the type of tests which may be carried out in the study of the RF wave-plasma attenuation problem falls into one of the following categories: (1) Diagnostic studies aimed at the experimental determination of electromagnetic plasma properties in reentry plasma layers, rocket plumes, and others, or the study and development of techniques and equipment for this purpose. Such techniques may be direct or passive and may involve probes, reflectometers, optical devices, and others. (2) Interaction studies aimed at understanding the basic nature of particular wave-plasma interaction mechanisms by comparison of experimental determinations with theoretically evaluated results of tenable models (ref. 33). (3) Simulated flight tests in which conditions are produced in laboratory configurations which largely reconstruct or simulate the particular flight communications problem and thereby allow for bulk experimental data (attenuation, VSWR, etc.) which might be representative of the actual flight situation. Some of the main difficulties in this idea are: (a) production of very high kinetic energy air flow at proper ambient conditions, (b) wave reflection problems from the walls of the facility, (c) interference from electrical equipment used in the production of the flow or for equipment power, and (d) the problem of scaling the results from small models to the full-size vehicle (ref. 34). Involved primarily in the scaling problem are the separate aspects of viscous-flow scaling and scaling of the reflection effects, the latter being very uncertain due to the opposing aspects of electron density gradients (dN_e/dy) and extent of the plasma (λ/Body scale) which are in turn dependent also upon the viscous scaling. (4) Actual flight communications tests using models or portions of the space vehicle under the flight conditions expected for the vehicle. This technique is, of course, not usually economical but may be necessary to establish necessary criteria otherwise indeterminate, or for expediency. The cost can certainly be far less than the actual space mission cost since the payload, range, and so forth, need not be nearly as large. For small flight models, the same scaling problems exist as for laboratory models.

Various experimental programs are underway at a number of laboratories, which involve one or more of the aforementioned approaches. A shock tunnel program at Cornell Aeronautical Laboratory (ref. 4) is used for simulated flight studies and employs a fiber-glass nozzle to permit microwave transmission to models in the test section. At the Langley Research Center a comprehensive program known as RAM (radio attenuation measurement) is underway which involves portions of each of the foregoing categories (refs. 20 and 35) with flight tests serving as verifications of the concepts

developed from theoretical and experimental ground studies.

CONCLUDING REMARKS

The problem of radio-frequency attenuation due to the interaction of an electromagnetic wave and a plasma layer has been reviewed with particular attention to that aspect dealing with communications during the reentry phase of space-flight missions. The electromagnetic plasma parameters have been discussed in relation to their influence on the wave propagation properties. It has been shown that theoretical models of wave-plasma interaction (absorption and reflection) can be synthesized to approximate the reentry plasma-layer problem; a comparison of flight results with those obtained with a simplified conceptual model was presented. Also, various means by which the attenuation problem may be alleviated or circumvented have been reviewed and the capabilities for laboratory and flight model tests have been discussed.

REFERENCES

1. ANON.: Results of the First U.S. Manned Orbital Space Flight February 20, 1962. Manned Spacecraft Center, NASA.
2. ROTHMAN, WALTER, and MELTZ, GERALD, eds.: Electromagnetic Effects of Re-Entry. Planetary and Space Sci., vol. 6, June 1961.
3. MARSHALL, L. A., and GIRAGOSIAN, P. A.: Hypersonic Aerodynamic Characteristics of Blunt Faced Lifting Reentry Vehicles. Paper No. 62–169, Inst. Aerospace Sci., June 1962.
4. ESCHENROEDER, A. Q., DAIBER, J. W., GOLIAN, T. C., and HERTZBERG, A.: Shock Tunnel Studies of High-Enthalpy Ionized Airflows. Rep. No. AF–1500–A–1 (AFOSR 3025), Cornell Aero. Lab., Inc., July 1962.
5. EDSALL, ROBERT H.: Calculation of Flow Fields About Blunt Bodies of Revolution Traveling at Escape Velocity. [Preprint] 2492–62, American Rocket Soc., July 1962.
6. PIPPERT, G. F., and EDELBERG, S.: The Electrical Properties of the Air Around a Reentering Body. Paper No. 61–40, Inst. Aerospace Sci., Jan. 1961.
7. BOWHILL, SIDNEY A.: The Ionosphere. Astronautics, vol. 7, no. 10, Oct. 1962, pp. 80–84.
8. MITRA, S. K.: The Upper Atmosphere. Second ed., The Asiatic Society (Calcutta, India), 1952. (Available from Hafner Pub. Co., New York.)
9. RATCLIFFE, J. A., ed.: Physics of the Upper Atmosphere. Academic Press, Inc. (New York), 1960.
10. RATCLIFFE, J. A.: The Magneto-Ionic Theory and Its Applications to the Ionosphere. Cambridge Univ. Press, 1959.
11. MARGENAU, H.: Conduction and Dispersion of Ionized Gases at High Frequencies. Phys. Rev., Second ser., vol. 69, nos. 9 and 10, May 1 and 15, 1946, pp. 508–513.
12. LINHART, J. G.: Plasma Physics. Second rev. ed., Interscience Publ., Inc., 1961.
13. STRATTON, JULIUS ADAMS: Electromagnetic Theory. McGraw-Hill Book Co., Inc., 1941.
14. CHAPMAN, SYDNEY, and COWLING, T. G.: The Mathematical Theory of Non-Uniform Gases. Cambridge Univ. Press, 1939, pp. 319–358.
15. MASSEY, H. S. W., and BURHOP, E. H. S.: Electronic and Ionic Impact Phenomena. The Clarendon Press (Oxford), 1952.
16. HAMMERLING, P., SHINE, W. W., and KIVEL, B.: Low Energy Elastic Scattering of Electrons by Oxygen and Nitrogen. Jour. Appl. Phys., vol. 28, no. 7, July 1957, pp. 760–764.
17. PENG, T. C., and PINDROH, A. L.: An Improved Calculation of Gas Properties at High Temperatures. Doc. No. D2–11722, Boeing Airplane Co., Feb. 23, 1962.
18. SCHULTZ, D. L.: Research at the National Physical Laboratory on the Ionization Properties of Gases at High Temperatures. NPL/Aero/378, British A.R.C., June 1959.
19. ELLIS, MACON C., Jr., and HUBER, PAUL W.: Real Gas Flow Conditions About Hypersonic Vehicles. Reentry Dynamics. Bull. of Virginia Polytechnic Inst., Eng. Exp. Station Ser. No. 150, vol. LV, no. 10, Aug. 1962, pp. 120–154.
20. HUBER, PAUL W., and EVANS, JOHN S.: Theoretical Shock-Layer Plasma Flow Properties for the Slender Probe and Comparison With the Flight Results. NASA paper presented at Second Symposium on the Plasma Sheath (Boston, Mass.), Apr. 10–12, 1962.

21. ALBINI, FRANK A., and JAHN, ROBERT G.: Reflection and Transmission of Electromagnetic Waves at Electron Density Gradients. Jour. Appl. Phys., vol. 32, no. 1, Jan. 1961, pp. 75–82.
22. HERRMANN, G. F.: The Absorption of Microwave Radiation in a Plasma Whose Electron Density Varies Linearly With Distance. Tech. Rep. No. 2 (RADC–TDR–62–87), Gen. Telephone and Electronics Labs., Inc., Feb. 1, 1962. (Available from ASTIA as AD No. 274126.)
23. GINZBURG, V. L. (Royer and Roger, trans.): Propagation of Electromagnetic Waves in Plasma. Gordon and Breach, Sci. Publ., Inc. (New York), c. 1961.
24. HODARA, H.: The Use of Magnetic Fields in the Elimination of the Re-Entry Radio Blackout. Proc. IRE, vol. 49, no. 12, Dec. 1961, pp. 1825–1830.
25. BALDWIN, K. M., BASSETT, O. E., HAWTHORNE, E. I., and LANGBERG, E.: Telecommunications During Re-Entry. Planetary and Space Sci., vol. 6, June 1961, pp. 207–218.
26. PAGE, F. M., and SUGDEN, T. M.: The Reduction of Attenuation of Microwave Radiation in Hydrogen/Air Flames Containing Alkali Metals by Chlorine, Bromine, and Iodine. Dept. Phys. Chem., Univ. of Cambridge, 1953. (Available as ASTIA Doc. AD 221440.)
27. LIN, S. C., GOLDBERG, W. P., and JANNEY, R. B.: Radio Echoes From the Ionized Trails Generated by a Manned Satellite During Re-Entry. Res. Rep. 127 (BSD–TDR–62–54), Avco-Everett Res. Lab., Apr. 1962.
28. FELDMAN, SAUL: Trails of Axi-Symmetric Hypersonic Blunt Bodies Flying Through the Atmosphere. Res. Rep. 82 (Contract No. DA–19–020–ORD–4765), Avco-Everett Res. Lab., Dec. 1959.
29. GOULARD, M., and GOULARD, R.: The Aerothermodynamics of Reentry Trails. Preprint 1145–60, American Rocket Soc., May 1960.
30. BLOOM, M. H., and STEIGER, MARTIN H.: Viscous Reacting Wake Flow—Symmetric and Axi-Symmetric. PIBAL Rep. No. 544, Polytechnic Inst., Brooklyn, 1960.
31. LEES, LESTER, and HROMAS, LESLIE: Turbulent Diffusion in the Wake of a Blunt-Nosed Body at Hypersonic Speeds. Aero. Dept. Rep. No. 50 (Contract AF 04(694)–1), Space Tech. Labs., Inc., July 1961.
32. SIMS, THEO E., and JONES, ROBERT F.: Rocket Exhaust Effects on Radio Frequency Propagation From a Scout Vehicle and Signal Recovery During the Injection of Decomposed Hydrogen Peroxide. NASA TM X–529, 1961.
33. HUBER, PAUL W., and GOODERUM, PAUL B. (With appendix A by THEO E. SIMS and DUNCAN E. MCIVER, JR., and appendix B by JOSEPH BURLOCK and WILLIAM L. GRANTHAM): Experiments With Plasmas Produced by Potassium-Seeded Cyanogen Oxygen Flames for Study of Radio Transmission at Simulated Reentry Vehicle Plasma Conditions. NASA TN D–627, 1961.
34. BEISER, A., and RAAB, B.: Hydromagnetic and Plasma Scaling Laws. The Physics of Fluids, vol. 4, no. 2, Feb. 1961, pp. 177–181.
35. SIMS, THEO E.: Measurement of VHF Signal Attenuation and Antenna Impedance During the Ascending Flight of a Slender Probe at Velocities up to 17,800 Feet per Second. NASA paper presented at Second Symposium on the Plasma Sheath (Boston, Mass.), Apr. 10–12, 1962.

62. Survey of Plasma Accelerator Research

By Macon C. Ellis, Jr.

MACON C. ELLIS, JR., *Head, Magnetoplasmadynamics Branch, Aero-Physics Division, NASA Langley Research Center, received his Bachelor of Science degree in aeronautical engineering from Alabama Polytechnic Institute in May 1939. Ellis joined the Langley Staff in November 1939 as an aeronautical engineer. He does research and exploration into the basic nature and mechanism of the fundamental physical processes involved in ionized gases interacting with magnetic and electrical fields. He successfully developed one of the first supersonic wind tunnels in this country (the Langley 9-inch supersonic tunnel); he conducted early jet propulsion studies and made the first objective study of supersonic ram jets and supersonic wind-tunnel experiments, leading to the proposal of a supersonic airplane in 1945; he conducted the first supersonic-tunnel test of the X–2 airplane configuration. He is a member of the American Rocket Society, the British Interplanetary Society, the American Geophysical Union, the Engineers' Club of the Virginia Peninsula, and an Associate Fellow in the Institute of the Aerospace Sciences. He serves as a member on a number of technical committees at Langley and presently is a member of the NASA Research Advisory Committee on Electrical Energy Systems.*

SUMMARY

A brief summary is given of the role of plasma acceleration in modern technology, including space exploration. The various types of plasma accelerators which are described and for which the current research status and problems are discussed include continuous-flow, direct-current, crossed-field accelerators; continuous-flow accelerators utilizing Hall currents; accelerators utilizing traveling-wave concepts; and pulsed, coaxial plasma guns.

INTRODUCTION

Modern technology continues to seek, for numerous objectives, means to accelerate gaseous media of greater density to higher and higher velocities. Since this effort has mostly concentrated on the conversion of thermal energy to kinetic energy, containment of the hot gas and survival of the container has related progress primarily to advances in high-temperature and high-strength materials and to advances in wall-cooling techniques. Eventually, however, radiation to the container walls from the hot gas at values of density desirable for many applications poses an upper limit on storage of thermal energy. It is obviously desirable then to seek means of adding directed energy to the gas by means which minimize the thermal energy added; use of electromagnetic forces on charged particles offers this possibility. An electromagnetic plasma accelerator avoids the necessity of containing a gas at its full stagnation temperature and pressure and alleviates the nozzle-throat heat-transfer problem.

The use of electric fields to accelerate ion and electron beams to velocities approaching that of light is a well-developed and documented science and art of the physicist; however, the

density of these beams is very low due to space-charge limitations. Hence, the interest here is in the possibilities of accelerating neutral plasmas where, in principle, no such space-charge limitations exist. Possible applications of high-velocity plasma streams are as follows:

- Efficient, high-exhaust-velocity thrusters for distant space missions
- Laboratory simulation of hypersonic flight (with quenched ionization in test flow)
- Plasma injectors in controlled thermonuclear fusion research
- Laboratory simulation of astrophysical phenomena
- Possible conversion of kinetic energy to radio-frequency energy
- Produce high-velocity plasma for other magnetoplasmadynamics, (MPD) research (e.g., MPD generators)
- Plasma acceleration studies increase basic MPD knowledge
- Furnishes primary exploitation of breakthrough in superconducting magnets

As related to the primary and continuing objectives of NASA space exploration, electric propulsion systems offer the promise of much greater payloads than do chemical or nuclear systems for the more distant space missions.

In the continuing effort to simulate, in the laboratory, hypersonic flight or reentry from orbital, lunar, and planetary flight, the attainable flight conditions are far in advance of the simulation capabilities. Inherent limitations of conversion of thermal to kinetic energy have already been mentioned; Mach numbers in the range of 15 to 18 appear as upper limits although radio-frequency (RF) or inductive heating of the supersonic stream may take this somewhat higher. Shock tubes have provided a wealth of data at real-gas conditions but simulate for very short times the flow only for blunt bodies or near the stagnation point, whereas study of flow around and behind the body is becoming increasingly more important. Use of electric body forces for acceleration thus appears as an attractive means of attaining high-velocity flows in the range of 26,000 to 60,000 feet per second. In contrast to plasma propulsion, where the efficiency of the thrust system directly affects the power system weight, efficiency for the flow simulator is of secondary importance and running or test time need not be more than seconds or minutes.

The other applications listed are self-explanatory except, perhaps, generation of high-power RF energy. Most present means for converting electrical energy to RF energy involve electron streams in one way or another and their energy-density is low, requiring large volumes of apparatus for high power. High-velocity plasma streams offer several possibilities for resonant excitation and extraction of RF radiation and, in addition, plasma instabilities, which are a troublesome problem in both controlled thermonuclear fusion (CTNF) and plasma acceleration efforts, might be trained to give up their "losses" as controlled RF energy.

The first application of plasma accelerators was listed as electric propulsion so a word more on this is in order to get an idea of the "fit" of plasma systems into the mission picture. In the analysis of reference 1, comparison has been made among chemical, nuclear, and electric propulsion systems for some distant missions. One aspect of this analysis is shown in figure 62–1. The missions shown at the left are in approximate order of increasing difficulty or characteristic vehicle velocity increment required. The gross payload shown is that delivered at the mission objective, and it is considered that minimum useful payloads are in the range of 1,500 to 2,000 pounds. Without going into such details as trip times and weights in earth orbit, the analysis shows that for the more distant missions only the electric propulsion systems will do the job. (The analysis of ref. 1 assumes ion

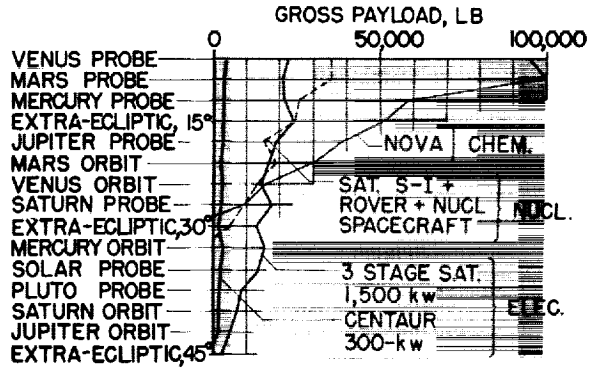

FIGURE 62–1.—Performance comparison of chemical, nuclear, and electric systems. (From ref. 1.)

thrust systems.) The final point is that tripling the output of the electric power system gives large gains in payload capabilities; therefore, the necessity for development of large space power systems is emphasized. These larger powers will be necessary if the potential advantage of higher thrust and shorter mission times for the plasma systems is to be realized. Furthermore, certain space missions call for variable specific impulse during flight, for example, from 2,000 to 40,000 seconds. (See refs. 2 and 3.) Magnetoplasmadynamic devices, at this time, appear to have no fundamental limitations on ability to vary exhaust velocity; thus, such devices potentially can encompass this specific-impulse range and at the same time offer high thrusts per unit area.

SYMBOLS

B	magnetic induction
E	electric field strength
j	current density
M	Mach number
p	static pressure
p_t	total pressure
T	temperature
u, v, V	velocity
x, z	distance in axial direction
y	distance in vertical direction
γ	ratio of specific heats
ρ	mass density
σ	scalar electrical conductivity
τ	mean free time between collisions
ω	cyclotron frequency
Subscripts:	
$i, +$	ion
$e, -$	electron
in	ion neutral
ϕ	angle from x-axis
θ	angle between ion and E/B direction or azimuthal direction
n	neutral particle
z	longitudinal or axial direction
R	radial direction
rot	rotational
$trans$	translational
$cath$	cathode

Bar over symbol indicates vector.

PLASMA-ACCELERATOR CATEGORIES

Many possibilities exist for the compounding of pieces and plasma principles to devise a plasma accelerator. In any attempt to categorize those that have been conceived or worked on, one faces the dilemma that is illustrated in the following list:

A given accelerator might be
- (a) Continuous or
- (b) Pulsed.

The device may use
- (a) Electrodes or
- (b) No electrodes.

The plasma may be generated
- (a) Separate from accelerating region or
- (b) As integral or initial part of acceleration process.

Basic acceleration process may utilize
- (a) Self-magnetic fields or
- (b) Applied magnetic fields

Coupled with
- (c) Applied current or
- (d) Hall current.

Basic containment of plasma may be
- (a) Magnetic or
- (b) Aerodynamic.

Plasma may be closer to
- (a) Collisionless or
- (b) Collision dominated.

A given accelerator scheme or device might be of the continuous-flow variety in the sense that a steady source of gas (or propellant) is fed in and accelerated in a continuum sense or it may be pulsed in several ways. If the pulse rate is sufficiently high to provide only small fluctuations with time in the resulting flow momentum, then it would be continuous. The device may utilize electrodes to feed the electrical energy in and the cathodes may be thermionic emitters or field- or photo-emitters or ion-bombardment emitters. Many forms of electrodes are possible—for example, the hollow cathode. If electrodeless, the accelerator may take numerous forms, depending on the detailed magnetic-field configurations and their variation with time. The plasma to be accelerated may be generated separately from the primary accelerating region, as in a seeded arc jet, or the generation may be inseparable, in principle, from the process of imposing directed electromagnetic forces on the plasma. The basic acceleration process may utilize, for the magnetic component of the driving force, either the field of the driving current or an applied magnetic field, or both. The primary driving

current can be the applied current or a Hall current or both may be utilized. The plasma containment may be either aerodynamic or magnetic. Aerodynamic containment depends upon collisions to restrict the diffusion rate of particles toward the walls and magnetic containment depends upon the absence of collisions to restrain the motion of charged particles to magnetic field lines, hence, away from the walls. The mean free time between collisions or inversely the mean free path of the electrons or ions, coupled with the velocity of the particles and the magnetic-field strength, may define an $\omega\tau$ domain of operation of a given acceleration scheme. Although not listed, RF energy may be used rather directly in the acceleration process or for plasma heating or may be combined in numerous fashions with other combinations of items shown. Plasma conditions and MPD principles force or restrict certain combinations; therefore, the choice of combinations is limited but still large. The subsequent discussion is thus restricted to those types of plasma accelerators which have been studied most extensively and which are hopefully farthest along toward their goals.

PLASMA ACCELERATION

The following table shows the general types of accelerators to be discussed briefly:

	Approximate number under study
Continuous-flow, d-c, linear, crossed-field accelerator	13
Continuous-flow accelerators utilizing Hall currents	8
Accelerators utilizing traveling-wave concepts	9
Pulsed, coaxial plasma guns	24
TOTAL	54

A search of the literature on the subject of plasma acceleration reveals the relatively large number of devices under study as shown. Each of these represents at least some experimental as well as analytical effort and it is probable that the list is not complete; it is obvious, however, from the numbers that there exists considerable interest and competition toward achievement of the apparent potentialities of such devices. The engineer seeks to attain the high velocities for his own uses whereas the scientist is fascinated with an application for this exploding science of magnetoplasmadynamics.

CONTINUOUS-FLOW, LINEAR, CROSSED-FIELD PLASMA ACCELERATORS

The basic concept of a continuous-flow, linear type of crossed-field, direct current (d-c) plasma accelerator is shown schematically in figure 62–2. The cathodes are shown in the upper wall, the anodes in the lower wall, and an externally imposed magnetic field is normal to and out of the plane of the paper; the electric field is in the plane of the paper and directed upward, perhaps at a slight angle for reasons to be discussed subsequently. Since the gas flow is ionized and is an electrical conductor, the elements of an electric motor are evident, and the electric-motor or Lorentz force per unit volume on the current is

$$\overline{F}=\overline{j}\times\overline{B}$$

that is, the cross product of the current density and the magnetic induction. The device may be considered analogous to a shunt-wound, d-c motor, but the deceptive simplicity of the concept fades as one begins to examine the details of the acceleration process and the particle motions. The concepts of operation, together with results of analysis and experiments for the accelerator as carried out by George P. Wood and associates at the Langely Research Center (refs. 4, 5, 6, and 7) are outlined in the following comments.

As stated previously, the accelerator incorporates a magnetic field normal to the electric field and uses the Lorentz force. Since the force exerted by a magnetic field on a moving charged particle is normal to the velocity of the particle, no work is done on the particle by a stationary magnetic field. The magnetic field

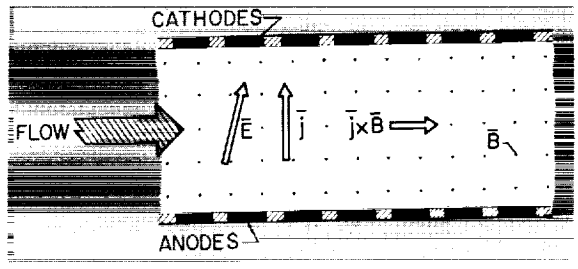

FIGURE 62–2.—Schematic of crossed-field accelerator.

simply determines in part the direction of the particle velocity. For the collisionless case, the two-dimentional projection of the ion and electron paths would by cycloids that lie along equipotential lines in a direction normal to both electric and magnetic fields. Because of the mass difference, the radii of gyration of the ions and electrons differ and the sense of rotation is opposite due to opposite sign of charge; however, the average drift direction and velocity are the same, and the drift velocity is E/B.

In the present instance, there is no interest in the low-density collisionless case, and the effects and results of collisions must be considered. From the macroscopic point of view, the driving force is the Lorentz force on a current in a magnetic field, $\overline{j}\times\overline{B}$ per unit volume, where the current consists principally of a flow of electrons. In the microscopic picture, it is desired that the ions be accelerated in the electric field, and then, by collisions, drive the neutral particles along the channel. The microscopic method is used to provide insight into the physics of the process and the macroscopic method is used to provide quantitative results for use in designing accelerators.

QUALITATIVE ANALYSIS FROM MICROSCOPIC POINT OF VIEW

Because of the large difference in the masses of electrons and ions, these two species behave differently in crossed fields in a three-component plasma; that is, they have different mean free times, different cyclotron frequencies, and different velocity directions and magnitudes. The desirable behavior on the part of each is discussed first.

Because of its comparatively small mass, an electron cannot impart much momentum at a collision with a neutral particle. It is therefore not undesirable that the electron make many cycles between collisions with neutral particles and thus have its velocity vector directed essentially at random just before collision. On the other hand, the ion should make, on the average, just a portion of a cycloid between collisions with neutral particles. It is perhaps well to reiterate here that the basic acceleration process is considered to be first the acquisition of additional momentum from the electric field by the ion, then the transfer of this additional momentum to a neutral particle by collision, and then the equal distribution, on the average, of this additional momentum over the more numerous neutral particles. The portion of the cycloid that it is desirable for the ion to traverse is one for which, on the average, three conditions are satisfied.

The first of these conditions is that, on the average, at collision the ion velocity is a specified amount greater than the average forward velocity of the neutral particle. Satisfying this condition allows additional momentum to be imparted to the neutral particle at a specified rate. Part of this additional momentum goes into random motion of the particle and tends to raise the temperature of the gas. On the other hand, the cooling effect associated with acceleration of the plasma tends to lower the temperature; thus satisfying this condition results in a partial control over temperature.

The second condition is that the collision occurs when, on the average, the instantaneous direction of motion of the ion is in the direction of the axis of the channel. The reason for this condition is that it is desirable to drive the neutral particles axially along the channel and not toward a wall.

The third condition is that the ion travels on the average along the axial direction—that is, in addition to moving axially at the time of collision, the average velocity of the ion should lie along the direction of the axis and not be directed toward a wall where on contact with an electrode the ion would be neutralized.

Some of these conditions are mutually contradictory, but usually not seriously so. As illustrated in figure 62–3, the ion path without collisions is cycloidal; however, the wish is that, on the average, the ion path will repeat a small section of this cycloid (the section between the two dashed lines), and that the initial and final directions will be nearly the same and will approximate a straight line.

In Wood's analysis (ref. 4), the first condition has been adopted that, on the average, at collision the ion velocity is a specified amount greater than the average forward velocity of the neutral particle; further, constant static temperature is assumed, so that the acceleration

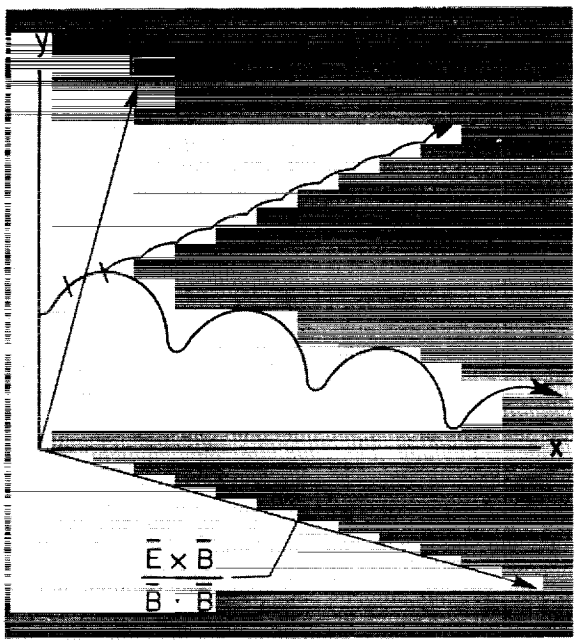

FIGURE 62–3.—Ion path with and without collisions.

rate is specified to be such that the decrease in temperature due to acceleration is just compensated by the increase in temperature due to Joule heating. The second condition is adopted in order that the driving force on the neutrals may be directed parallel to the axis of the channel. A choice can be made between the second and third conditions, that is, the ions or the neutrals may be directed along the axis. If it is desired to direct the neutrals along the axis, then the electric field may be tilted in such a way that the x-components of ion and electron velocities are equal as shown in figure 62–4, thereby making the axial current zero. The direction of the ions is tilted but the angle for practical cases is extremely small.

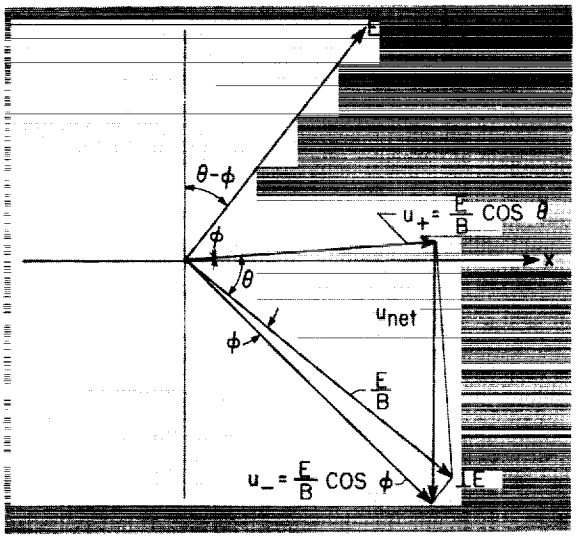

FIGURE 62–4.—Orientation of ion and electron velocities.

QUANTITATIVE RESULTS FROM ANALYSIS FROM MACROSCOPIC POINT OF VIEW

At this point then, what do the results of macroscopic analyses show in terms of geometry and operating characteristics of such an accelerator? Figure 62–5 shows the Mach number as a function of normalized length for the conditions of constant cross-sectional area, constant static temperature, constant applied magnetic field, Lorentz force directed along the channel axis, small degree of ionization, no friction and heat transfer, and γM^2 greater than unity. The

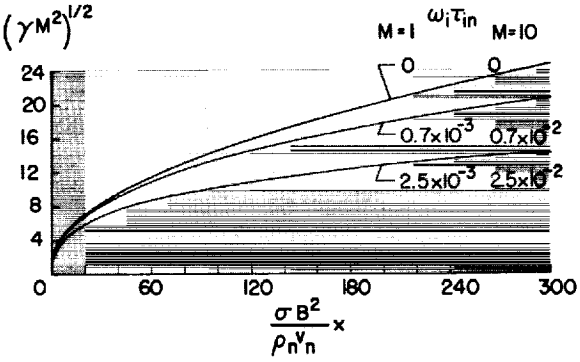

FIGURE 62–5.—Mach number as function of length.

curves show essentially the Mach number at a given longitudinal distance x from the $M=1$ station as a function of the distance normalized by the parameter $\frac{\sigma B^2}{\rho_n V_n}$. Reference 4 takes into account the Joule heating due to ion slip as well as the conventional Joule heating due to resistance and the three curves show the effect in terms of $\omega\tau$ where ω_i is for the ions and τ_{in} is for the ion-neutral collisions. Increasing $\omega_i\tau_{in}$ corresponds to increasing the heating due to ion slip. The current, hence the acceleration, must correspondingly be decreased at a given x-station to preserve the balance between heating and cooling due to acceleration; the accelerator

length is then greater in order to reach a given Mach number. The detrimental effects of ion-slip heating on accelerator length can, however, be overcome by the cooling effect of a slight area expansion of the accelerator channel. Typical values of $\omega_i \tau_{in}$ for the following experiments are approximately 10^{-3} radian.

CROSSED-FIELD ACCELERATOR EXPERIMENTS

The elements of the early experimental apparatus used at Langley to study crossed-field accelerators are shown schematically in figure 62–6. The source of plasma is a seeded arc jet, wherein the arc is magnetically rotated by the coils shown around the outer chamber wall. A typical mass flow of N_2 is 2.6 g/sec with final enthalpy of 8,860 Btu/lb and corresponding temperature of 6,900° K. Cesium is fed at constant rate through a resistance-heated vaporizer to the hot nitrogen flow after the arc. The resulting plasma emerges from a Mach 2 nozzle at the entrance to the EM acceleration region at a temperature of 5,500° K with ionization levels of 1- to 4-percent mole fraction corresponding to nearly complete ionization of the cesium seed. The accelerator channel, shown in the low-pressure chamber, is 1 cm × 1 cm × 8 cm. Magnetic fields up to 11,000 gauss are imposed across the channel through pole faces contacting nonmagnetic walls of the channel. As shown in the schematic, a total-pressure tube is shown at the flow exit. Static-pressure orifices are also incorporated along the channel walls. Figure 62–7 shows a cross section through the accelerator indicating the components and the segmented electrodes. Cathodes used have mostly been of thoriated tungsten. The current loop through the gas between opposing electrodes is closed separately for each pair through external batteries, and voltage and current may be controlled separately for independent pairs.

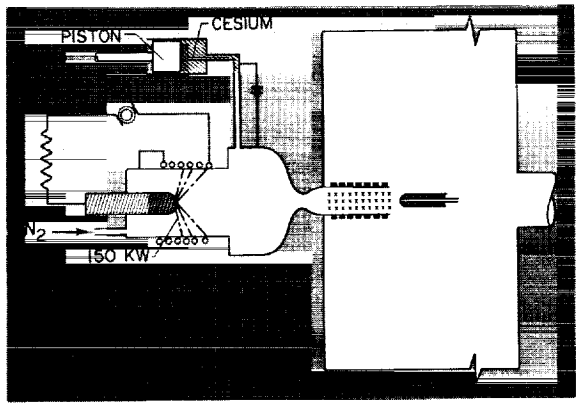

FIGURE 62–6.—Schematic of apparatus.

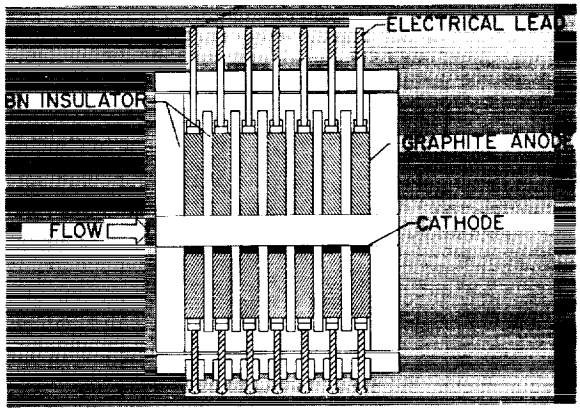

FIGURE 62–7.—Longitudinal section through accelerator.

The significance of the pressure measurements is indicated from the following equations:

$$\frac{\Delta p_t}{p_t} = \frac{2\gamma M^2}{[2+(\gamma-1)M^2]\rho u^2}\left[jB - \frac{(\gamma-1)M^2 j^2}{2\sigma u}\right]\Delta x$$

$$\frac{\Delta p}{p} = -\frac{\gamma M^2}{(M^2-1)\rho u^2}\left[jB - \frac{(\gamma-1)M^2 j^2}{\sigma u}\right]\Delta x$$

The equations show the relative change in total pressure p_t and in static pressure p. For the two terms in the brackets of each equation, the first is the effect of the Lorentz accelerating force and the second is the effect of Joule heating; therefore, an increase in total pressure and a decrease in static pressure (note negative sign of static-pressure equation) indicates a win for the accelerating force.

Typical results of several tests are shown in table 62–I. The column headings show mass flow, total current flow across the channel, and total pressures at the accelerator channel exit for the cases of current flowing and no current flowing. By sensing the change in total and static pressure (latter not shown) due to switching on the current flow, the fact that the accelerator was truly accelerating could be easily and directly observed. Typical runs are shown for two sets of pressure or density in the

TABLE 62–I.—*Representative Data for 1 cm×1 cm×8 cm Accelerator*

Mass flow, g/sec	Accelerator current, amp	p_t, mm Hg		$\frac{(\Delta p_t)on}{(p_t)off}$
		Current off	Current on	
1.37	66	143	214	0. 50
1.37	110	145	245	. 69
1.37	114	136	260	. 91
2.74	160	342	520	. 52
2.74	125	325	460	. 42
2.74	144	357	501	. 40

channel and it is seen that for all cases an increase in total pressure occurs; this increase indicates that the Lorentz force exceeds the effects of Joule heating in diminishing this force. By using the equations with known values of x, B, ρu and M, estimated values of γ, and calculated values of σ, a calculated value of the total-pressure change can be made. The experimental values average between 50 and 60 percent of the calculated values and corresponding velocity increases implied from the measurements are about 30 percent. For this small accelerator, efficiencies from measurements are misleading mainly because of the losses associated with the large voltage drop through the cathode and anode sheaths. For larger accelerators this loss would be a far smaller fraction of the total losses. If these losses are ignored, efficiencies of conversion of electrical to kinetic energy of about 70 percent are indicated. Many other detailed measurements have been made with the use of this small accelerator and much has been learned concerning, for example, electrode materials, insulator materials, seeding techniques, temperature measurements, accelerator construction, and many other details. It is obvious that the small size of the apparatus greatly exaggerates wall losses and limits many measurements, especially probing-type measurements, and that a larger accelerator with higher power and greater acceleration is the desirable next step. A larger accelerator has been built at the Langley Research Center and operation has just started; the principal features of this larger facility are shown in the

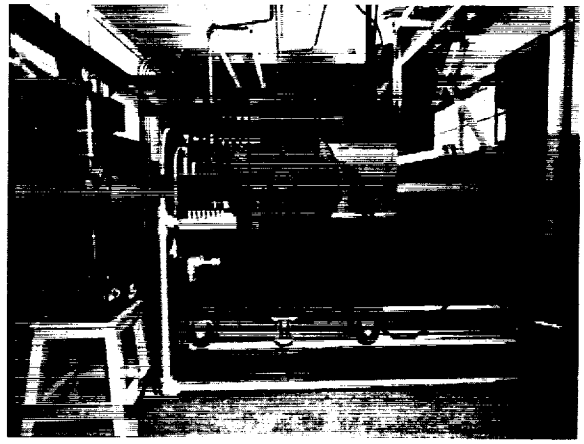

FIGURE 62–8.—Langley 1-inch-square plasma accelerator.

photograph of figure 62–8. Unfortunately, the accelerator channel and many details of the arc chamber are hidden behind the large electromagnet. The arc is at the left and the low-pressure discharge pipe is at the right.

The characteristics of the arc plasma source and estimated performance of the accelerator are shown in table 62–II. In the table, a consistent set of nominal operating conditions are given; however, it is emphasized that the potential of the primary apparatus will permit still greater velocity increases than are shown (2,000 to 4,000 m/sec) as research progresses.

TABLE 62–II.—*Langley 1-Inch-Square Plasma Accelerator*

Arc plasma source:	
Arc potential and current	200 v, 2,500 amps
Arc-chamber pressure	1 atm
Gas flow rate	7 g/sec
Gas enthalpy	8,000 Btu/lb
Gas temperature	7,000° K
Gas ionization (Cs seed)	≈ 2 percent
Accelerator:	
Dimensions	1 in. × 1 in. × 12 in.
Number of electrodes	24 pairs
Magnetic field	10,000 gauss
Power source	400, 12-v battery
Potential across electrodes	135 to 225 v
Current through plasma	1,700 amps
Power into Joule heat	70 kw } 250 kw
Power into Lorentz force	180 kw } into gas
Pressure	70 mm Hg
Velocity at entrance	2,000 m/sec
Velocity at exit	4,000 m/sec

Other Investigations of Crossed-Field Accelerators

Other experimental work on crossed-field accelerators is included in references 8 to 12. The experiments of Demetriades (ref. 8) are noteworthy in that he has achieved the highest thrust and velocity increase due to the Lorentz force and has reached an efficiency of 54 percent. His accelerator incorporates three pairs of electrodes, and the whole assembly of channel, electrodes, and magnet is mounted on a thrust stand, separate from the arc-jet plasma source; thus, direct measurements of thrust due to electromagnetic forces can be made. He reports thrusts up to 3.6 pounds at an acceleration efficiency of 54 percent. The specific impluse increment due to the plasma accelerator was reported to be 1,200 seconds, corresponding to an addition of 300 percent to the specific impluse of the arc jet used. In his experiments, he has made systematic variation in the electric parameters; for example, in tests where the voltage and current were held constant and thrust measured as a function of magnetic-field strength, he shows linear increase as expected up to a peak where the back electromotive force and Hall current predominate and cause a decrease. He has also made extensive study of electrode configurations, both flush and protruding. All his experiments are fairly short-time tests; thus, problems such as electrode erosion and so forth still remain.

Hellund and Blackman and their group have carried out experiments on crossed-field accelerators and have concentrated on properties of gases for use in such devices, especially as influencing choice of propellant and use of their nonequilibrium characteristics. (See ref. 9.)

Hogan (ref. 10) has carried out short-duration experiments at high-power and high-magnetic induction levels by the ingenious combination of an ionized shock-tube flow, a transverse magnetic field generated by the discharge of capacitor through a coil, and a transverse electric field supplied by another capacitor system. He obtained results which, although for a small 1½-inch channel, are for power inputs to the gas up to 5 megawatts and show that, for his range of conditions, deceleration due to eddy currents in the gas as it leaves the magnetic field were small, electrical energy chargeable as loss to the boundary layer was relatively small (smaller with increase in power), and that overall efficiencies up to 70 percent were realizable.

Problems and Future Research on Crossed-Field Accelerators

For the crossed-field accelerator, the detail problems and loss mechanisms deserving attention are numerous and have been elaborated recently by several authors. Janes has discussed the various loss mechanisms in an accelerator channel which he believes to be crucial (ref. 13) and implies from his summary and later comments (ref. 14) that because of wall loss and heating limitations of such aerodynamically contained accelerators, magnetically contained arrangements hold greater promise for the highest possible exhaust velocities. He has made approximate analyses (ref. 13), considered separately, of thermal-leaving losses, frozen-flow losses, electrical conductivity, propellant choice, eddy-current effects, Hall current limitations, ion-slip heat losses, wall effects, transport coefficients in a magnetic field, electronic heat conduction and thermal equilibrium, electrode boundary layers, insulator boundary layers, and Joule field coil losses. Obviously numbers of these effects are so interrelated that they must be considered simultaneously as pointed out in reference 15; consequently, as pointed out in reference 9, there is considerable doubt as to the accuracy of such analyses in that, at best, only trends can be indicated. One very important technological development subsequent to most of these discussions of problems is that of the superconducting magnet; Joule field coil losses will be nearly nonexistent and magnet weight will be very small.

In any case, it is safe to conclude that much more fundamental work, both theoretical and experimental, is needed to study

(1) both macroscopic and particle characteristics of basic gas and acceleration processes,
(2) nonequilibrium gas effects for a variety of gases that are potential propellants,
(3) highest possible velocities to uncover limitations,
(4) electrode characteristics,
(5) insulator characteristics.

A number of groups including Langley Research Center are pursuing these studies with optimism, at this stage, for the future of the crossed-field accelerator.

Continuous-Flow Accelerators Utilizing Hall Currents

The rectangular plasma accelerator discussed in the previous section used, as its plasma source, the seeded, high-temperature gas from an arc jet. This arc jet was a coaxial device in which an externally imposed axial magnetic field B_Z and a radial current density j_R combined to exert a $j_R B_Z$ force/volume in the azimuthal direction as shown schematically at the lower left of figure 62–9. This force rotates a radial arc sector or disk as shown. In the arc jet used as a high-temperature gas or plasma generator, rotation of the arc serves to distribute the Joule heating of the gas and inhibit electrode erosion by avoiding stationary arc spots (or moving arc spots when a disk is formed). The question naturally arises as to whether it would be possible to use $j_R B_Z$ to put work into rotation of the gas and to convert rotational energy directly to translational energy. Such conversion can take place in a nozzle, as shown in the figure, into which the rotating gas moves and the centrifugal forces are balanced by the wall reaction, converting angular to axial momentum. In order to put the plasma into rotation, it is generally more efficient to use a uniformly distributed force derived from a current distributed over an arc disk interacting with the axial magnetic field, rather than the "line force" derived from the current concentrated in an arc spoke. Such a view then gives a picture of a continuous azimuthal or Hall current. The differential motion of electrons and ions due to their different drift velocities in the azimuthal direction normal to both the radial electric field and the axial magnetic field constitutes a circular drift current mainly caused by the motion of the lighter electrons relative to heavier ions. It should be emphasized that even for the arc spoke covering a sector between the coaxial electrodes, a Hall current can exist within the spoke since the current follows the streamlines formed by the azimuthal components of the curved particle motion. Such components can then exist if $\omega\tau > 0$; however, the primary point of interest for application to accelerators is to determine all the conditions necessary for a uniformally distributed discharge and continuous Hall current and these include not only the $\omega\tau$ values but other conditions such as emission from the cathode.

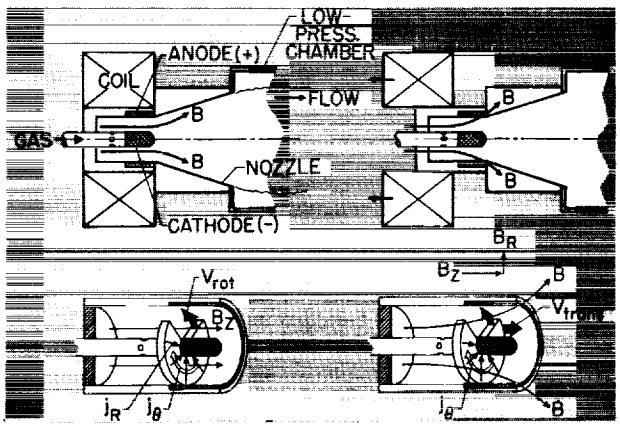

FIGURE 62–9.—Plasma rotation and Hall current acceleration.

Shown at the upper left of figure 62–9 is a schematic of an experimental apparatus at Langley Research Center for producing plasma rotation and conversion to translation. If the magnetic-field coil is slid back, as shown at the right, the magnetic field is no longer purely axial in the region of the discharge, but is divergent so that a radial component B_R exists. The second mode of operation of the accelerator is then evident whereby the azimuthal Hall current j_θ and the radial component of the magnetic field B_R produce a $j_\theta B_R$ force/volume which acts in the longitudinal direction. Conversion of residual rotational energy to translation can again utilize a mechanical nozzle and, in addition, the diverging magnetic-field lines can be used for magnetic guiding or containment. Both of these concepts of operation of this coaxial scheme, that is, conversion of rotation energy and Hall current operation, were first described in references 16 and 17. Both modes of operation have been the object of research at Langley for the past 2 years. Results of this research and those from studies of similar devices at other laboratories will be discusssed in subsequent sections.

Experiments With Coaxial Hall Current Devices

An experiment can be devised to show the Hall current operation of this coaxial device. For Hall current operation, the direction of acceleration changes with the polarity of the electric field which changes the direction of the Hall current. For a given direction, the magnetic field enters as the second power; thus, its direction does not affect the direction of acceleration. Experiments using an apparatus similar to that shown in the upper right-hand sketch (fig. 62–9) were made in which the electric field was reversed. These early experiments showed that the coaxial device can act in a diamagnetic fashion (pushing the plasma toward the weaker magnetic field) or in a paramagnetic fashion (pushing the plasma toward the stronger magnetic field).

One of the first objectives of study obviously is to determine the nature of the discharge in some detail, especially the conditions for a disk or uniform discharge. Patrick and Powers find experimentally that when $\omega_e\tau_e>1$, the discharge is stable and the arc is uniform through the channel (refs. 18 and 19). Experiments at Langley in this range also give uniform discharges; however, it has also been found that the cathode temperature has a primary effect on the discharge. The two photographs of figure 62–10 indicate the effect of cathode temperature, where all other conditions are the same. The photograph in figure 62–10(a) is from a film sequence taken at 4,000 frames per second and is for a relatively cold cathode. For this condition, the spokes (and possibly retrograde motion) are evident. As the cathode is heated to the conditions shown for the photograph in figure 62–10(b), the discharge is uniform, since at the Kerr cell shutter speed of 0.1 microsecond for this photograph, any probable spoke motion would be resolved if spokes existed. It is to be noted that at the temperature shown for the tungsten cathode, thermionic emission is very small but, even at this low value, is very effective in uniformizing the discharge. Further experiments on cathode conditions and materials are in progress, including gas and alkali-metal injection through the cathode.

Experiments on both modes of operation have been made and are still in progress at both Langley and Avco-Everett Research Laboratory. At Langley, concentration has been on

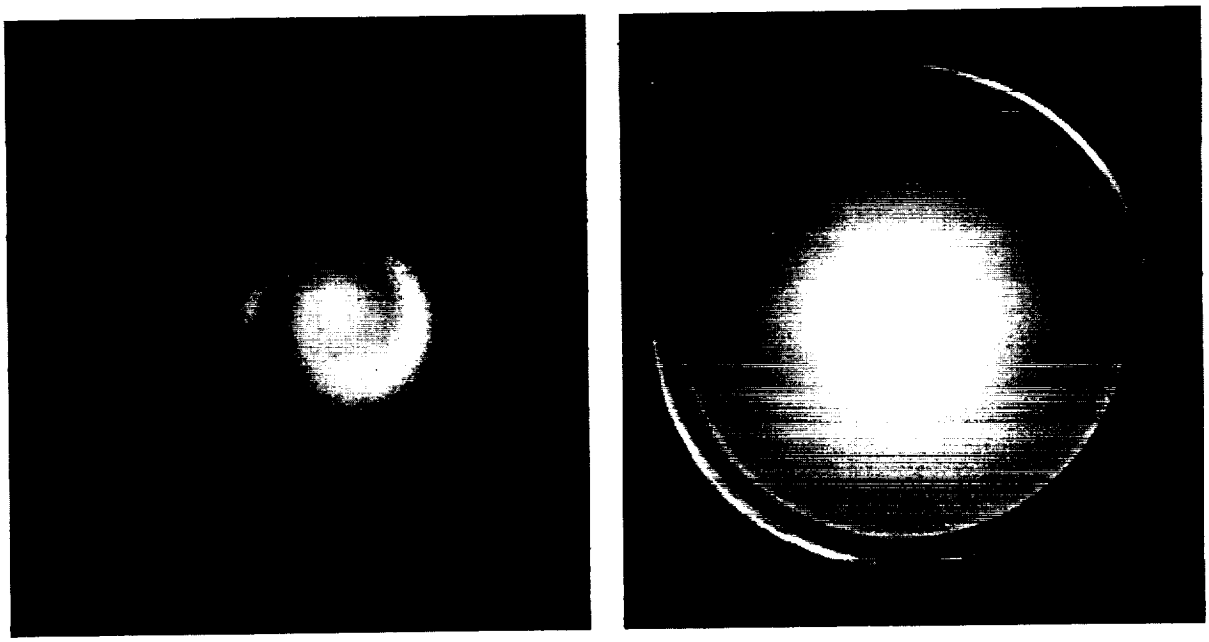

(a) Rotating spokes. Cold cathode. (b) Uniform discharge. T_{cath}=2,360° K; exposure time, 0.1 μsec.

FIGURE 62–10.—Effect of cathode temperature on coaxial discharge in B_z field.

the discharge itself (refs. 20 and 21) as well as the means of feeding lithium into the system in such a fashion that it is vaporized in one step (without contacting the walls) and enters the accelerating region in a second step. Lithium is a desirable propellant because of the low frozen-ionization losses in the density range in which these devices operate and because it will permit higher power inputs. A Hall current acceleration device with a 50,000-gauss solenoid is nearing completion at the Langley Research Center.

Results of detailed measurements at Avco-Everett Research Laboratory for both modes of operation of the coaxial accelerator are given in reference 19. For the case in which rotation is converted to translation by means of a shallow nozzle (20°), a thrust of 0.7 pound was produced with an overall efficiency of 15 to 20 percent. These results led the investigators to a wide angle (50°) nozzle seeking to convert azimuthal motion more rapidly to axial motion. Figure 62–11 (taken from ref. 19) shows schematically the geometry and configurations of fields and currents that might be expected. Since a magnetic field with a large radial component could be produced in this nozzle, full advantage could be taken of the possible large Hall currents to produce additional body forces in the axial direction. In such a configuration, for $\omega\tau > 1$, current lines are pushed out of the annulus and are forced downstream by the Hall effect. In the arrangement shown, the interaction of the Hall currents and both components of the magnetic field provide both acceleration and containment; that is the $j \times B$ forces can be largely in a direction which accelerates the plasma away from the channel walls and in the thrust direction. They made very detailed pressure, mass-flow rate, velocity, and electric-probe surveys of the flow field for both the shallow and wide angle nozzles and found that the basic concepts were realized; however, large plasma-swirl effects were predominant, more so for the narrow nozzle. An average exhaust velocity corresponding to a specific impulse of 600 seconds was attained with an overall thrust efficiency of 25 percent for the 50° nozzle.

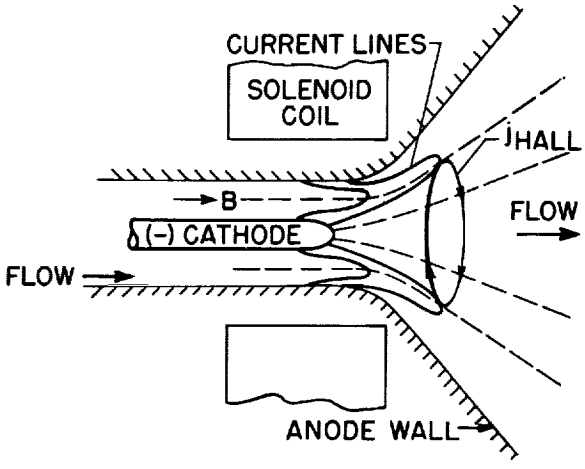

FIGURE 62–11.—Magnetic annular arc. (From ref. 19.)

In general, for these coaxial devices in the "high-density plasma" range, principles have been proven and much progress has been made in studies of detail flows and mechanisms. The primary advantages this coaxial arrangement has in comparison with other devices are its combination of arc jet with the accelerator portion and the possibilities of magnetic containment of the plasma. The principal problems that must be studied arise from the nonuniformities in the flow which stem from the rotation of the jet. It appears that rational choices or compromises must be made between the requirements for best conditions for MPD acceleration and magnetic containment or nozzle requirements. For example, in figure 62–11, the current lines close back almost along magnetic field lines, this case being ideal for containment; however, these conditions are dissipative as far as acceleration is concerned. For best MPD acceleration, the desire is to cut the current lines with the magnetic field lines as near normal as possible. One way of doing this is to provide a series of segmented electrodes in the center cathode and the outer wall. In the latter case, however, the magnetic nozzle is lost. Another advantageous factor in these accelerators stems from the fact that the azimuthal driving current is larger than the radial current between electrodes; the direct losses to the electrodes because of the lesser thermionic emission required should thus be smaller than in the linear crossed-field accelerator. In continuing studies to improve these coaxial devices, it is desired to have available large variations in magnetic-

field configurations. The solenoidal coil is readily adaptable to produce wide variations in field geometry; however, most important are the high field strengths that can conveniently be obtained with superconducting solenoids.

Low-Density Longitudinal Electric-Field Hall Current Accelerators

Several investigators have studied coaxial arrangements incorporating radial magnetic fields and longitudinal electric fields. (See refs. 22 to 27.) A class of these low-density devices may be considered to be nonspace-charge limited ion accelerators, wherein by a suitable choice of electric and magnetic fields, ions are electrostatically accelerated in a plasma in the presence of trapped electrons.

The apparatus described in reference 26 was designed at the Langley Research Center to study the basic phenomena in an axial electric field or discharge and a predominantly radial magnetic field. A cross-sectional view of this apparatus is shown in figure 62–12. Note the iron core which concentrates the field lines from the solenoid to make a predominantly radial magnetic field where the field strengths are highest. The iron core is laminated to prevent radical distortion of the electric field and is insulated from the discharge by an enclosing glass tube. The experiments with this apparatus covered a range of pressures from 15 to 150 microns of mercury, arc voltages to 700, currents to 80 amperes and average radial magnetic-field strengths to 450 gauss. The important distinction of these conditions from those of the Hall accelerator of the previous section is that it operated at high-density, small ion-slip, and low ionization. In this case operation is at low density, small ion-slip and high ionization. In terms of the pertinent plasma parameters in the experiments here, both the ion gyro radius and ion mean-free path are large compared with the apparatus size, the electron gyro radius is small compared with the apparatus size and the electron mean-free path. Under these conditions, the ions may be accelerated in the electric field in the presence of electrons trapped in rotary E/B motion about the axis with small drift in the axial direction. As mentioned in reference 27 the $j \times B$ force/volume is produced by the azimuthal Hall current and the radial magnetic field. For low density, highly ionized plasmas having few collisions, the $j \times B$ force equals the electrostatic force from the electric field on the ions.

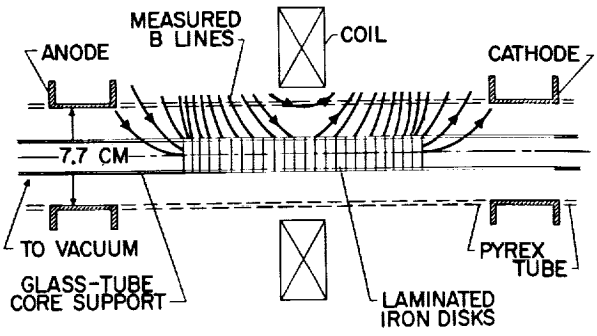

FIGURE 62–12.—Ion acceleration in a plasma using Hall currents.

The apparatus shown represents an element of such an accelerator wherein studies of the plasma conditions have been made in terms of arc voltage and current, charge particle distribution and density, potential distribution, and Hall current. These experiments have generally indicated that the device operates as expected, but have, of course, brought out many problems requiring further study. Briefly the experiments gave the following results:

(1) A positive slope volt-ampere characteristic was observed; the slope increased with increasing magnetic field or decreasing pressure.

(2) Approximate values of the Hall current were observed by using a technique wherein a ballistic galvanometer sensed the Hall current by switching off the discharge with the magnetic field left on. Hall current values agreed "order-of-magnitude-wise" with those predicted. Ratios of Hall current densities to axial-current densities in the range of 10 to 15 were observed.

(3) The pressure at the cathode was observed to increase depending on the direction of the electric field or ion motion.

(4) At the lower pressures, anomalous diffusion effects became more pronounced, as expected, for fewer collisions.

An apparatus using the same principles as just outlined has been investigated by Janes, Dotson,

and Wilson (ref. 22). Their accelerator shown in figure 62–13 does not have the oppositely rotating Hall currents that are in the apparatus at Langley. In their apparatus, ionization is produced by a Phillips Ionization Gage (P.I.G.) type discharge occurring between the ionizer filament and anode. Ion acceleration takes place in an electrically neutral region immediately below. The filament at the exit only serves to release electrons which are necessary to neutralize the outgoing plasma. Results with this apparatus have not yet been reported; however, extensive measurements using a cusped-field arrangement with predominantly radical fields have been made. A device similar to the one shown in figure 62–13 but smaller has been used in reference 28. Also, in this accelerator, no ionizer filament was included so that ionization had to be provided by the normal collision mechanism resulting from axial leakage of electrons. In all of these devices it is intended that the axial mobility of electrons will be sufficiently restricted by the magnetic fields to permit the plasma to sustain a significant voltage associated with the electric fields necessary to accelerate the ions as current carriers. Electrons produced near the anode are carried to the exit through an external circuit and there emitted from a hot filament to obtain an electrically neutral plasma-exit beam. The cusped-field apparatus shown in figure 62–14 has been used in the experiments of reference 22. For moderate magnetic fields (and specific impulse values) it was found (ref. 22) that specific impulse I_{sp} first increased linearly as a function of B but flattened out at a value of I_{sp}

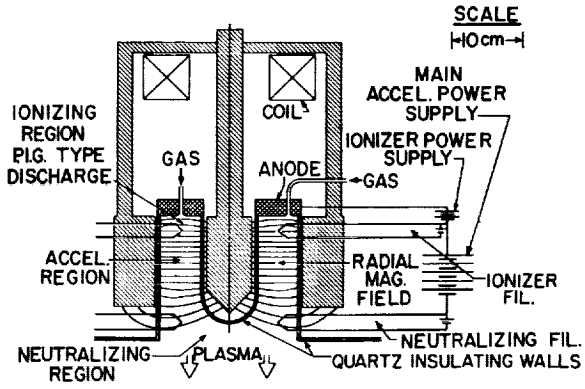

FIGURE 62–13.—Annular two-stage E.M. region d–c plasma accelerator. (From ref. 22.)

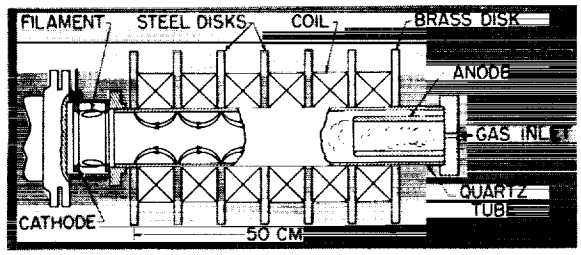

FIGURE 62—14.—E.M. region d–c cusp plasma accelerator. (From ref. 22.)

of 1,200 at the highest magnetic fields. This apparent saturation in the observable specific impulse was probably associated with decrease in ratio of ion gyro radius to tube radius well below a value of 1.0. The use of stronger magnetic fields to produce greater I_{sp} produced difficulties in detachment of the plasma from the magnetic field at the exit; this difficulty was partially circumvented by sloping the magnetic field at the exit to provide a gradual decrease in strength—that is, a magnetic nozzle. (See ref. 22.) Also, at the higher magnetic-field strengths, high localized wall heating was observed at the radial cusp points. At high values of the magnetic-field strength, large oscillations appeared in the anode to cathode voltage, of order 100 kc and of amplitudes exceeding several hundred volts. This experiment was modified to include a plug in the center of the tube in order to separate electron leakage arising as a result of the null point in the magnetic field from electron leakage associated with diffusion of electrons across magnetic-field lines. The plug greatly reduced the backstreaming of electrons.

On the basis of the experiments of references 22 and 28, it was concluded that electron diffusion rates were 100 to 1,000 times the currents predicted by classical diffusion theory but obeyed fairly well the anomalous diffusion law of Bohm as discussed in reference 27. Furthermore, the voltage across the discharge is proportional to B rather than B^2. The turbulence responsible for the enhanced diffusion observed is not well understood, and the large voltage oscillation observed may be associated with this turbulence. Similar oscillations were observed and the diffusion mechanism was discussed in some detail in connection with the studies of the Hall accelerator discussed in reference 17.

The potential engineering advantages of "EM region" d-c plasma accelerators are listed by Janes as follows (ref. 22):

(1) Freedom from space-charge limitations of conventional ion rockets

(2) Magnetic containment possibilities.

(3) High acceleration voltages which depend only upon the specific impulse rather than upon the instantaneous power level, thereby minimizing arc-voltage-drop problems

(4) A readily variable specific impulse and power level

(5) Extreme simplicity in the associated electrical circuitry

(6) Convenient physical size together with moderate power levels, electrostatic voltage gradients, magnetic-field strengths, and heat-transfer rates

The principal study on these devices at the present time is directed toward an understanding of electron-diffusion mechanisms. If means cannot be found to reduce or circumvent the high diffusion rates indicated thus far by the experiments, the overall performance of these devices will be limited.

PULSED PLASMA GUNS

Perhaps the most extensively studied of all plasma acceleration ideas is that of impulsively creating and accelerating a blob of plasma using simple geometric devices such as a pair of rail electrodes or a coaxial arrangement of electrodes. The problems and progress of such devices can be conveniently discussed by confining oneself to the coaxial arrangement. Lovberg has recently written an excellent summary paper (ref. 29) on his views and experiences in research with coaxial plasma guns and some of the following remarks and illustrations are drawn from his presentation.

The simplest embodiment of an impulsive plasma accelerator is the "rail gun," shown schematically in figure 62–15. It is nothing more than a pair of parallel conductors enclosed in a low-pressure system connected to a charged capacitor. When a gas is admitted to the region between the rails, electrical breakdown occurs, and current is conducted around the closed contour. Since it is a general property of unconstrained inductive circuits to move toward larger inductance and particularly of current loops to expand, this particular current loop will seek to expand through a motion of the conducting plasma toward the gun muzzle at the right. In perhaps more fundamental terms, the plasma current interacts with its self-field to produce a $j \times B$ force toward the right. In figure 62–16 the two rails have become a pair of coaxial cylinders in order that complications associated with the side forces on the plasma arising from the free edge interacting with the magnetic field may be avoided. Such essentially simple devices show fair promise as efficient propulsion units.

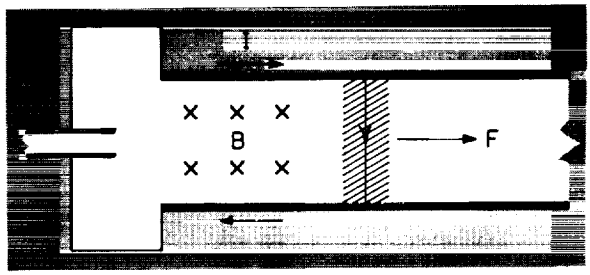

FIGURE 62–15.—Rail-gun plasma-accelerator concept.

The development problems associated with making a plasma gun into an efficient propulsive device fall into two categories; those having to do with the physical processes in an accelerated plasma and those concerned with engineering questions involving components such as capacitors, switches, valves, insulators, electrodes, and so forth. Lovberg has said that a long road of fairly fundamental plasma physics still lies ahead before the plasma engine has reached the state of development of ion engines.

Some of the problems in coaxial plasma-gun development and requirements that may be

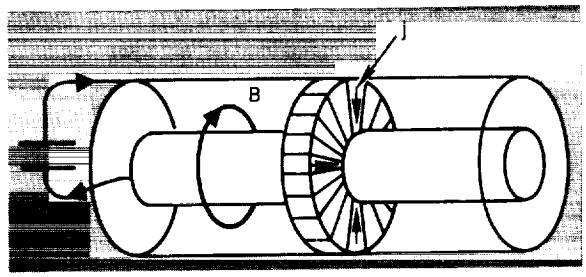

FIGURE 62–16.—Evolution of rail gun into coaxial accelerator. (From ref. 29.)

dictated by certain of these problems might be as follows:

(1) Fairly high electron temperatures, although a nonpropulsive energy loss, might be tolerated; however, high ion temperatures mean transverse thermal speeds which can be very effective in moving ions into electrodes where they lose their entire kinetic energy. Ordinarily, the presence of magnetic fields inhibits these thermal drifts; nevertheless, for long narrow accelerating channels, the electrode loss for even slow transverse speeds can be intolerable. The requirement is thus made that the channel be limited in length compared to diameter so that the acceleration is over before the ions have had time to move transversely a significant amount. (At Langley, analysis has been made of the role of the attainable or limiting velocity of a plasma gun and it is indicated that a primary factor may be the axial component of momentum lost at the electrodes by the ions associated with the current.)

(2) Instabilities of the plasma configuration arise from the previously stated theorem that if any part of a circuit is unconstrained, it will seek out the configuration of highest possible inductance. The propulsion purpose is achieved if the fluid can be coerced to move smoothly along only one possible avenue of inductance-increase toward the muzzle of a coaxial gun. The system, however, usually finds all such avenues, most of which are destructive to the goal. The discharge in a coaxial system not only moves axially, but tends to lose its initial azimuthal symmetry and gather up into a single spoke on one side of the tube as shown in figure 62–17. When this occurs, the discharge is no longer effective in imparting axial momentum to the gas. The spoke also develops violent instabilities of its own, and absorbs field energy, much like a resistor. Recognizing these instabilities (which occur also in a wide variety of accelerators), the requirement is made that conditions be found, if possible, to avoid them or to provide conditions such that their growth rate is small compared with the linear acceleration rate.

(3) The beam energy should be as close as possible to stored energy in the capacitors and the plasma should have absorbed this energy

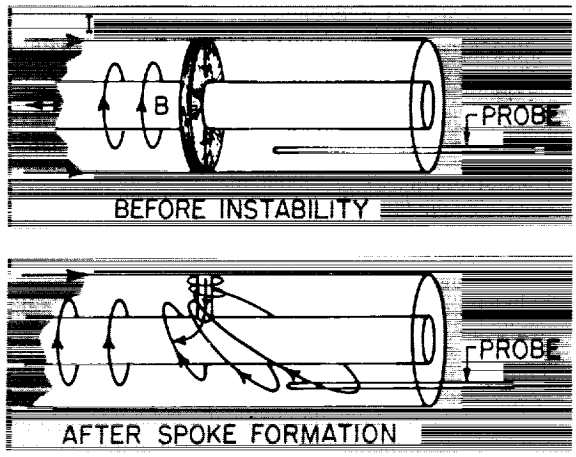

FIGURE 62–17.—Symmetric and spoked current distribution in pulsed coaxial accelerator. (From ref. 29.)

by the time it emerges from the gun. It can be shown that very low inductance energy sources will correspondingly be required for efficient engines.

Lovberg and his associates have built and carried out experiments with a number of coaxial plasma-gun arrangements. They have made extensive interior diagnostics of the discharge with probes which measure the electric and magnetic fields inside the plasma. Through data obtained with these probes they are able to make inferences of several important parameters, for example, ion density and directed ion velocity. Highlights of their observations (ref. 29) are briefed as follows:

(1) A distinct layer of radial current was accelerated toward the gun muzzle at about 10^7 cm/μ sec ($I_{sp}=10^4$ sec); however, the plasma ions were not accelerated to anything like the current layer speed. It was concluded that the accelerating current layer does not necessarily act as a piston as has been generally supposed. It has the character of a strong ionizing shock which does impart momentum to the propellant but at a speed which has to be determined by other means. They found, by using time-of-flight techniques that in some cases, the plasma and current layer move nearly together.

(2) A primary source of losses was attributed to a tendency of the gun to "crowbar," that is, set up a secondary discharge near the insulator after about one-half cycle of the oscillating gun current. This energy is sealed off

from the plasma and lost. Efforts to overcome this problem have not yet been successful and it continues to be a source of worry.

(3) The efficiency of transfer of field energy to the plasma was good, that is to say, losses associated with drift into the electrodes or plasma radiation do not appear to be ruinous.

(4) Heat transfer from electrons to ions is slow, that is, over the time of the total gun pulse, ion heating is small.

(5) Extensive surveys of conditions under which spoke instabilities are troublesome are not conclusive, however, "good" conditions to avoid these can be met. However, small departures of pressure, propellant, and voltage from values giving "good" condition could reestablish detrimental instabilities.

(6) Distribution of propellent gas in the barrel just prior to breakdown has a major influence on crowbarring at the insulator.

At Langley, extensive experiments have been made with various coaxial plasma-gun arrangements, and one development that has been made in reference 30 is schematically shown in figure 62–18. The gun is connected directly to a 50-kilojoule capacitor bank without a switch in the line; however, the gas pressure in the gun is sufficiently low that, for the standoff voltage and electrode spacing, breakdown does not occur. When the coil is switched on, an axial magnetic field is imposed between the electrodes, and for the desired electric and magnetic conditions, a breakdown occurs in a very short time interval. Part of the conditions are that the ion cyclotron radius is much larger than the electrode spacing, as indicated in the lower sketch, the electron cyclotron radius is smaller than the spacing and smaller than the mean-free path. The electrons will perform cycloidal motions in the crossed fields between collisions and, at each collision, the electron takes up a new cycloid closer to the anode by about one cyclotron radius. The avalanche progresses by the production of enough ion pairs on collisions with neutrals so that breakdown occurs very rapidly. Another view is that the electron transit distance is too small to produce collisions in the electric field alone and that the greatly increased transit distance in the crossed fields makes enough collisions possible. The theory for this breakdown process has been developed and experimentally proven. With a 36-microfarad bank charged to 48,000 volts, a peak current of 1,300,000 amperes was achieved with a current rise time of only 2 microseconds. Advantages of magnetic-ignition are: losses associated with external switching are avoided, the high rate of discharge generally means efficient energy transfer to the plasma, and the gun can be operated at very low pressures where many difficulties are avoided.

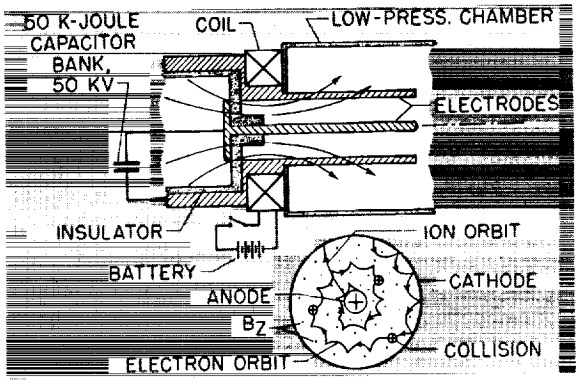

FIGURE 62–18.—Magnetically ignited coaxial discharge.

It may be somewhat puzzling that low-pressure operation is listed as an advantage for the coaxial plasma gun; however, many problems encountered at higher pressures can, in fact, be avoided. At Langley, a coaxial plasma gun was operated in this low-pressure region (10^{-5} mm Hg) with magnetic switching, and the following general findings were noted: conversion efficiency of electrical to beam energy of 50 percent was attained, no crowbarring or instability was observed, and the plasma is almost entirely electrode material; however, it is not inconceivable that a propulsion device could utilize consumable electrodes.

Other research at Langley has included development of a new approach to determination of the limiting velocity of plasma guns wherein the primary factor is that the axial component of the ion current is lost at the electrode (ref. 31). Estimates based on this approach check experimental values; however, the detail mechanisms at the electrodes require much further research. Also, spectrographic observations of the plasma show large contamination by electrode material; thus, a study of electrode conditions is being made. In all experimental

studies of plasma guns, the short duration of observation demands ever improved diagnostic techniques; at Langley a new type of magnetic probe has been developed recently (ref. 32).

TRAVELING-WAVE ACCELERATORS

There is great attraction, in principle, to acceleration schemes which avoid electrodes, since in all the devices so far discussed electrodes are used and present energy-loss or survival problems to varying degrees—worst probably for the plasma guns with their very high initial current concentration at the electrodes. Characteristically, the electrodeless devices make use of time-varying magnetic fields which induce currents in the plasma; these in turn interact with the magnetic field to produce acceleration. Invariably, one is led to the idea of traveling magnetic fields or magnetic "traveling waves" so that the plasma may be effectively continuously accelerated or accelerated in magnetically contained plasma "bunches." Reduction of wall losses by magnetic containment is also a desirable advantage offered by these concepts. A fairly large variety of traveling-wave schemes have been conceived and studied extensively (see bibliographies of refs. 33 and 34 and ref. 35). Description and distinction of the shemes from each other can become exceedingly involved in detail; thus, this brief summary seeks only to point out some broad categories.

Probably the simplest concept of an induction accelerator, which might constitute one stage of a traveling-wave scheme, is the so-called ring accelerator. In one form of this scheme, a capacitor discharge (or RF) is fed into a single loop of conductor around a tube containing low-pressure gas. The varying magnetic field associated with this loop induces an azimuthal electric field in the gas of sufficient intensity to ionize the gas. The resulting azimuthal current in the gas interacts with the magnetic field to produce a Lorentz force radially inward and axially away from the coil. This single-coil scheme can provide large instantaneous forces, but the short range of magnetic forces makes it inefficient. One is led immediately to a phased string of coils down the tube as shown in the lower part of figure 62–19. These coils might be single turns with properly

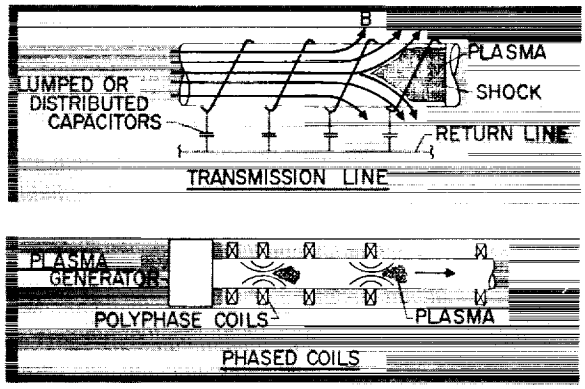

FIGURE 62–19.—Traveling-wave plasma-accelerator concepts.

timed discharges from a series of capacitors fed to each coil, or multiturn coils properly phased with the plasma velocity or with the coil spacing increasing with plasma velocity as shown. For these staged arrangements, the coils are not inductively independent and are effectively a transmission line. This arrangement has been called a timed-sequenced device in which it is sought to synchronize the driving currents with the plasma position.

The upper part of figure 62–19 shows a transmission line arrangement which gives more regular fields. A traveling magnetic piston drives the plasma down the tube; the shock wave preceding this piston ionizes the gas. With lumped capacitors, large amounts of energy can be stored for pulsed operation. However, repetitive operations imposes switching and capacitor problems. Another variation of the arrangement shown is to provide an RF generator instead of the switched pulses, and the device becomes a continuously operating transmission line; thus the high voltages and currents of the pulsed device are circumvented.

A number of persons have studied a variety of traveling-wave schemes. For the single-coil arrangements, very high velocities have been obtained, but at efficiencies of only a few percent. Penfold (ref. 36) has studied and operated a pulsed device which accelerates plasma toroids by means of an arrangement incorporating 19 one-turn coils spaced 1 inch apart along a 6-inch-diameter pyrex vacuum tube. The velocity of the magnetic field at the end of this this sequenced array of coils was 11 cm/μsec and experimental observations with microwave

and photomultiplier techniques indicated that the toroids were, in fact, achieving this velocity. He has made extensive diagnostic measurements with the device.

One of the most extensive investigations of a traveling-wave device has been made by Janes (ref. 22) and is shown schematically in figure 62–20. The conditions of his operation are

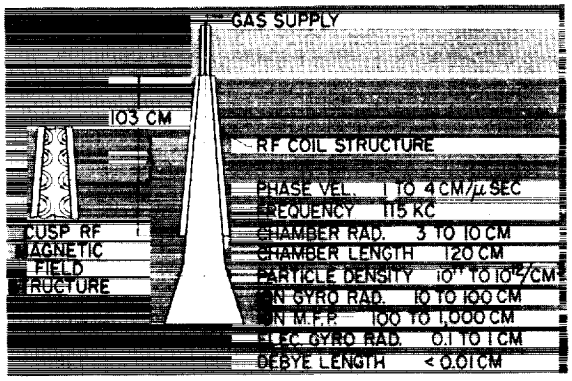

FIGURE 62–20.—E.M. region RF traveling-wave plasma accelerator. (From ref. 22.)

shown in the figure. With this apparatus, he has made measurements of mass-flow rate, RF power absorption in the plasma, local and integrated wall heat-transfer rates, and integrated axial voltage gradients. He also measured distribution of the local momentum flow with a quartz thrust plate. From these and extensive Langmuir probe measurements of ion flux, plasma potential and electron temperatures he found that the E.M. region accelerating mechanism was remarkably effective, the most striking feature being the appearance of strong electrostatic fields which were closely correlated with the ion accelerations. Specific impulses of 2,600 were computed from the measurements corresponding to two-thirds of the phase velocity of the cusps. His observation suggested that an external axial voltage be applied and experiments with such an axial field indicated the mean plasma velocity could be about doubled. His experience with this device led him to studies with the E.M. region steady-flow plasma accelerators previously mentioned.

Most of the traveling-wave schemes considered operate at high conductivities because of the moderate magnetic fields available, and at low densities, implying low thrusts. At low densities, diffusion losses to the walls are important; these could be reduced by longitudinal bias magneteic fields, but it has been found that this decouples the driving fields from the plasma and prevents acceleration.

It has been questioned whether traveling-wave devices can ever reach reasonable efficiency unless some way of using magnetic fields or other means to reduce losses are found. Even if this were so, their use as a laboratory device such as a hypersonic wind tunnel would still be attractive, especially if seeding could be avoided and exiting ionization quenched.

CONCLUDING REMARKS

It is emphasized that in this presentation, it has not been possible to cite all the important contributions to plasma accelerator research, which field has now reached such proportions that one type of accelerator alone has recently been the subject of a several-day meeting. The purpose here has been to show the broad possibilities of plasma acceleration schemes and to mention a few of the problems arising from active research. Accomplishments in the field of sufficient dramatic impact to impress those outside are few; however, the growing bulk of knowledge from many detailed findings lends increasing encouragement and full expectation that practical plasma-acceleration devices will be a reality in the very near future. Perhaps the greatest encouragement stems from the fact that a large number of outstanding scientists are working in the field. These numbers include those working towerd controlled thermonuclear fusion, which research effort feeds much basic plasma physics information into the plasma acceleration efforts and vice versa.

REFERENCES

1. JAFFE, LEONARD D., LUCAS, JOHN W., MERRILL, OWEN S., SHAFER, JOHN I., and SPENCER, DWAIN F.: Nuclear Electric Spacecraft for Unmanned Planetary and Interplanetary Missions. [Preprint] 2389–62, American Rocket Soc., Mar. 1962.
2. SPEISER, E. W.: A Preliminary Study of Advanced Propulsion Spacecraft Payload

Capabilities. Tech. Memo. No. 33–42 (Contract No. NASw–6), Jet Propulsion Lab., C.I.T., May 10, 1961.

3. Speiser, Evelyn W.: Performance of Nuclear-Electric Propulsion Systems in Space Exploration. Tech. Rep. No. 32–159 (Contract No. NASw–6), Jet Propulsion Lab., C.I.T., Dec. 15, 1961.
4. Wood, George P., Carter, Arlen F., Lintz, Hubert K., and Pennington, J. Byron: A Theoretical Treatment of the Steady-Flow, Linear, Crossed-Field, Direct-Current Plasma Accelerator for Inviscid, Adiabatic, Isothermal, Constant-Area Flow. NASA TR R–114, 1961.
5. Wood, George P., and Carter, Arlen F.: Considerations in the Design of a Steady DC Plasma Accelerator. Dynamics of Conducting Gases, Ali Bulent Cambel and John B. Fenn., eds., Northwestern Univ. Press (Evanston, Ill.), c.1960, pp. 201–212.
6. Carter, Arlen F., Wood, George P., Sabol, Alexander P., and Weinstein, Richard H.: Experiments in Steady-State High-Density Plasma Acceleration. Engineering Aspects of Magnetohydrodynamics, Clifford Mannal and Normal W. Mather, eds., Columbia Univ. Press, 1962, pp. 45–55.
7. Wood, George P., Carter, Arlen F., Sabol, Alexander P., and Weinstein, Richard H.: Experiments in Steady State Crossed-Field Acceleration of Plasma. The Physics of Fluids (Letters to the Editor), vol. 4, no. 5, May 1961, pp. 652–653.
8. Demetriades, Sterge T.: Experimental Magnetogasdynamic Engine for Argon, Nitrogen, and Air. Engineering Aspects of Magnetohydrodynamics, Clifford Mannal and Norman W. Mather, eds., Columbia Univ. Press, 1962, pp. 19–44.
9. Hellund, Emil J., and Blackman, Vernon H.: Crossed Field Accelerators. [Preprint] 2128–61, American Rocket Soc., Oct. 1961.
10. Hogan, William T.: Experiments With a Transient D.C. Crossed-Field Accelerator at High Power Levels. Third Symposium on Engineering Aspects of Magnetohydrodynamics, Univ. of Rochester, Mar. 28–30, 1962.
11. Ragusa, Domenico, and Baker, Jerome: Experimental Results With a Direct Current Electromagnetic Plasma Accelerator. Engineering Aspects of Magnetohydrodynamics, Clifford Mannal and Norman W. Mather, eds., Columbia Univ. Press, 1962, pp. 56–63.
12. Rausa, G. J., and Gearhart, L. M.: Plasma Acceleration Studies. Engineering Aspects of Magnetohydrodynamics, Clifford Mannal and Norman W. Mather, eds., Columbia Univ. Press, 1962, pp. 64–80.
13. Janes, G. Sargent: Magnetohydrodynamic Propulsion. Res. Rep. 90 (AFOSR TN 60–955), Avco-Everett Res. Lab., Aug. 1960.
14. Janes, G. Sargent: Introduction. Engineering Aspects of Magnetohydrodynamics, Clifford Mannal and Norman W. Mather, eds., Columbia Univ. Press, 1962, pp. 3–4.
15. Sutton, George W., and Gloersen, Per: Magnetohydrodynamic Power and Propulsion. Magnetohydrodynamics, Ali Bulent Cambel, Thomas P. Anderson, and Milton M. Slawsky, eds., Northwestern Univ. Press (Evanston, Ill.), c.1962, pp. 243–268.
16. Hess, Robert V.: Experiments and Theory for Continuous Steady Acceleration of Low Density Plasmas. Vol I of Proc XIth Int. Astronautical, Carl W. P. Reuterswärd, ed., Springer-Verlag (Vienna), 1961, pp. 404–411.
17. Hess, R. V., Burlock, J., Sevier, J. R., and Brockman, P.: Theory and Experiments for the Role of Space-Charge in Plasma Acceleration. Electromagnetics and Fluid Dynamics of Gaseous Plasma, Vol. XI of Microwave Res. Inst. Symposia Ser., Polytechnic Press of Polytechnic Inst. of Brooklyn, c.1962, pp. 269–305.
18. Powers, William E., and Patrick, Richard M.: Magnetic Annular Arc. The Physics of Fluids, vol. 5, no. 10, Oct. 1962, pp. 1196–1206. (Also, available as Avco-Everett Res. Rep. 129.)
19. Patrick, R. M., and Powers, W. E.: Plasma Flow in a Magnetic Annular Arc Nozzle. Presented at Third Symposium on Advanced Propulsion Concepts (Cincinnati, Ohio), Oct. 2–4, 1962. (Sponsored by U.S. Air Force and Gen. Elec. Co.)
20. Weinstein, Richard H., and Hess, Robert V.: New Experiments With Hollow Cathode Discharges (For Application to Plasma Accelerators). Third Symposium on Engineering Aspects on Magnetohydrodynamics, Univ. of Rochester, Mar. 28–30, 1962.
21. Grossmann, William, Jr., and Hess, Robert V.: Existence of a Voltage Plateau for a

Discharge Crossed With a Magnetic Field at Elevated Pressures. Presented at the Summer Meeting, American Phys. Soc. (Seattle, Wash.), Aug. 27, 1962.

22. JANES, G. S., DOTSON, J., and WILSON, T.: Electrostatic Acceleration of Neutral Plasmas—Momentum Transfer Through Magnetic Fields. Presented at Third Symposium on Advanced Propulsion Concepts (Cincinnati, Ohio), Oct. 2–4, 1962. (Sponsored by U.S. Air Force and Gen. Elec. Co.)
23. LARY, E. C., MEYERAND, R. G., Jr., and SALZ, F.: Ion Acceleration in a Gyro-Dominated Neutral Plasma—Theory. Bull. American Phys. Soc., ser. II, vol. 7, no. 7, Aug. 27, 1962, p. 441.
24. SEIKEL, G. R., and RESHOTKO, E.: Hall Current Ion Accelerator. Bull. American Phys. Soc., ser. II. vol. 7, no. 6, June 19, 1962, p. 414.
25. CANN, G. L., TEEM, J. M., BUHLER, R. D., and BRANSON, L. K.: Magnetogasdynamics Accelerator Techniques. AEDC–TDR–62–145 (Contract No. AF 40(600)–939), Arnold Eng. Dev. Center, July 1962.
26. RIGBY, ROBERT NORRIS: Some Physical Properties of an Axial Electric Arc in a Radial Magnetic Field. M. S. Thesis, The College of William and Mary in Virginia, 1962.
27. HESS, ROBERT V.: Fundamentals of Plasma Interaction With Electric and Magnetic Fields. NASA University Conference, 1962. (Paper no. 62 of present compilation.)
28. SALZ, F., MEYERAND, R. G., Jr., and LARY, E. C.: Ion Acceleration in a Gyro-Dominated Neutral Plasma—Experiment. Bull. American Phys. Soc., ser. II, vol. 7, no. 7, Aug. 27, 1962, p. 441.
29. LOVBERG, R. H.: Impulsive MHD Devices as Space Engines. Presented at Third Symposium on Advanced Propulsion Concepts (Cincinnati, Ohio), Oct. 2–4, 1962. (Sponsored by U.S. Air Force and Gen. Elec. Co.)
30. THOM, KARLHEINZ, and NORWOOD, JOSEPH, Jr.: Magnetic Ignition of Pulsed Gas Discharges in Air of Low Pressure in a Coaxial Plasma Gun. NASA TN D–910, 1961.
31. THOM, K., NORWOOD, J., and JALUFKA, N.: Velocity Limitation of a Coaxial Plasma Gun. NASA Paper presented at the International Symposium on Coaxial Plasma Gun (Cleveland, Ohio), Sept. 6–7, 1962.
32. THOM, KARLHEINZ, and NORWOOD, JOSEPH, Jr.: Novel Method for Measuring the Electrical Conductivity of a Moving Conductor. Bull. American Phys. Soc., ser. II, vol. 7, no. 7, Aug. 27, 1962, p. 432.
33. BREWER, G. R., CURRIE, M. R., and KNECHTLI, R. C.: Ionic and Plasma Propulsion for Space Vehicles. Proc. IRE, vol. 49, no. 12, Dec. 1961, pp. 1789–1821.
34. GOURDINE, MEREDITH C.: Recent Advances in Magnetohydrodynamic Propulsion. ARS Jour., vol. 31, no. 12, Dec. 1961, pp. 1670–1677.
35. ANON.: Third Symposium on the Engineering Aspects of Magnetohydronamics. Univ. of Rochester, Mar. 28–30, 1962.
36. PENFOLD, ALAN S.: Estimating the Mass of a Fast Plasma Toroid. Ion and Plasma Propulsion Research, AFOSR 3–62, U.S. Air Force, Mar. 1962, pp. 28–29.